Investigating how ubiquitin-mediated proteolysis of AURKA contributes to its activity in the cell cycle

Ahmed Mohamed Abdelbaki Abdelaal

Churchill College

Department of Pharmacology

A thesis submitted on September 2020 for the Degree of Doctor of Philosophy

For my family

Declaration

This thesis:

- is my own work and contains nothing which is the outcome of work done in collaboration with others, except where specified in the text;
- is not substantially the same as any that I have submitted for a degree or diploma or other qualification at any other university; and
- does not exceed the prescribed limited of 60,000 words.

Ahmed Mohamed Abdelbaki Abdelaal

September 2020

Title: Investigating how ubiquitin-mediated proteolysis of AURKA contributes to its activity in the cell cycle
Name: Ahmed Mohamed Abdelbaki Abdelaal

Abstract

Aurora kinase A (AURKA) is a major mitotic regulatory kinase required for mitotic entry, the formation of a bipolar mitotic spindle, and the completion of cytokinesis. In recent years AURKA has been identified as an upstream regulator for many interphase functions such as cilia disassembly and mitochondrial fragmentation. AURKA is overexpressed in many tumours and has a pivotal role in the acquisition of malignant cell phenotypes. Therefore, it is considered a highly attractive drug target for anti-cancer therapy.

The activity of AURKA is regulated by phosphorylation at the active loop or the interaction with binding partners. TPX2 is a well-known binding partner of AURKA. It activates AURKA through stabilizing the T-loop and is required for targeting AURKA to the mitotic spindle. Phosphorylation and binding partners may act synergistically to induce hyperactivity of the kinase. Previous research from my lab has highlighted that AURKA is frequently co-expressed with TPX2 in human cancers and proposed AURKA/TPX2 complex as an oncogenic holoenzyme in a variety of cancers. AURKA protein is targeted for proteasome-mediated degradation by the FZR1 activated form of APC/C at the end of mitosis. This study focuses on characterisation of AURKA degrons, the contribution of APC/C-FZR1 in the timing of AURKA inactivation, identifying the physiological consequences of AURKA deregulation outside mitosis, and examining the role of Short Linear motifs (SLiMs) within AURKA N-terminal domain in regulating its stability and activity.

I show that the previously known D-box-like motif ($R_{371}xxL_{374}$) within C-terminal is not a functional degron. I also reveal that the A-box motif may act as an atypical D-box that is sufficient to drive protein degradation. I use a new tool CRISPR/Cas9 FZR1 knockout cell line and a FRET-based biosensor for measuring AURKA activity to investigate directly whether AURKA inactivation is regulated simply by destruction. These, in combination with time-lapse imaging, show that inactivation of AURKA is identical in wild-type and FZR1KO cells, despite the difference in protein levels between the two cell lines. I demonstrate that the timing of AURKA inactivation is regulated via the degradation of its activator TPX2 at mitotic exit. Moreover, the destruction of AURKA is required to regulate its interphase activity. I also identify that extra AURKA activity can have consequences on the morphology of the

mitochondrial network outside of mitosis. My time-lapse imaging reveals that FZR1-restricted degradation of AURKA controls mitochondrial dynamics. This mechanism links the destruction machinery, through AURKA signaling to the mitochondrial dynamics of the cell.

I further explore the role of the N-terminal domain in the regulation of AURKA activity through the detailed analysis of the potential SLiMs. I find that K_{23}RVL has a role in mediating the autoinhibition of AURKA. I then investigate the hypothesis that calmodulin (CaM) protects AURKA from degradation through its binding to the A-box SLiM. I find that AURKA degradation is not affected by inhibition of Ca2+/CaM.

In summary, this work sheds light not only on the molecular mechanisms of AURKA activity and stability but also on the physiological relevance outside mitosis, which is urgently needed in the field to understand the oncogenic activity of AURKA and to improve therapeutic applications of cancer patients.

Ahmed Mohamed Abdelbaki Abdelaal

Acknowledgements

I would like to thank my supervisor, Dr. Catherine Lindon, for her support and encouragement during the last 4 years. She encouraged me to work hard throughout my studies. She has guided me to becoming an independent researcher. I learned so much from her expertise in the field. Also, I would like to express my very great appreciation to Dr Giulia Guarguaglini and Dr Olivier Gavet for their valuable support and collaboration in shaping up this project.

The relationships that I have established within the Lindon lab also greatly impacted my life and scientific career. I would like to thank Dr. Begum Akman, Camilla Ascanelli, Cynthia Okoye, Richard Wang, Roberta Cacioppo, Siân Stockton, Thomas Brand, Anja Hagting, and Arianna Rossi for their great feedback on my project. They helped me to think about the project and discuss my experiments to achieve my project goals. I am particularly grateful for the assistance given by Dr. Ahmed Balboula who has been willing to talk with me and always suggested interesting idea for my work. I would like to express my sincere gratitude to my professors, Dr. Abdel Badie Elattar, Dr. Al Ahmady AL Zahaby, Dr. Reham Abou-ElKahair at Zagazig University for their unconditional support and all considerate guidance.

A big thank you to my sister (Rehab), my brother (Hossam), his wife (Amal), Aseel, Mohamed and my loving parents. My deepest gratitude is to Churchill College and my friends: Omer Bayazeid, Mohamed EL-Gazzar, Dina Tahboub, Omar quoqas, Anwar Gaber, Abdelhamid Youssef, Marwa Shykhon, Youmna Hussein, Samuel Gabra, Noura, Ibrahim, Alim, Assad, Nadi, Omar, Steven, Mahmoud Bahansawi, Mohamed Elzek, Abdallah, Moataz, Malak, Bilal, Salma, Ghalia, Ban dodin, and Ahmed Talaat.

I would like to offer my special thanks to the funding sources of my PhD: Cambridge Overseas Trust, Youssef Jameel Foundation and Cambridge Philosophical Society. It would not be possible to do PhD in University of Cambridge without their financial support.

Last but not least, I would like to thank people who have comforted and sustained me all the way through my graduate study. I deeply appreciate their belief in me.

Ahmed Abdelbaki Abdelaal

Abbreviations

PTMs	Post-translational modifications
IDRs	Intrinsically disordered regions
SLiMs	Short linear motifs
CDKs	Cyclin-dependent kinases
APC/C	Anaphase-promoting complex/cyclosome
Plk1	Polo-like kinase 1
AURKA	Aurora A
AURKB	Aurora B
AURKC	Aurora C
MPF	M-phase-promoting factor
SAC	Spindle Assembly Checkpoint
MCC	Mitotic checkpoint complex
PPi	Pyrophosphate
E1	Ubiquitin-activating enzyme
E2	Ubiquitin-conjugating enzyme
E3	Ubiquitin ligase
CPC	Chromosomal passenger complex
INCENP	Inner centromere protein
GSK3 β	Glycogen synthase kinase 3 β
MAP	Microtubule-Associated Protein
PCM	Pericentriolar material
Cep192	Centrosomal protein 192
PKD	Polycystic kidney disease
HCCs	Hepatocellular carcinomas
SAC	Spindle assembly checkpoint

ΔΔG	Gibbs free energy variations
WT	Wild type
Plk1	Polo-like kinase 1
HRP	Horseradish peroxidase
LB	Luria broth
MLN	MLN8237
PCR	Polymerase chain reaction
ZM	ZM447439
UPS	Ubiquitin- proteasome system
FZR1	Fizzy and cell division cycle 20 related 1
FRET	Förster resonance energy transfer
NEB	Nuclear envelope breakdown
PM	Prometaphase
CFP	Cyan fluorescent protein
YFP	Yellow fluorescent protein
VCL	Vinculin
CCNB1	Cyclin B1

Table of Contents

List of Figures

List of Tables

Chapter 1 Introduction

Cells carry out various functions through specific proteins expressed by approximately 20,000 genes. Protein function is determined by conformation, and the regulated modulation of conformation underlies cell signaling, function, and fate. The ability of proteins to transduce signals to one another in the cell is affected by their intracellular concentrations, post-translational modifications, and intracellular localization. Post-translational modifications (PTMs) cause rapid changes in a protein's response to the stimulus. PTMs range from global modification to highly specific regulatory events on small pools of molecules and include methylation, glycosylation, ubiquitination, and phosphorylation. The addition and removal of PTMs are controlled by tight enzymatic regulation. For example, phosphorylation, the process by which a phosphate group is covalently attached to a protein on serine, threonine or tyrosine, residues are catalyzed by enzymes called kinases. On the other hand, the removal of phosphate groups is achieved by enzymes called phosphatases. These tight regulations by kinases and phosphatases are essential for the regulation of signal cascades and cellular decisions. They alter the structure and properties of proteins reversibly or irreversibly through biochemical reactions. PTMs regulate activities as diverse as cellular gene expression, cell-cell interaction, protein-protein interaction, and communication with the extracellular environment. The perturbation of PTMs will, therefore, affect cell physiology (Deribe et al., 2010; Mowen and David, 2014).

Proteins typically have a variety of conformational modules within the protein sequence that both determine their overall structure and allow them to bind other proteins with great specificity and avidity. This specificity of action enables proteins to amplify, attenuate, and/or integrate signals to achieve different cellular decisions. The majority of proteins contain a mixture of globular domains and intrinsically disordered regions (IDRs) in their structure (Darling and Uversky, 2018). IDRs can be divided based on the length of the amino acid sequence into a short linear motif (SLiMs): 3- 10 amino acids; and an intrinsic disorder domain (IDD): 20-50 amino acids. SLiMs are short, conserved motifs that act as interaction modules recognized by additional biomolecules and are involved in the regulation of protein destruction, localization, function, and PTMs (Lemas et al., 2016). PTMs occur in IDRs at a much higher frequency than in globular domains (Darling and Uversky, 2018; Davey et al., 2017; Min et al.,

2013), reflecting the fact that IDRs are under less evolutionary constraint and evolve more rapidly than structured domains. They are thus natural sites of functional specialization, and much of this functional fine-tuning can be explained through PTM-mediated modulation of SLiM structure and binding to other proteins (Van Roey et al., 2014). For example, some SLiM classes are in a functionally inactive state that becomes active only after the addition of a specific PTM which primes them for recognition by their target domains (Davey et al., 2015). These complex regulations are important to temporally and spatially control the activity of proteins directing major events in the life of the cell. The paradigm of a PTM-driven cellular event, during which the cell undergoes the most extreme physiological and morphological changes, is mitosis.

1.1 Mitosis

Mitosis is a type of cell division that is important for separating the genetic material and organelles between the daughter cells (Yanagida, 2014). It occurs through precise initiation and execution of two distinct processes. First, the segregation of replicated chromosomes into two distinct daughter nuclei by a process termed as karyokinesis. This is then followed by a process known as cytokinesis, by which the cell cytoplasm is partitioned into two daughter cells. Morphologically, mitosis can be classified into five different stages, which marks irreversible changes in the structure of the chromosomes in the cell (Sullivan and Morgan, 2007; Wieser and Pines, 2015).

The start of mitosis is called prophase. It begins with chromosome condensation and ends with subsequent breakdown of the nuclear membrane. It is then followed by a process called prometaphase. It is defined as the time from the breakdown of the nuclear membrane to the beginning of metaphase stage, where all chromosomes align at the middle of the mitotic spindle. This is subsequently followed by anaphase which involves separation of the sister chromatids and their migration to the opposite poles. In telophase, the microtubule-based midbody start to assemble, the chromosomes reform nuclei near the poles, the nuclear envelope reforms, followed by cytokinesis, and finally the two daughter cells are cleaved from the mother cell (Pines, 2012). The morphological description of mitosis could be problematic because chromatin condensation can occur at the beginning of the interphase stage in some organisms rather than the end. Moreover, the nuclear membrane persists until anaphase in C. elegans (Gorjanacz et al., 2007). Therefore, although the microscopic classification of mitosis is often

useful, most of these changes can be described more precisely at the molecular level (Pines and Rieder, 2001).

1.1.1 Phosphorylation and Ubiquitination drive mitosis

Mitotic phases can be described at the molecular level by the changes in the activity of mitotic regulators such as cyclin-dependent kinases (CDKs) and the anaphase-promoting complex/cyclosome (APC/C). CDKs are families of proteins that play critical role in triggering G1 to S and from G2 to M transition by phosphorylating downstream substrates to modulate their intracellular activities. The APC/C is a large E3 ligase that targets mitotic substrates for ubiquitination and proteasomal degradation (Acquaviva and Pines, 2006; Pesin and Orr-Weaver, 2008; Peters, 2006; Sivakumar and Gorbsky, 2015). The activity of these mitotic regulators can precisely describe mitotic progression because they do not depend on chromosome structure, alignment, and nuclear membrane breakdown.

Higher eukaryotic cells do not commit to mitosis until near the time of nuclear membrane breakdown. Cyclin A–CDK has been shown to play a dominant role throughout G2, as well as other mitotic kinases such as Polo-like kinase (PLK1) and the Aurora kinases, Aurora A (AURKA) and Aurora B (AURKB), in preparing the cell for mitosis.

The commitment to mitosis is determined by the rapid activation of the master regulator kinase CDK1 associated with its activating subunit cyclin B, which are the components of the M-phase-promoting factor (MPF). The phosphorylation and dephosphorylation events of key residues of Cyclin B/CDK1 can positively and negatively regulate its activity within mitosis. During prophase, Cyclin B /CDK1 accumulates within the nucleus. As with the nuclear accumulation of cyclin B, Cdc25 phosphatase moves to the nucleus, where it dephosphorylates and activates Cyclin B/ CDK1 (Lindqvist et al., 2009; Nasa and Kettenbach, 2018). This enzyme can phosphorylate multiple, distinct substrate proteins within the cell, which alter their activity, location, and function. As a result, the nuclear membrane starts to break down, and organelles are induced to fragment into small vesicles that segregate equally into the two daughter cells. Many of these substrates are phosphorylated on IDRs. For example, CDK1/Cyclin B phosphorylation of the phosphatase PP2A-B56 SLiM motif (LpSPIxE) regulates its subcellular localization for subsequent control of mitotic exit (Qian et al., 2015).

During the metaphase/anaphase transition, equal segregation of the chromosomes is required to avoid aneuploidy. In most cases, cells with the wrong number of chromosomes often die or undergo uncontrolled proliferation. Therefore, cells have evolved a surveillance mechanism pathway to enhance the accuracy of chromosomes segregation. The fidelity of chromosome segregation is achieved by checkpoint pathways. This mechanism stops or delays cell division until a specific event is satisfied. During mitosis, the accuracy of microtubule-kinetochore attachment is monitored by the spindle assembly checkpoint (SAC).

The SAC delays metaphase/anaphase transition to ensure that all kinetochores become properly attached to the mitotic spindles. The presence of free kinetochores leads to the formation of a complex consisting of a molecular signal that causes inhibition of anaphase onset. This signal, which is composed of a multimeric protein complex called the mitotic checkpoint complex (MCC), prevents anaphase onset by inhibition of the APC/C (Barford, 2019; Liu and Zhang, 2016). Activation of the APC/C marks the onset of mitotic exit, since it rapidly eliminates mitotic cyclin B. Once ubiquitin-mediated proteolysis has started, it continues through the mitotic exit to regulate many processes to prepare cells for interphase (Kapuy et al., 2009). This pathway ensures that the APC/C does not target proteins that are required for chromosome disjunction and mitotic exit until proper kinetochore- spindle attachment is achieved.

Yet another important process in mitosis is organelle inheritance which is essential for cell viability, including the inheritance of the Golgi apparatus, the mitochondria, the endoplasmic reticulum, and the nuclear membrane. The inheritance of organelles into daughter cells occurs in a two-step process. First, the organelle networks are broken down into a large number of smaller units. Thereafter, the dispersing small units are distributed randomly at the mother cell and segregated into the daughter cells (Knoblach and Rachubinski, 2015; Mascanzoni et al., 2019; Valente and Colanzi, 2015).

At the end of mitotic division, the two daughter cells end up with a centrosome, a single complement of chromosomes, and subunits for building their organelles and cytoskeletal reassembly. Fragmentation and dispersion of organelles at mitosis occur under the control of the master mitotic regulatory kinase, Cyclin B/CDK1, and other mitotic kinases such as Aurora-A (AURKA) (Peng and Weisman, 2008; Yamano and Youle, 2011). The functional inactivation of mitotic kinases by APC/C-mediated ubiquitin signaling is therefore thought to determine the return to an interphase state at the end of mitosis.

1.2 Cell cycle regulation by ubiquitination

1.2.1 Ubiquitin biology and mechanism of protein ubiquitination

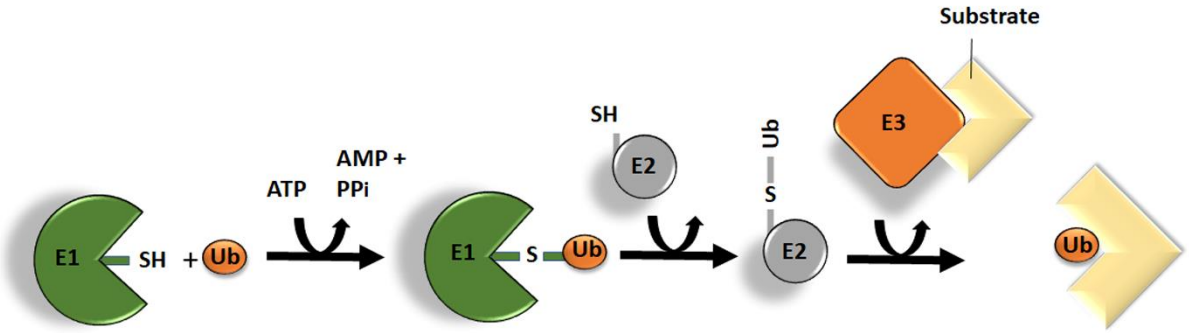

Figure 1-1 Mechanism of protein ubiquitination. Protein ubiquitination is achieved by three-enzymes E1, E2, and E3. The E1 enzyme is responsible for activating ubiquitin. E1 enzyme, along with ATP, binds to the ubiquitin protein to form high energy E1~Ub thioester linkage between an E1 catalytic cysteine residue and the C-terminus of Ub. E1 then passes the activated ubiquitin to E2, and E3 catalyzes the transfer of ubiquitin from E2 to the substrate protein.

Rapid transitions in the cell cycle depend on activation, inactivation, and the timely destruction of cell cycle regulators. Ubiquitin-mediated proteolysis allows modular regulatory elements of the cell cycle to disappear quickly, thus regulating the cell cycle positively and negatively to promote synchronization of the cellular machinery (Bassermann et al., 2014). The ubiquitin pathway was identified by Avram Hershko and Aaron Ciechanover in the late 1970s and early 1980s (Ciechanover et al., 1980; Goldknopf and Busch, 1977; Mahajan et al., 1997; Schwartz and Hochstrasser, 2003). The ubiquitin-proteasome system relies on three enzymes known as a ubiquitin-activating enzyme (E1), the ubiquitin-conjugating enzyme (E2), and ubiquitin ligase (E3). Ubiquitin is a small 76 amino-acid (8 kDa) protein that is conjugated to the target proteins by a process called ubiquitination. E1 can activate ubiquitin by forming a thioester-linkage linking the ubiquitin and the cysteine in the active site of the E1 enzyme (UBA1 or UBA6) (Groen and Gillingwater, 2015; Liu et al., 2017). This reaction requires energy in the form of ATP (Pastore, 2010). Once the ubiquitin is activated, the E1 can bring the ubiquitin to the cysteine in the active site of an E2, the Ubiquitin Conjugating Enzyme (these are called UBCs). E2 will then transfer it to the target substrate. Multiple rounds of protein ubiquitination will create a long chain of ubiquitin on the substrate (Fiskin et al., 2017). The reaction requires the activity of E3s (Ubiquitin ligases), which bring together E2 and substrates. Some E3s are enzymes playing a role in forming an intermediate thioester bond via an active

site cysteine such as the HECT class, and most E3s including the APC/C, are allosteric activators of E2s through a non-enzymatic scaffolding function (**Figure 1-1**) (Weber et al., 2019; Zheng and Shabek, 2017).

Once the substrate is ubiquitinated, it can be recognized by a large proteolytic complex known as 26S Proteasome which binds to the ubiquitinated substrates and degrades them inside the central channel (Bassermann et al., 2014; Heride et al., 2014; Pastore, 2010). Ubiquitin signaling does not only regulate proteolysis as a major outcome but also regulate protein-protein interactions, activity and localization in signaling pathways. Polyubiquitination can have different linkages through one of the different lysine residues of ubiquitin, or the N-terminal amino group (M1, K6, K11, K27, K29, K33, K48, and K63) (Ikeda and Dikic, 2008; Kim et al., 2009). The classical view of the function of polyubiquitination is that specific linkages target protein for degradation. However, specific ubiquitination linkage types do not definitively lead to degradation; they may have other non-proteolytic functions such as regulation of transcriptional activity and the activation of the ubiquitin selective chaperone (Kaiser P et al., 2000; Jentsch S et al., 2007). Since all types of linkages, including branched ones, are possible, this can offer countless possibilities (Castaneda et al., 2016; Kim et al., 2007; Komander and Rape, 2012). There are a large number of E3 ubiquitin ligases (more than 800 in human cells) that create the specificity in this PTM pathway through specific substrate recognition.

Recognition of target proteins by E3s is achieved through a minimal element within a protein sequence called a degron. Most known degrons are embedded as SLiMs within the IDRs of target proteins. Degrons have been shown to control some important cellular functions, such as monitoring cellular hypoxia (via the ubiquitin regulated HIF1 transcription factors), and cell cycle progression (Davey and Morgan, 2016; Van Roey et al., 2014). However, despite the large number of E3 ubiquitin ligases known, the majority of them have poorly defined target degrons. One of the best known E3 ligase-degron recognition modules is that of the APC/C with its mitotic targets.

1.2.1.1 Ubiquitin-dependent proteolysis in mitosis

Whereas the activation of CDK1 and other mitosis-specific protein kinases are required for chromosome condensation, spindle assembly and organelle fragmentation in early events of mitosis, the subsequent activation of ubiquitin-dependent 26S Proteasome-mediated

destruction is required to achieve the separation of sister chromatids and the events of mitotic exit (Prosser and Pelletier, 2017; Rousseau and Bertolotti, 2018; Strzyz, 2018). Mitotic cyclin proteolysis is the major mechanism for the inactivation of CDK1. Securin, an inhibitor of sister chromatid separation, is one of the most prominent key regulators of chromosome segregation. It was initially identified in fission yeast (Cohen-Fix et al., 1996; Funabiki et al., 1996; Holloway et al., 1993; Yamamoto et al., 1996). Simultaneous degradation of securin, the inhibitor of the Separase enzyme, allows activation of Separase activity to cleave the Cohesin protein that holds the sister chromatids together at metaphase. Inactivation of mitotic cyclin and destruction of securin are thus the two events required for anaphase entry. More recent studies have revealed that proteolysis of other substrates regulates events that follow anaphase entry, including the disassembly of the central spindle, chromosome decondensation, and reformation of the nuclear membrane. The earlier genetic studies in budding yeast had identified a number of subunits of a complex essential for metaphase/anaphase transition (i.e. for degrading mitotic cyclin and securin) and called it the APC/C. The APC/C was finally purified in 1996 and was shown to be a complex of at least 14 subunits, including recognizable components of an E3 ligase such as the APC2 ‘cullin’ and APC11 ‘Ring Finger’ subunits (Peters, 2006; Pines, 2011)

1.2.2 Anaphase-Promoting Complex/Cyclosome (APC/C)

APC/C is an E3 ubiquitin ligase that catalyzes the attachment of ubiquitin onto the substrate proteins during the cell cycle (Thornton and Toczyski, 2006). Cdc20 and Cdh1 (FZR1) are the two co-activators of APC/C and are required both to activate it and to allow it to bind to substrates (He et al., 2013). APC/C activity is controlled by the MCC, which sequesters Cdc20. Once all the kinetochores on every pair of chromosomes are properly captured by the mitotic spindle, Cdc20 is released from the MCC (Di Fiore et al., 2016) and APC/C interacts with its activator Cdc20. The APC/C-Cdc20 complex targets cyclin B1 and Securin during metaphase to promote the onset of anaphase. After anaphase onset, APC/C-Cdc20 targets a large number of additional substrates, and APC/C-FZR1 (inhibited under conditions of high CDK1 activity) also becomes active. APC/C-FZR1 specifically degrades Aurora kinases, and Cdc6 early in mitotic exit, and then takes over to target all other APC/C substrates, including Cdc20, in G1 phase (Burton and Solomon, 2001; Kraft et al., 2005; Wasch et al., 2010). This mode of regulation ensures the precise timing of APC/C activation and degradation of its target proteins. APC/C can recognize its target substrates through a composite receptor between APC3, APC10, and Cdc20 or FZR1 (Chang et al., 2015) (**Figure 1-2**). These APC/C regulatory subunits form

a binding pocket, facilitating the interaction of the complex with degrons. In general, there are five types of degrons that have been identified by their role in substrate degradation: the destruction box (D-box), the KEN box, CRY box, A-box, and the ABBA motif. The D-box and KEN motifs are common to most substrates. CRY box was identified in cdc20, A-box in AURKA while ABBA motif was found in cyclin A (Davey and Morgan, 2016). The D-box, KEN, and ABBA motifs have been shown to provide high complementarity to the core-motif binding pockets on the APC/C complex. Recognition of the substrates by the APC/C E3 ligase does not require phosphorylation on the target substrate, unlike other E3 ubiquitin ligases (Barford, 2011). In some cases, phosphorylation has been shown to block the degradation of the target protein.

The orderly return to interphase is coordinated by the sequential degradation of at least 200 substrates, all coordinated by the APC/C. Sequential degradation is thought to be achieved by differences in the timing of substrate ubiquitination, and in the number, linkage type and topology of the ubiquitin chains added to substrates. Recent work has shown that the APC/C promotes efficient degradation of substrates by recruiting 2 different E2 enzymes: UBE2C and Ube2S (Ye and Rape, 2009). The first ubiquitin chain is added to the target substrate by UBE2C ("priming"). E2 enzyme Ube2S directs the synthesis of ubiquitin conjugates to the substrates linked through lysine 11 (k11) rather than the conventional k48-linked degradation signal to the substrates (Lindon et al., 2015; Min et al., 2015). One important substrate of the APC/C-FZR1 at this time is AURKA.

1.3 Aurora kinase family

Aurora kinases are serine/threonine kinases essential for the accuracy of mitosis. The Aurora kinase family is composed of three members in vertebrates: Aurora-A (AURKA), Aurora B (AURKB), and Aurora C (AURKC). There are two types in the *Xenopus*, *Drosophila and C. elegans* (the A- and B-types), and only one in budding yeast (Ipl1) and fission yeast (Ark1). Because the kinases were recognized separately many times in independent studies, their nomenclature early on was widely variable. Therefore, scientists agreed to designate the family members' names as AURKA, AURKB, and AURKC (Andresson and Ruderman, 1998; Paris and Philippe, 1990; Roghi et al., 1998).

In somatic cells, Aurora kinases activities peak in parallel to the protein level in mitosis and then drop dramatically at mitotic exit. Aurora kinase genes are frequently amplified or

overexpressed in cancer cells. Moreover, overexpression of all Aurora kinases interferes with mitotic progression (Carmena and Earnshaw, 2003; Willems et al., 2018). Detailed analysis of the structures of Aurora kinases indicates that they are composed of the C-terminal globular, catalytic domain, and an N-terminal IDR. The C-terminal catalytic domain shows only small differences in sequence, and yet we still have an incomplete understanding of how these variations may be important functionally. The N-terminal domains vary in size and amino acid sequence. AURKA possesses the longest IDR among the Aurora kinases proteins (Cheetham et al., 2002; Richards et al., 2016) and AURKC has the shortest. Aurora kinases have similar substrate specificity but have different functions according to their subcellular location (Seeling et al., 2017).

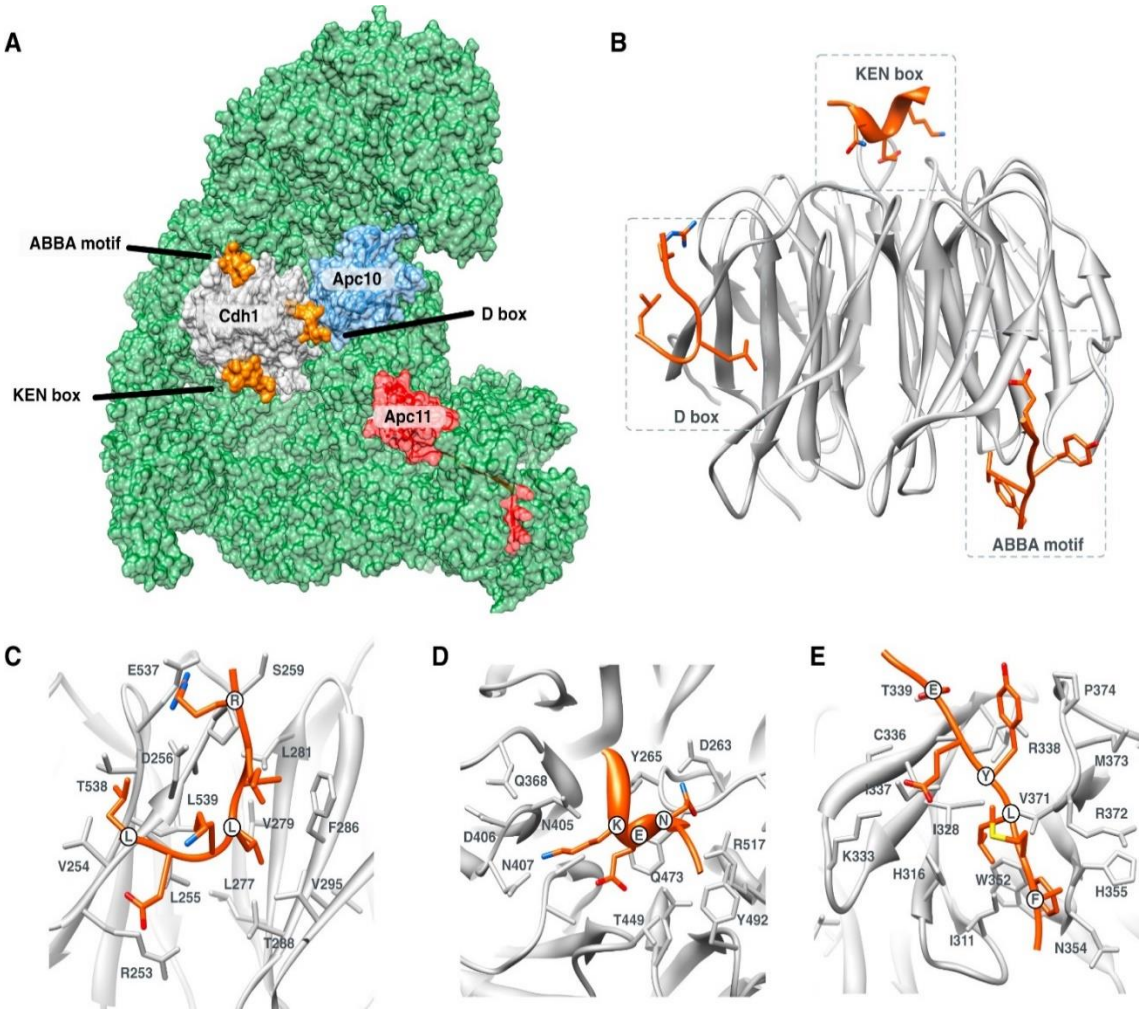

Figure 1-2 WD40 domain structure and the specificity of degrons receptors in FZR1. A) the FZR1/Cdh1(gray) is shown together with APC/C subunits (green) including Apc10 subunit (blue), the Apc11 RING subunit (red) (He et al., 2013; Chang et al., 2015). FZR1 receptors are also shown in orange. B) FZR1 receptors interact with at least three binding motifs: D box, KEN box, and ABBA C) The D box receptor binds its ligand. (D) The KEN receptor binds its

ligand. (E) The ABBA receptor binds its ligand. This figure is taken from (Davey and Morgan, 2016).

AURKA plays an important role in controlling the entry and progression into mitosis through setting up the mitotic spindle and reorganizing spindle microtubules for central spindle assembly at mitotic exit (Barr and Gergely, 2007; Courtheoux et al., 2018). Studies have shown that AURKA may have additional, non-mitotic roles, specifically with regards to the cytoplasmic organization of eukaryotic cells (Mahankali et al., 2015). On the other hand, AURKB is known to be localized with chromosome arms, and it relocalizes to the microtubules of the central spindle at anaphase (Kelly et al., 2007). AURKB is a part of the chromosomal passenger complex proteins (CPC) that consists of four proteins: AURKB, inner centromere protein (INCENP), borealin, and survivin (Vader et al., 2006). They are required to maintain chromosome segregation and cytokinesis (Bertran-Alamillo et al., 2019). Cells that have been deprived of AURKB activity by siRNA-mediated knockdown have a markedly increased polyploidy. During late cytokinesis, AURKB phosphorylates and activates RACGAP1 which activates GAP activity toward RhoA, a protein needed for the execution of cytokinesis (Carmena et al., 2009; Carmena et al., 2012; Ma and Poon, 2011; Sessa et al., 2005). AURKC was found to localize to the centromere in spermatocytes and oocytes and is thought to play a similar role to AURKB during meiosis (Kimmins et al., 2007; Quartuccio and Schindler, 2015).

1.4 AURKA

AURKA is a major mitotic serine/threonine kinase responsible for centrosome maturation, bipolar spindle, and robust central spindle assembly at anaphase. It also has a number of reported interphase roles, including cilia disassembly, regulation of mitochondrial morphology, stabilization of the Myc family of TFs (Asteriti et al., 2015; Grant et al., 2018; Hannak et al., 2001; Korobeynikov et al., 2017; Schumacher et al., 1998). AURKA has been detected in the late S phase at the centrosome, and expression levels subsequently increase in the G2-M phase. Photobleaching experiments reveal that centrosome associated AURKA is rapidly exchanging with cytoplasmic AURKA. The amount and the activity of AURKA increase at the centrosome, after which, at prophase, a fraction of the total active AURKA moves to the nucleus, coincident with chromatin condensation (Hegarat et al., 2011; Lioutas and Vernos, 2013; Reboutier et al., 2013). During metaphase, AURKA is observed at both spindle poles and on the bipolar spindle. During anaphase, the chromosomes move apart, and the spindle begins to disassemble which coincides with the degradation of AURKA by APC/C-FZR1 (Floyd et al., 2008; Lindon et al.,

2015). In telophase, only a small fraction can be seen in the centrosome and spindles. During cytokinesis and telophase, AURKA levels are further decreased in parallel to the kinase activity (Barr and Gergely, 2007) (**Figure 1-3**).

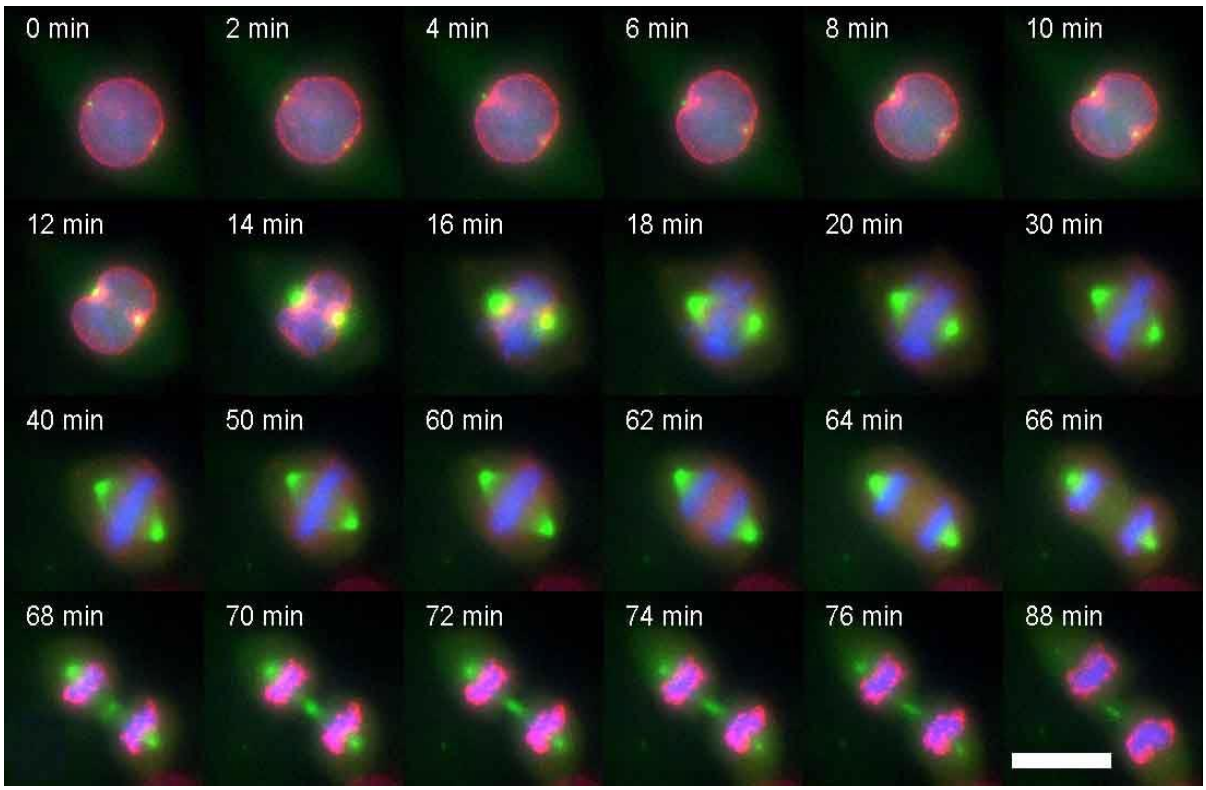

Figure 1-3 Molecular behavior of GFP-AURKA throughout mitosis in a human MDA-435 cell line. Time-lapse images were captured at 2 min intervals of cell expressing CFP-histone H3, GFP-Aurora-A and DsRed-importin Bar: 10 μM. This figure is taken from (Sugimoto et al., 2002).

1.4.1 Regulation of AURKA activity in Mitosis

AURKA is a member of the AGC subfamily of serine/threonine kinase. AGC kinases contain a specific hydrophobic pocket on the N-lobe between the β -sheet and the C-helix called the PIF pocket. The active conformation of AGC kinases is generally induced by the movement of a hydrophobic (HF) motif within the C-lobe that docks into the PIF pocket (Bayliss et al., 2017).

The active conformational changes of many AGC kinases are also stabilized by phosphorylation in their activation loop or in the catalytic domain (Bayliss et al., 2003; Eyers et al., 2003; Tsai et al., 2003). Unlike other AGC kinases, AURKA lacks the N- and C-terminal extensions. Crystal structure studies revealed that the binding partner TPX2 interacts and

activates AURKA. The association of the binding partner provides AURKA with the HF motif and F/W side chains that increases the kinase activity (Bayliss et al., 2017; Bayliss et al., 2003; Giubettini et al., 2011; Kufer et al., 2002) (**Figure 1-4**).

The stimulatory phosphorylation has a clear impact on AURKA activity and functions. Mass spectroscopy shows that there are four major phosphorylation sites of Xenopus AURKA in metaphase: S53, T294, T295, and S349 (equivalent to S51, T287, T288 and S342 in human AURKA). S349A mutation does not seem to affect AURKA activity significantly, whereas the S349D inhibits its kinase activity (Littlepage et al., 2002). On the other hand, T288 autophosphorylation is identified as one of the key regulatory mechanisms for AURKA activation at different subcellular locations and in mitosis (**Figure 1-5**). However, the mechanism of autophosphorylation remains unclear. Phosphorylation of two threonine residues within the activation loop of the kinase, T287, and T288, induces a conformational change in the kinase domain and results in changes in the kinase activity (Rowan et al., 2013; Shagisultanova et al., 2015).

A number of studies suggest that other phosphorylation sites modulate AURKA activity and stability. For example, phosphorylation by Glycogen synthase kinase 3 β (GSK3 β) at residue S342 suppresses the activity of AURKA through the downregulation of T288 phosphorylation (Lee et al., 2013). The interaction between AURKA and its binding partner Nucleophosmin does not cause autophosphorylation at T288 as expected but instead induces the kinase activity through autophosphorylation at S89, a conserved serine residue in the N-terminal disordered region (Reboutier et al., 2012). Moreover, Ajuba binds to the N-terminal domain of AURKA at the centrosome and induces its activation by autophosphorylation at T288 (Hirota et al., 2003).

S51 has been shown in several studies to be a bona fide phosphorylation site and phosphor-mimic mutation of this site blocks AURKA degradation completely (Ferrari et al., 2005). S51/L in AURKA gene was detected as a cancer-associated mutation at the COSMIC database (Forbes SA et al., 2011). PP2A has been identified as a functional phosphatase at this site (Horn et al., 2007). Interestingly, Calmodulin physically interacts with AURKA via the pS51 version of the A-box and causes its activation by inducing autophosphorylation at T288 (Plotnikova et al., 2012). By contrast, inactivation of AURKA involves dephosphorylation by phosphatase 1 (PP1) and PP6 in cells and extracts (Katayama et al., 2001; Kettenbach et al., 2018; Zorba et al., 2014). These observations suggest that there is a complex regulatory network along with

T288 phosphoregulation responsible for forming a fully active conformation of AURKA, and we do not yet fully understand how full AURKA activity is reached, and how much residual activity it has outside of mitosis.

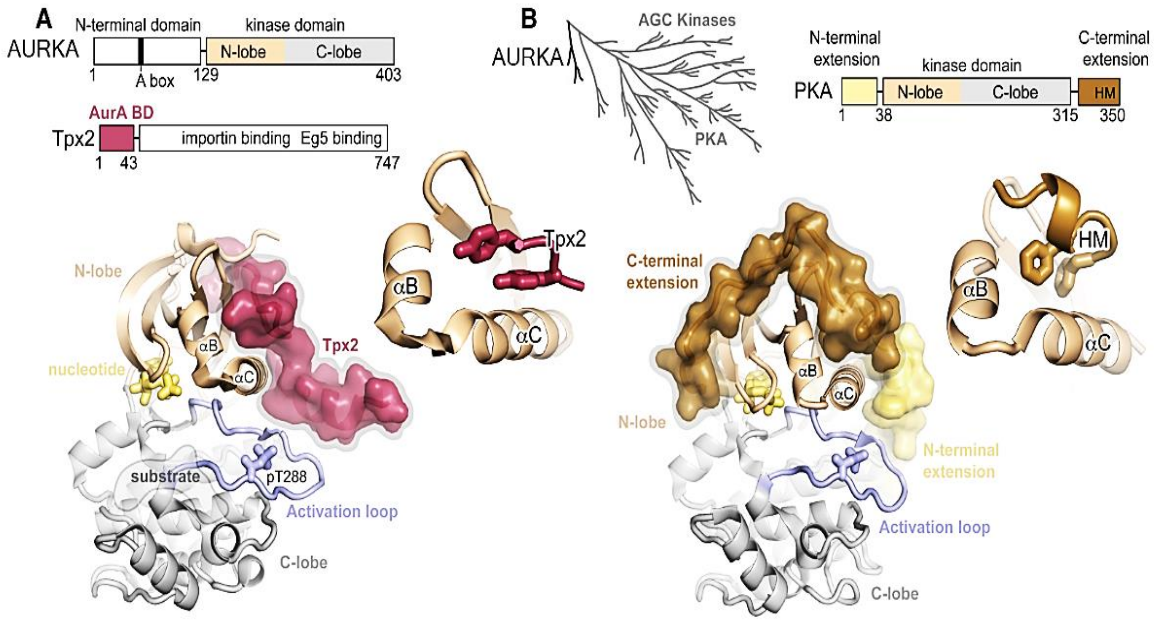

Figure 1-4 AURKA and the AGC-family kinases share a common regulatory architecture. A) Top: AURKA and TPX2 domains are shown, including the N-terminal disorder region and kinase domain of AURKA, and the AURKA -binding domain (AURKA BD) of TPX2. The kinase domain of AURKA is composed of the N-lobe and C-lobe. The location of the A-box in the N-terminal domain of AURKA, which targets the kinase for destruction, is also shown. Bottom: X-ray structure of the AURKA kinase domain bound to residues 1-43 of human TPX2 (PDB ID: 1OL5). The N-lobe and C-lobe are shown in beige and gray, respectively, the activation loop in blue and TPX2 in magenta. The inset shows an expanded view of the docking site of TPX2 on the N-lobe. B) Top: A phylogenetic tree illustrating the relationship of the Aurora kinases to the AGC kinase family is shown on the left, and the domain architecture of the AGC kinase PKA is shown on the right. Bottom: Structure of PKA (PDB ID: 1L3R) with the C-terminal tail containing the HM colored brown, the N-terminal extension colored yellow, and the remainder of the kinase domain colored as in (A). The inset shows the docking of the HM to the PIF pocket of the kinase. This figure adapted from ref (Levinson, 2018).

1.4.2 Binding partners of AURKA

AURKA activity is regulated by binding with different proteins such as the microtubule-associated protein (MAP) TPX2, Phosphatase inhibitor-2, mitotic spindle-associated TACC3, the centrosomal protein Cep192, the ciliary protein Pifo and the transcription factor N-Myc (Dodson and Bayliss, 2012; Levinson, 2018; Ruff et al., 2018; Zorba et al., 2014). These

regulatory binding partners stimulate AURKA activity by binding and stimulating autophosphorylation.

`

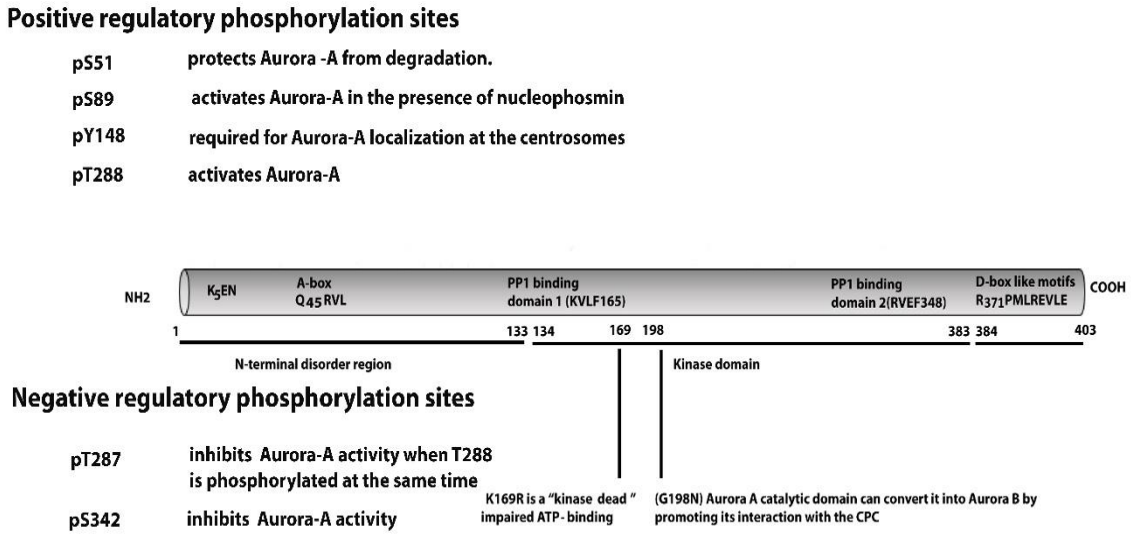

Figure 1-5 Phosphorylation sites and motifs within AURKA protein sequence. Ca2+/calmodulin binds to AURKA and induces its autophosphorylation at S51, S53, S66, and S98. Nucleophosmin (NPM) binds to N-terminal AURKA and induces the kinase activity through autophosphorylation at S89. Phosphorylation by GSK3 at S342 residue suppresses the activity of AURKA. Atypical protein kinase C (aPKC) phosphorylates AURKA at T287 and induces the kinase activity of AURKA. Serine/threonine-protein kinase (PAK 1) phosphorylates at T288 and S342. S4, and S41 have been reported to be phosphorylated in vivo. N-terminal domain of AURKA (amino acids 1-133) contains two important degrons, KEN box and A-box. C-terminal domain of AURKA (amino acids 134-383) contains two Protein Phosphatase 1 (PP1) binding motifs and D-box like motifs. C-terminal tail (384-403) is a disordered region.

The best characterised of all of these partner proteins is TPX2. It is a well-known interactor, controls AURKA localization, activation, and stability during mitosis (Giubettini et al., 2011). Activation of AURKA by TPX2 does not require phosphorylation, as it stimulates activity even when T288 is mutated to a non-phosphorylatable residue. This is important because PP6 has been reported to interact with the AURKA-TPX2 complex to maintain the hypoactive form of AURKA activity at the spindle. *In vitro*, binding with TPX2 and autophosphorylation act synergistically to produce a hyperactive form of the kinase. Moreover, TPX2 also protects pT288 by favoring movement of the phosphorylated residue to an inaccessible position that cannot be reached by PP1 phosphatase (Bayliss et al., 2003; Giubettini et al., 2011; Kufer et al., 2002). TPX2 expression level is low but detectable during G1 phase, rising in S phase until it

reaches its maximum level in mitosis. TPX2 in association with AURKA provides a major MT nucleation activity for mitotic spindle assembly. In interphase, importin-α bindsTPX2. During prophase, local generation of a Ran-GTP gradient in the proximity of the chromosome induces the dissociation of TPX2 from the importin alpha complex (Tsai et al., 2003). Therefore, TPX2 becomes available to bind and activate AURKA which then targets it to the mitotic spindle. However, it remains unclear whether TPX2 degradation or dissociation contributes to AURKA inactivation at mitotic exit. At mitotic exit, TPX2 levels decrease due to its degradation by APC/C. There is evidence that TPX2 protects Aurora-A from protein degradation, helping to regulate the intracellular levels and the activity of the protein at mitosis (Giubettini et al., 2011).

1.4.3 Ubiquitin-mediated proteolysis of AURKA

In most cell types, AURKA activity is regulated by phosphorylation, interaction with a binding partner, or degradation. Degradation of AURKA is mediated by the ubiquitin-proteasome system in a manner that depends on the APC/C-FZR1 (Clijsters et al., 2013; Floyd et al., 2008; Min et al., 2015). AURKA ubiquitination and degradation are directed by the accessible orientation of its degrons in co-operation with phosphorylation events, interaction with binding partners, or both (Castro et al., 2002; Floyd et al., 2008; Littlepage and Ruderman, 2002; Taguchi et al., 2002). A number of studies of AURKA degradation have identified putative degrons, two of them in the N-terminal IDR, where analysis of evolutionary sequence conservation identifies them as SLiMs. The SLiMs in AURKA IDR are around a KEN motif at K5 and the ‘A-box’ (centered on Q45RVL), both of which are identified as degrons (**Figure 1-6**). Cell-based assays revealed that KEN box lysine K5 was ubiquitinated at mitotic exit (Lindon et al., 2015). Considering that KEN-box is not present in the *Drosophila melanogaster* or the *Caenorhabditis elegans* homologues, this indicates that KEN box is less likely to control AURKA degradation, but they may be a site for ubiquitination. These observations suggest that there could be additional degradation signal motifs that ensure a proper time of degradation.

AURKA has been found to contain D-box like motifs within the C-terminal domain. The effect of D-box like motifs on AURKA degradation is quite contradictory. It has been reported that the ubiquitination level in AURKA D-box like motif mutants was significantly lower than wild-type AURKA, whereas the degradation was similar to the wild-type (Honda et al., 2000). This observation suggests that AURKA D-box like motifs could be a signal for ubiquitination, not for the degradation of AURKA. Degrons normally reside in IDRs, therefore, it would be less likely for AURKA D-box inside a globular domain to be functional. However, the double

point mutation in (D-box like motif) R371xxL374 interfered with the degradation of AURKA *in vitro* (Arlot-Bonnemains et al., 2001; Castro et al., 2002). *In vivo* assessment of D-Box's role is still problematic because the double point mutation of D-box R371AxxL374A in human AURKA abrogates its localization in all mitotic structures which can be argued as misfolding of AURKA (**Supplementary figure B-1**).

Interestingly, a chimera between the disordered N-terminal domain of AURKA and the kinase domain of AURKB is degraded in the same way as AURKA (Chiara Marcozzi, Master's Thesis 2012), which indicates that the degrons required for efficient degradation of AURKA are located in the N-terminal IDR. Indeed, the major degron in this region was identified and named the A-Box by Joan Ruderman's lab (Littlepage and Ruderman, 2002). S51, which is phosphorylated in mitosis, may block AURKA destruction until late mitotic exit. Two possibilities have been postulated to explain the function of A-box. First, the A-box could contribute directly to recruit AURKA to the APC/C. Second, the A-box could modify the three-dimensional conformation of AURKA to interact with FZR1 through its D-box (the D-box Activating Domain or 'DAD' hypothesis) (Castro 2002). Interestingly, the same A-box motif has been reported to bind with calmodulin for activation (Plotnikova et al., 2010). These observations suggest that both degradation and activation of AURKA can be achieved through the A-box and raises the question of whether AURKA activation and degradation are competing processes.

1.5 The role of AURKA in centrosome function

The accuracy of chromosome segregation requires accurate duplication, maturation, separation, and positioning of centrosomes. The centrosome is a microtubule-organizing center in mammals, consists of two centrioles, and surrounded by pericentriolar material (PCM) including the γ-tubulin and other microtubule regulators. The onset of duplication of centrioles occurs in the G1/S transition. During G2/M, the centrosomes are separated and migrate to opposite poles. In mitotic cells, PCM accumulates around centrosomes five-fold more than interphase cells. This process of PCM recruitment to the centrosome is called centrosome maturation. Inhibition of AURKA interferes with centrosome maturation. Studies in several systems have shown that AURKA is a key player for centrosome maturation (Mahen and Venkitaraman, 2012; Palazzo et al., 2000). AURKA localization at the centrosome is mainly dependent on Centrosomal protein 192 (Cep192) in vertebrates (Joukov et al., 2010). At the

centrosome, AURKA promotes spindle assembly via phosphorylating and recruiting several key players including γ-tubulin, CKAP5, TACC3, LATS2, and kinesin-like protein KIF11 to stabilize microtubules (Toji et al., 2004). AURKA function is not limited to centrosomes. The fact that the AURKA phosphorylates histone H3 on T118 residue during mitosis provides some indication of the chromatin-related functions (Wike et al., 2016).

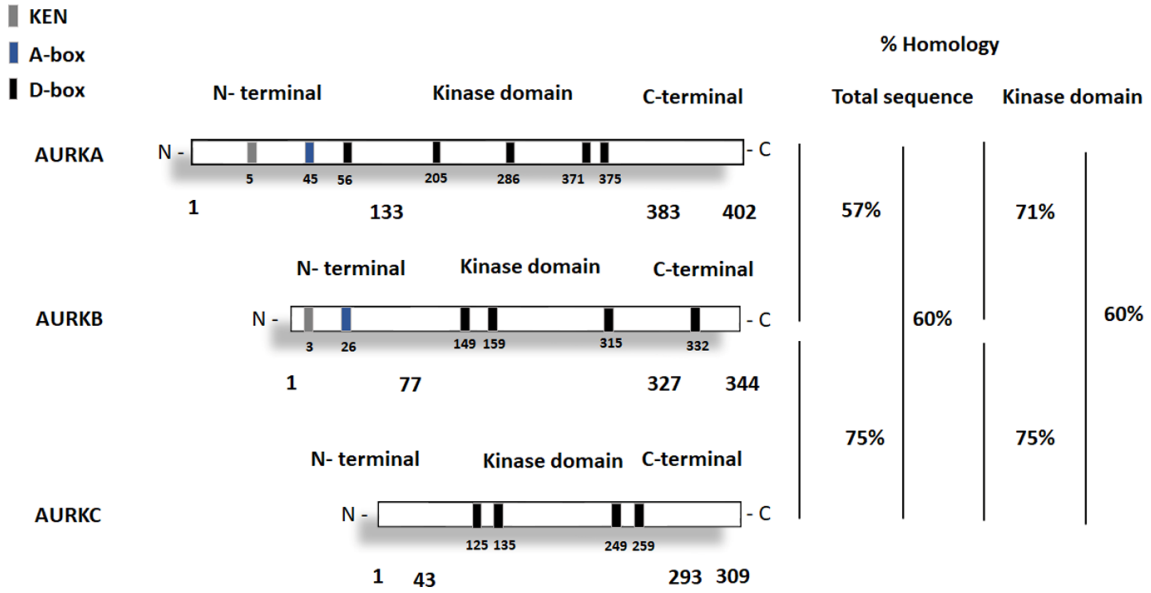

Figure 1-6 Structure of Aurora kinase domains. Schematic representation of the structure of three Aurora family members. Aurora kinases are composed of the N-terminal domain and the C-terminal domain. The percentages show the similarities in amino acid sequences between Aurora-A, Aurora-B and Aurora-C. AURKA, and AURKB contain D-box like motifs, a KEN motif, and an A-box motif that are important protein degradation at the end of mitosis (Willems et al., 2018).

1.6 AURKA and mitotic entry

Cells enter mitosis by the action of kinases and phosphatases. AURKA mediates the timing of mitotic entry via promoting CDK1 activation (De Souza et al., 2000; Jackman et al., 2003). The most important way of achieving this regulation depends upon controlling the activity of PLK1 and polyadenylation-dependent translation of specific mRNAs. During G2, AURKA and Bora form complexes that activate PLK1 kinase by phosphorylating the active T-loop at T210 (Chan et al., 2008; Seki et al., 2008). After that, active PLK1 begins to prepare for the activation of CDK1/cyclin B by promoting the destruction of the CDK-inhibitory kinase WEE1, and by activating phosphatase CDC25C, thereby allowing cells to enter mitosis (Dutertre et al., 2004; van Vugt et al., 2004). Moreover, active PLK1 kinase also appears to protect AURKA from the action of PP6, which creates a feedback loop that allowing AURKA and PLK1 to reach their

maximal activities during mitosis (Kettenbach et al., 2018). AURKA has been shown to regulate translational targets such as mos and cyclin B mRNAs in Xenopus and mouse oocytes. In oocytes, AURKA specifically phosphorylates polyadenylation element (CPEB) on S174 that induces cyclin-B1 mRNA polyadenylation and translation (Cao and Richter, 2002; Groisman et al., 2000; Groisman et al., 2002; Mendez et al., 2000). However, this important role of AURKA has not yet been revealed in somatic cells.

1.7 AURKA role in interphase

Although AURKA was first identified as a regulator of mitosis, it has become clear in recent years that it is also present in interphase and is responsible for a number of important non-mitotic functions (Mahankali et al., 2015; Shagisultanova et al., 2015) (**Figure 1-7**). It is thought that these functions may be relevant to the persistent association of AURKA amplification, overexpression or misregulation with cancer. However, the regulation of AURKA activity in interphase cells remains poorly understood.

1.7.1 Cilia / flagellar disassembly

The role of AURKA in flagellar disassembly was first described by Junmin Pan and William Snell using Chlamydomonas as a model (Pan and Snell, 2000). In AURKA-depleted cells, cells retain their flagella, even after they have passed to a pH shock (Snell et al., 2004). This observation suggests that the flagella disassembly system is likely to be disrupted by the depletion of AURKA. Therefore, active AURKA is a part of the flagella disassembly system and a marker for flagella length (Luo et al., 2011). Moreover, recent studies have revealed an interesting biological function of AURKA that appears to be involved in controlling primary cilia disassembly in mammals. Overexpression of AURKA causes cilia resorption at G1 in human cells. However, inactive mutant AURKA could not cause deciliation which suggests that this function depends on AURKA kinase activity (Plotnikova et al., 2012; Pugacheva et al., 2007). An important inducer of AURKA activation in the basal body is HEF1. The kinase activity has been reported to increase rapidly by binding to its co-activator HEF1 in the basal body after adding a serum to quiescent cells (Pugacheva et al., 2007). This interaction in response to extracellular cues leads to cilia disassembly in G0/G1. Modulation of the active state of AURKA in the mother centriole by its binding partner enables the kinase enzyme to interact with an effector protein HDAC6 and phosphorylate it on serine and threonine residues

to evoke the cilia disassembly response through deacetylation of axonemal microtubules (Kozyreva et al., 2014). Ciliary defects can lead to human diseases such as polycystic kidney disease (PKD), and nephronophthisis. In the future, it will be important to determine whether non-degradable AURKA inhibits cilia formation.

1.7.2 Mitochondrial fragmentation

Mitochondria are cytoplasmic organelles that produce a cell's energy. They undergo fission and fusion throughout the cell cycle. Previous reports have shown that the number of mitochondria changes during the cell cycle stages. The number of mitochondria in mitosis increases to twice that in the G1 phase. In the early G1 phase, mitochondrial fusion reduces the mitochondrial number to 50% compared to the number present at mitosis. During the transition from G2 to M phase, mitochondrial fission leads to an increase in the number of mitochondria (Arnoult, 2007; Zorov et al., 2019). Nishida and colleagues revealed, using high-resolution imaging, that mitotic spindles and mitochondria are associated together during mitosis, indicating there is a relationship between mitochondrial segregation and mitosis (Nishida et al., 2005).

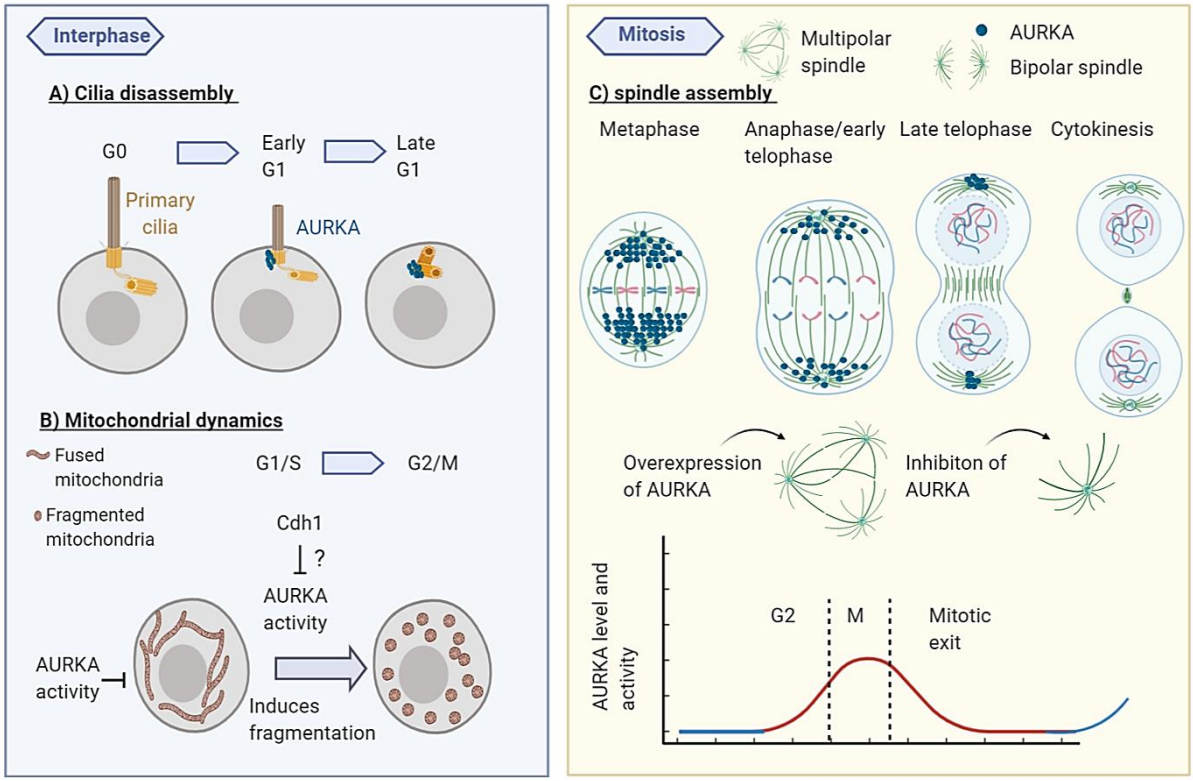

Figure 1-7 Aurora-A kinase functions in interphase and mitosis. A) During early/late G1, AURKA begins to accumulate significantly at centrosomes and induces cilia disassembly. B) Cytoplasmic AURKA is associated with mitochondria and promotes mitochondrial fragmentation. C) During mitosis, AURKA promotes bipolar spindle assembly, and its activity drops at the mitotic exit. Overexpression of AURKA leads to multipolar spindle defects while its inhibition causes the formation of monopolar spindle.

In early mitosis, mitochondria are fragmented into smaller subunits that are equally distributed into each daughter cell. Active DRP1 plays a major role in regulating the mitochondrial fragmentation process. The mitotic kinase CDK1/cyclin B directly phosphorylates DRP1 at a conserved serine S616 to activate it to trigger mitochondrial fragmentation. During mitosis, AURKA acts as an upstream regulator to direct the activity of CDK1/cyclin B onto DRP1 (Bertolin et al., 2018; Grant et al., 2018; Kashatus et al., 2011). AURKA has also been shown to localize at mitochondria to control the mitochondrial fragmentation effect and enhance ATP production. The relationship between AURKA and mitochondria may be one of the mechanisms that facilitate the association between the over-activity of AURKA and transformed cells (Dutertre et al., 2002), though the details of this mechanism remain to be fully explicated.

1.8 AURKA oncogenic activity

AURKA is a clinically important oncogene. Several reports showed that 40 % of breast cancer cell lines, 18% of primary breast tumours, and 52% of primary colorectal tumours were associated with gene amplification leading to a significant increase in both mRNA transcript and protein (Katsha et al., 2015), whereas in gastric cancers only 5% of the cases were detected to be associated with gene amplification (Hu et al., 2005; Zhou et al., 1998). In other types of cancer, however, the upregulation of AURKA mRNA and proteins are much more frequent than gene amplification. For example, *AURKA* gene amplification in hepatocellular carcinomas (HCCs) is 3%, while 60% of HCCs with overexpressed AURKA mRNA and protein (Jeng et al., 2004). These data suggest that there is a change in expression or stability of the protein, that can contribute to cancer initiation or progression.

It has been proposed that AURKA overexpression requires the upregulation of activator factors for its oncogenic potential. The TPX2/AURKA complex seems to form an oncogenic holoenzyme since the activation and spindle localisation of AURKA require its binding to its regulator TPX2. Co-expression of TPX2 may be a way for activating and protecting AURKA from degradation in tumors, contributing to extra AURKA activity after 20q amplification because AURKA and TPX2 are found at the chromosome 20 (Asteriti et al., 2010; Chang et al., 2017; Shah et al., 2019).

Abnormal expression or activation of AURKA can result in unusual chromosomal aberrations. These chromosomal aberrations can be a consequence of errors in spindle formation, chromosome alignment, or failure of kinetochores to capture free microtubule ends (Giet et al., 2005; Lassus et al., 2011). Moreover, inhibition of AURKA leads to loss of the SAC, even in the presence of microtubule destabilizing or stabilizing drugs (nocodazole/ Taxol) (Courtheoux et al., 2018; Wysong et al., 2009). When AURKA was overexpressed, MAD2 staining remained attached to the kinetochores even after anaphase onset indicating that overexpression of AURKA can bypass SAC controls (Yang et al., 2005). However, errors in chromosome segregation are not necessarily enough to provoke uncontrolled proliferation.

1.9 Checkpoint disruption and chromosomal instability

DNA damage during G2 delays entry into mitosis through activation of the ATM checkpoint kinase and blocks the activation of cyclin B/CDK1. However, forced

overexpression of AURKA has been found to override the G2 checkpoint and allows cells with damaged DNA to enter mitosis (Marumoto et al., 2002). This result indicates that AURKA plays a role in G2/M checkpoint control.

An additional level of complexity comes from the distinct collaboration between AURKA and tumor suppressors or oncogenes such as P53 and N-Myc that might contribute to tumorigenesis. P53 is a tumor suppressor protein that is essential for protecting genomic stability in response to the DNA damage and aberrant oncogene activation. It acts as a transcription factor that regulates several target genes, thereby causing cell cycle arrest and protecting against transformation (Zilfou and Lowe, 2009). Knockdown of P53 results in centrosomal amplification and spindle defects in living cells (Bischoff et al., 1998; Marumoto et al., 2002). Human p53 protein interacts with AURKA and inhibits its kinase activity. AURKA also appears able to phosphorylate p53 at serine S315 to mediate its recognition by MDM2 for ubiquitination and degradation (Katayama et al., 2004; Sasai et al., 2016). These data suggest that P53 is negatively regulated in AURKA-overexpressing cells, resulting in the disruption of DNA damage checkpoint and the trigger of apoptotic responses. Characterising the regions that are required for the interactions with AURKA, and the exact mechanism by which p53 suppresses AURKA activity are important questions.

N-Myc is a growth-promoting transcription factor that localizes in the nucleus and binds E-box DNA sequences. The oncogenic activity of N-Myc deregulates the cancer transcriptome, proteome, and metabolome (Beltran, 2014). The communication between AURKA and N-Myc mediates its oncogenic effect in cancers. N-Myc physically interacts with AURKA; this interaction has been shown to protect N-Myc from destruction by its cognate E3 FBXW7 (Richards et al., 2016). Since developing drugs that directly target N-Myc is very challenging, a new approach has been adopted to disrupt the native conformation of AURKA to cause the degradation of N-Myc protein in N-Myc -driven neuroblastoma (Brockmann et al., 2013; Otto et al., 2009). There is a very large body of literature concerning the regulation and functions of AURKA, and we do not yet have a complete picture of how AURKA is regulated through the cell cycle via its different modes of activation, and how deregulation of AURKA stability and activity contribute to the cancer phenotypes. Unveiling the regulation of AURKA activity within the cell, therefore, provides critical insight into the oncogenic activity of AURKA and the design of therapeutic drugs for cancer treatment.

1.10 Aims and objectives

Although we have some insight into what is required for the regulated activation of AURKA for mitosis and its destruction during mitotic exit, we are lacking understanding of how activation and destruction are linked to each other to regulate AURKA activity through the whole cell cycle. Fully understanding the regulation will help to develop therapeutics against this target. The overall aim of my project is to discover how the activation and degradation of AURKA are integrated through the SLiMs in the N-terminal IDR. Towards this, the specific objectives of my project were outlined as follow:

- To investigate AURKA degrons within the protein sequence that mediate AURKA degradation and evaluate their contribution to AURKA stability in live, single cells (Chapter 3).
- To address the longstanding question of how degradation and inactivation of AURKA are coupled at mitotic exit, using a novel FRET-based activity probe for AURKA. (Chapter 4).
- To investigate the relative contribution of activity and stability of AURKA on regulating its non-mitotic functions in interphase (mitochondrial dynamics) (Chapter 5).
- To investigate the potential SLiMs located in the N-terminal AURKA and test the hypothesis that Ca2+/Calmodulin signaling can influence AURKA activity and degradation during mitotic exit. (Chapter 6).

Chapter 2 Materials and methods

2.1 Cell culture

Table 2-1: Cell culture reagents and inhibitors.

Name	Company
Dulbecco's modified Eagle's medium	Sigma Aldrich St. Louis
RPMI-1640	Sigma Aldrich St. Louis
DMEM/F-12	Calbiochem, San Diego, CA
Hank's balanced salt solution (HBSS)	Life Technologies
0.05% Trypsin-EDTA	Life Technologies
Leibovitz's, L-15 Medium,	Life Technologies™
0.1 μg/mL cholera toxin	Calbiochem, San Diego, CA
Eight-well plastic-bottom slides	Ibidi GmbH, Martinsried, Germa
Fluorescently labeled secondary antibodies	LI-COR bioscience
NuPAGE gradient gel	Thermo Fisher Scientific Leicestershire, UK
Red CMXRos	Thermo Fisher Scientific Leicestershire, UK
Aurora-A kinase MLN8237 10mM	Millennium Pharmaceuticals
Thapsigargin (THAPSI) 5 μM	Sigma Aldrich St. Louis
Ionomycin 5 μM	Sigma Aldrich St. Louis
Penicillin-Streptomycin (P/S)	Thermo Scientific™
10 μg/mL insulin	Sigma Aldrich St. Louis
0.5 μg/mL hydrocortisone	Sigma Aldrich St. Louis
Calmidazolium (CMZ)	Sigma Aldrich St. Louis

2.2 Cell culture and transfection

The human cancer cell lines U2OS, U2OSFZR1 Knockout, MDA-MB-231, and MDA-MB-157 were cultured in Dulbecco's modified Eagle's medium (Sigma) containing 10% fetal bovine serum (FBS). T47D, BT549, and HCC 1143 were maintained in RPMI-1640 (Sigma-Aldrich; St Louis, MO) supplemented with 10% FBS and 10 μg/mL insulin (Sigma-Aldrich; St Louis, MO). MCF10A was maintained in DMEM/F-12 supplemented with 0.1 μg/mL cholera toxin (Calbiochem; San Diego, CA), 10 μg/mL insulin, 0.5 μg/mL hydrocortisone (Sigma-

Aldrich), 0.02 μg/mL EGF (Upstate Biotechnology; Lake Placid, NY), and 5% horse serum (Invitrogen; Carlsbad, CA). hTERT RPE-1 were cultured in DMEM: F12 medium containing 10% FBS and 0.01 mg/mL hygromycin B. Cells were transfected using electroporation with Neon Transfection System using the following parameters: pulse voltage 1500V, pulse width 10 ms, and 2 pulses total on the transfection device.

2.3 *In vivo* degradation assays

U2OS cells were electroporated with wild type AURKA-Venus and mutants, then seeded at 2×10^4 onto eight-well plastic-bottom slides (Ibidi GmbH, Martinsried, Germany) for time-lapse analyses. Imaging medium was L-15 supplemented with FBS and antibiotics(P/S). Time-lapse imaging was carried out on an Olympus Cell R imaging platform comprised of Olympus IX81 motorized inverted microscope, Orca CCD camera (Hamamatsu Photonics, Japan), motorized stage (Prior Scientific, Cambridge, UK) and 37°C incubation chamber (Solent Scientific, Segensworth, UK). Epifluorescent and DIC images were acquired with 2 × 2 bin using appropriate filter sets and 40× NA 1.3 oil objective, at 2 min intervals. Image sequences were exported as 12-bit tiff files for analysis in ImageJ. Cell images meeting the following requirement were analysed using image J software:

- Cell is expressing the fluorescent protein.
- The cell is not close to another fluorescent object to avoid fluorescence overlap.
- The maximum fluorescence level of the cell is not saturated (maximum pixel value less than 10000)

Fluorescence intensity= area x (mean cell – mean background).

2.4 Folding free energy (ΔΔG) calculation and molecular modeling approach

The AURKA 3D structure (from PDB ID: 1mq4) was mutagenized in silico using the "BuildModel" protocol of the FoldX software suite. Using this protocol, we predicted the change of the folding free energy (ΔΔG) of AURKA upon point mutations of the D-box sequence. Positive ΔΔG values indicate an increase in folding free energy of the mutant form, corresponding to a destabilizing effect of the mutation. Predicted values of ΔΔG values of >

1.84 kcal mol-1 are considered to be highly destabilizing for a protein structure (Studer et al., 2014; Tokuriki et al., 2008).

Using a 3D molecular modeling approach, we examined whether the atypical Q_{45}RVL degron (A-box) might bind a known degron receptor site on FZR1. Employing the FlexPepDock server, we docked the peptide Q_{45}RVLCPSNS into three known peptide binding sites on FZR1, that is, the D-box, KEN, and ABBA sites.

To serve as a control, we also performed similar docking experiments with a series of control peptides: The D-box and KEN-box peptides from AURKA, and panels of known H. Sapiens D-box, KEN-box and ABBA-box motif peptides. The sequences of these peptides were obtained from the SLiMs database (http://slim.icr.ac.uk/apc/index.php?page=instances). The input receptor-peptide complex 3D models for peptide docking on the D-box, KEN, and ABBA binding sites of FZR1 were obtained through homology modeling using the MODELLER program. *S. cerevisiae* Cdh1 (50% sequence identity with human FZR1) was used as a template (PDB ID: 4BH6). The models were submitted to the FlexPepDock server, which carried out a local docking procedure to optimize the receptor-peptide interactions. Scoring of the output receptor-peptide complexes was performed using the Statistically Optimized Atomic Potential Protein-Protein (SOAP-PP) function (Dong et al., 2013). FlexPepDock returns as an output 10 different models for each receptor-peptide complex and the SOAP-PP scores reported in the figures are the average scores of the 10 models of each complex (error bars are standard deviation values). Lower SOAP-PP scores correspond to more stable receptor-peptide binding interfaces.

2.5 Western blot

Cells were lysed in 1% Triton X-100, 150 mM NaCl, 10 mM Tris–HCl at pH 7.5, and EDTA-free protease inhibitor cocktail (Roche)., and PhosSTOP™ inhibitor for phosphatase (Sigma-Aldrich). After 30 min on ice, the lysate was centrifuged at 14,000 rpm (4°C) for 10 min. The amount of proteins was quantified using Bradford measurement of absorbance at 590 nm. For immunoblotting, an equal amount of protein (20 μg) was loaded into SDS-PAGE 4-12% pre-cast gradient gel. Proteins were then transferred to Immobilon-P or Immobilon-FL membranes using the XCell IITM Blot Module according to the manufacturer's instructions. Membranes were blocked in PBS-0.1% Tween-20-5% BSA and processed for immunoblotting with primary antibodies. Primary antibodies for western blot were as follows: AURKA mouse

mAb (1:1000; Clone 4/IAK1; BD Transduction Laboratories), phospho-Aurora A (Thr288)/Aurora B (Thr232)/Aurora C (1:1000; clone D13A11 XP® Rabbit mAb, Cell Signalling), rabbit polyclonal TPX2 antibody (1:1000; Novus Biological), FZR1 mouse mAb (1:50; a gift from T. Hunt and J. Gannon), Cdc20 mouse mAb (1:1000; Santa Cruz sc13162), AURKB rabbit polyclonal antibody (1:1000, Abcam ab2254), mouse monoclonal CyclinB1 (1:1000, BD 554177), DRP1 rabbit polyclonal (1:500, Bethyl lab), rabbit polyclonal Tubulin (1:2000; Abcam ab6046), mouse mAb anti-Vinculin (1:1000; clone hVIN-1; Sigma-Aldrich), rabbit anti-GFP (1:1000; 11814460001; Roche). After washing with TBS-T three times, the membranes were incubated with a secondary antibody. Secondary antibodies used were HRP-conjugated, or IRDye® 680RD- or 800CW-conjugated at 1:1,000 dilution for quantitative fluorescence measurements on an Odyssey® Fc Dual-Mode Imaging System (LICOR Biosciences). Quantitative immunoblotting was carried out using IRDye® 680RD and 800CW fluorescent secondary antibodies scanned on an Odyssey® Imaging System (LI-COR Biosciences).

Table 2-2: Protein analysis buffers. FBS, fetal bovine serum; PBS, phosphate-buffered saline; SDS, sodium dodecyl sulfate.

	Ingredients
Transfer buffer	1X NuPAGE transfer buffer, 10% (v/v) ethanol, in ultrapure water
Blocking buffer	5% (w/v) milk, 0.1% (v/v) Tween-20, in PBS
Fluorescence buffer	5% (w/v) FBS, 0.1% (v/v) Tween-20, 0.01% (w/v) SDS in PBS

2.6 Cell culture, synchronization and drug treatments

U2OS and FZR1KO cells were cultured in DMEM (Thermo Fisher Scientific) supplemented with 10% FBS, 200 μM Glutamax-1, 100 U/mL penicillin, 100 μg/mL streptomycin, and 250 ng/mL fungizone at 37°C with 5% CO2. For mitotic exit synchronizations, cells were collected in mitosis by 12 h treatment with 10 μM STLC (Tocris Bioscience) to trigger the Spindle Assembly Checkpoint (SAC) and then released at different time points by treatment with 10 μM AZ3146 (Generon, Slough, UK), an inhibitor of the SAC kinase Mps1. Cells were synchronized at different cell cycle stages as follows: For G0, cells were starved for 48 hr in DMEM without serum for 48 h. For G1, G0-arrested cells were

released into serum-containing media for 2 h. For G1/S, cells were incubated with media containing 2 mM thymidine for 16 h, washed with PBS, released into regular media for 12 h, and then incubated in media containing 2 mM thymidine for 15 h. S-phase cells were prepared by releasing G1/S phase cells into regular media minus thymidine for 5 h. For M-phase cell population, cells were incubated with 10 μM STLC for 12 h. Mitotic cells were then collected by shake-off. Aurora kinase inhibitors MLN8237 (Stratech, Ely, UK), MK5108 (Axon Medchem, Groningen, Netherlands), ZM447439 (Generon) and AZD1152-HPQA (Sigma-Aldrich UK) were used at the doses indicated.

2.7 Site directed mutagenesis

Mutations in D-box like motifs of AURKA and PLK1 were generated in pVenus-N1-AURKA and pVenus-N1-PLK1 (Previously made in the lab) using site direct mutagenesis technique and primers according to **Table 2-3**.

Table 2-3: The oligonucleotide forward and reverse primers.

Mutants	Forward	Reverse
AURKA $L_{374}I$	5’CCAGAGGCCAATGATCAGA GAAGTACTTG-3'	5’CAAGTACTTCTCTGATCAT TGGCCTCTGG-3'
AURKA $R_{371}A$	5’CCAGCCAGGCGCCAATGCT CAGA -3'	5’TCTGAGCATTGGCGCCTGG CTGG-3'
PLK1 $L_{340}I$	5’ACCCCAGCAACCGGAAGCC CATC -3'	5’GATGGGCTTCCGGTTGCTG GGGT -3'
AURKA Kpn1	5’GAGGTACCATGGACCGATC TAAAGAAAAC-3'	
AURKA $K_{23}R$	5’GGTCCAAGACGTGTTCTCGT GAC-3'	5’GTCACGAGAACACGTCTTG GACC-3'
AURKA K_{23}RVL/A AAA	5’GGTCCAGCAGCTGCTGCCGT G-3'	5’CACGGCAGCAGCTGCTGG ACC3'

Forwards and reverse primers were designed containing the mutation in question. The two primers overlap by about 10 nucleotides around the mutation to make the second step of the PCR easier. Site-directed mutagenesis was done in two PCR steps. First Step PCR was used to generate the mutations and end up with two fragments sequence rather than the whole one. To generate the 5' mutagenised fragment, I used the forward outside primer and the reverse mutagenic primer. To generate the 3' mutagenised fragment, I used the forward Mutagenic Primer and the Reverse outside Primer. For each mutant two 50 µL reactions were set up as follow:

Table 2-4: First step PCR reaction component.

Reagents	5' Fragment	3' Fragment
Water/ µL	31	31
Phusion HF buffer/ µL	10	10
2.5mM dNTPs/ µL	4	4
100 µM 5' Primer/ µL	1 (Forward outside)	1(Forward mutagenic)
100 µM 3' Primer/ µL	1 (Reverse mutagenic)	1 (Reverse outside)
100ng/µL Template DNA/ µL	1	1
DMSO/ µL	1.5	1.5
Phusion Polymerase/ µL	0.5	0.5

Table 2-5: First PCR step thermocycling conditions.

Step	Temperature	Time
Initial Denaturing Step	98ºC	2 min
Low temperature cycle 3x	45ºC	30 sec
Annealing temperature of homologous region	72ºC	60 sec
Denaturing Step	98ºC	30 sec
High temperature cycle x12	65 ºC	30 sec
Annealing temperature of whole primers	72ºC	60 sec
Final Elongation Step	72ºC	2 min

Second Step PCR: This step was used to stick the two fragments generated in the first step back together to give a whole gene with a specific point mutation.

Table 2-6: Second PCR step reaction.

Reagents	
Water/ µL	Make up to 50 µL (Including primers to be added later)
Phusion HF buffer/ µL	10
2.5mM dNTPs/ µL	4
5' Template Fragment/ µL	3
3' Template Fragment/ µL	3
DMSO/ µL	1.5
Phusion Polymerase/ µL	0.5

Table 2-7: Second PCR thermocycling conditions A for a routine PCR.

Steps	**Temperature and time**
Initial denaturing step	98ºC; 2 min
Cycle x5	98ºC, 30 sec Annealing temperature of overlap region; 30 sec 72ºC; 60 sec
Final Elongation Step	72ºC; 2 min

After these 5 cycles, the reaction was stopped and 1 µL of each of the outside primers were added and run for a further 20 cycles.

Table 2-8: Second PCR thermocycling conditions B for a routine PCR .

Steps	**Temperature and time**
Initial Denaturing Step	98ºC; 2 min
Cycle x20	98ºC, 30 sec Annealing temperature of overlap region; 30 sec 72ºC; 60 sec
Final Elongation Step	72ºC; 2 min

PCR products were separated by electrophoresis. Electrophoresis was performed in TAE buffer at 100 V for 40 min. DNA fragments of correct weight were excised and were purified using a QIAquick Gel Extraction Kit and according to the manufacturer's instruction. Digested DNA fragments and vectors were ligated using T4 Rapid DNA ligation Kit. Ligation was conducted in a 10 µL reaction at room temperature. Ligation reaction products were used to transform 50 µL DH5-alpha competent cells by heat shock method at 42 °C for 40 sec. Bacteria

are then recovered in 1mL Luria Broth (LB) at 37 °C for 40 min. Transformed bacteria were spread in Agar plates containing the appropriate antibiotic (Kanamycin 50 μg/mL). Colonies were picked and amplifies in LB with the antibiotic overnight. DNA was harvest using midiprep a QIAprep spin plasmid kit according to the manufacturer instructions.

2.8 Immunofluorescence analysis

Cells were seeded at 2 x 10^4 onto glass coverslips and then fixed with cold 100% methanol (−20°C), permeabilized with 0.5% Triton X-100 in PBS, and blocked in 2% bovine serum albumin (BSA), 0.2% Triton X-100 in PBS (blocking buffer) for 1 h at room temperature. Cells were then incubated overnight with primary antibodies diluted in blocking buffer at 4 °C. The following primary antibodies were used: mouse anti-γ-tubulin (Abcam ab6046) and rabbit anti-phospho-AURKA T288 (1:1000; clone D13A11 XP® Rabbit mAb, Cell Signalling). Cells were then washed three times with PBS and incubated with secondary antibodies at 1:1,000 dilution. FITC-conjugated anti-mouse (Sigma) and rabbit Alexa Fluor 568 (Invitrogen) were used as the secondary antibodies. DNA was stained with DAPI. Coverslips were mounted with Prolong Gold antifade reagent. Epifluorescent stacks were acquired using a 500-nm step with 2× 2 bin using appropriate filter sets and 40× NA 1.3 oil objective. The best in-focus images were selected and integrated intensities were measured by ImageJ (http://rsb.info.nih.gov/ij/; National Institutes of Health, Bethesda, MD), and the results were processed by Adobe Illustrator and Adobe Photoshop.

2.9 Mitochondrial imaging and analysis

Cells were seeded at 2 × 10^4 onto eight-well plastic-bottom slides (Ibidi GmbH, Martinsried, Germany) for live-cell imaging. To stain the mitochondria, the cells were incubated with 100 nM Mitotracker® Red CMXRos (M7512, Thermofisher) for 15 min, replaced with L-15 medium supplemented with FBS. Epifluorescent images were acquired with a 40X NA 1.3 oil objective on an Olympus IX81 motorized inverted microscope (Olympus Life Science, Southend-on-Sea, UK). The automated imaging platform included PE4000 LED illumination source (CoolLED, Andover, UK), Retiga R6 CCD camera (QImaging, Birmingham, UK), motorized stage (Prior Scientific, , UK) and 37°C incubation chamber (Solent Scientific, Segensworth, UK), all controlled by Micro-Manager (Edelstein 2014). Images were collected with 2 x 2 bin applied, exported as tiff files, and analysed using MicroP (Grant et al., 2018; Peng et al., 2011).

2.10 Time-lapse imaging and FRET quantification

Cells were imaged cells in L-15 medium with 10% FBS at 37°C using an automated epifluorescence imaging platform composed of Olympus IX83 motorized inverted microscope, Spectra-X multi-channel LED widefield illuminator (Lumencor, Beaverton, OR, USA), Optospin filter wheel (Cairn Research, Faversham, UK), CoolSnap MYO CCD camera (Photometrics, Tuscon, AZ, USA), automated XY stage (ASI, Eugene, OR, USA) and climate chamber (Digital Pixel, Brighton, UK) and controlled using Micro-Manager. FRET imaging was performed using a 40X NA 0.95 objective and ECFP/EYFP/mCherry beamsplitter (Chroma, Bellows Falls, VT, USA) for ratiometric comparison of CFP and YFP emission upon excitation of CFP. ImageJ software (National Institutes of Health) was used to quantify CFP and YFP signal across the whole cell and AURKA activity expressed as CFP/YFP ratio (1/FRET).

2.11 Statistical Analysis

Data analyses were performed in GraphPad 6.01 (San Diego, CA, USA). Results were analyzed with Student's t-test or Mann-Whitney U-test (non-parametric) as indicated in figure legends. Significant results are indicated as $p < 0.05$ (*), $p \leq 0.01$ (**) or $p \leq 0.001$(***). Values are stated as the mean ± standard deviations.

Chapter 3 Characterisation of AURKA degrons

3.1 Introduction

During mitotic exit, the ubiquitin-proteasome pathway is necessary and sufficient for the destruction of mitotic regulators to permits cells exit mitosis. The destruction of mitotic regulators is mainly mediated by the multisubunit ubiquitin E3 ligase APC/C. The activity of APC/C is tightly controlled by two major activator Cdc20 and FZR1. Active APC/C recognizes the substrates through short SLiM degrons leading to their ubiquitination and subsequent degradation. These degrons are important to generate the increased affinity of APC/C-substrate interaction that is required for efficient ubiquitination. As discussed by Davey et al., 2016, lack of strict conservation of degron sequences can be explained by multivalency of degron-E3 interactions and participation of residues outside the consensus (Davey and Morgan, 2016). These features go hand in hand with the flexibility of IDRs. The flexibility in sequences surrounding the degron is essential for substrate lysines to be able to mount a nucleophilic attack on a nearby ubiquitin thioester linkage. The lack of sequence conservation between degrons has contributed to historic confusion in the field, with some atypical degrons described as 'novel' being subsequently redefined as variants on known degrons (i.e. they dock to the known receptor sites on the APC/C) (Davey and Morgan, 2016).

AURKA is an unusual substrate that is degraded by the FZR1-activated form of APC/C (Floyd et al., 2008; Min et al., 2015; Pines, 2011). Deregulated AURKA is a common driver of cancer and cancer resistance (D'Assoro et al., 2015). Previous investigations have identified several potential degron within AURKA sequence through *in vitro* studies, including the 'A-box' motif and putative canonical KEN, and D-boxes (Castro et al., 2002; Crane et al., 2004b; Littlepage and Ruderman, 2002) **(Figure 3-1)**. The existence of N-terminal domain is required for destruction of AURKA during mitotic exit (Littlepage and Ruderman, 2002). Mutation of the C-terminal D box completely stabilized AURKA during mitotic exit *in vitro* or living cells. However, the crystal structure of the AURKA kinase domain revealed that the putative D-box is buried (Bayliss et al., 2003). This should make the degron inaccessible to APC/C raising the question of whether the D- box-like motif in C-terminal is a functional D-box.

In vivo assessment of D-Box's role has remained problematic because it had been observed by researchers in the Lindon Lab that the double point mutation of D-box $R_{371}AxxL_{374}A$ in Venus-tagged AURKA abrogates its localization in all mitotic structures, which can be argued as interfering with the folding of AURKA or with the interaction of binding partners (Lindon et al., 2015). Here I describe a study undertaken to provide a more complete characterisation of AURKA degrons and to resolve the status of the putative D-box of AURKA.

3.2 Results

It has been previously reported that D-box like motif $R_{371}XXL_{374}$ is required for AURKA degradation **(Figure 3-1)**. Crystal structure of AURKA show that the D box motif is buried in the kinase domain and inaccessible for APC/C recognition (Davey and Morgan, 2016; Lindon et al., 2015). I carried out *in silico* modelling to test the likely effect of different D-box mutations on the structure of AURKA. The structure of AURKA kinase domain (122-403) was examined in PyMol and variations in free energy resulting from different point mutations in the putative D-box ($R_{371}xxL_{374}$) were calculated using FoldX3 software **(Figure 3-2)**. The *in-silico* work was carried out in the lab of Dr. Alessandro Paiardini at Sapienza University, Rome, Italy.

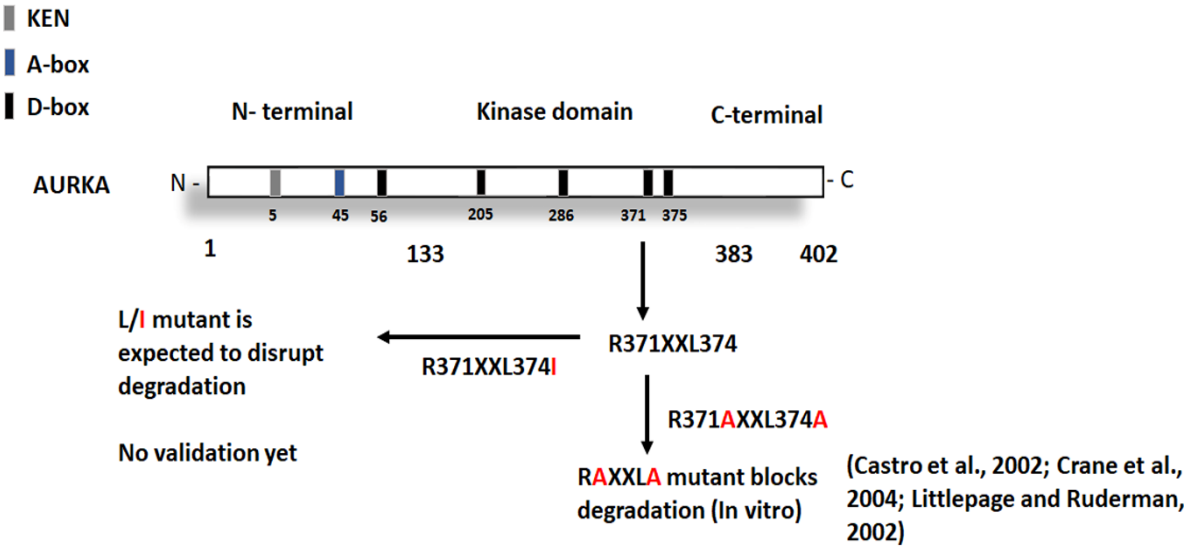

Figure 3-1 Schematic of putative D-box sequences of AURKA and mutants for testing D-box functionality. $R_{371}xxL_{374}$ was described as D-box regulating the destruction of AURKA at mitotic exit.

3.2.1 *In silico* evaluation of the folding state of different AURKA D-box mutants

The molecular structure of the putative D-box shows L_{374} fitted into the hydrophobic aliphatic pocket on the kinase domain. Moreover, there is a salt bridge established between R_{371} and conserved residue E_{299} that contribute to the observed structure **(Figure 3-2 A)**. FoldX3 software predicted the change of the folding free energy upon point mutations of the D-box sequence. Gibbs free energy variations (ΔΔG) for the protein folding state predicted that the RxxL>AxxA substitution frequently used to test for D-box function is strongly destabilizing to the structure ($R_{371}A/L_{374}A$, ΔΔG = 5.8 kcal mol-1). Free energy differences $R_{371}A$ and $L_{374}A$ (ΔΔG = 4.9, 2.6 kcal mol-1) were also much larger than $L_{374}I$ (ΔΔG = 1.6 kcal mol-1) **(Figure 3-2 B)**. The conserved substitution $L_{374}I$ has the lowest free energy variations (ΔΔG) for the protein folding of all D-box mutants (ΔΔG = 1.6 kcal mol-1). I concluded that $R_{371}A/L_{374}A$ is likely to strongly disrupt the folding of AURKA.

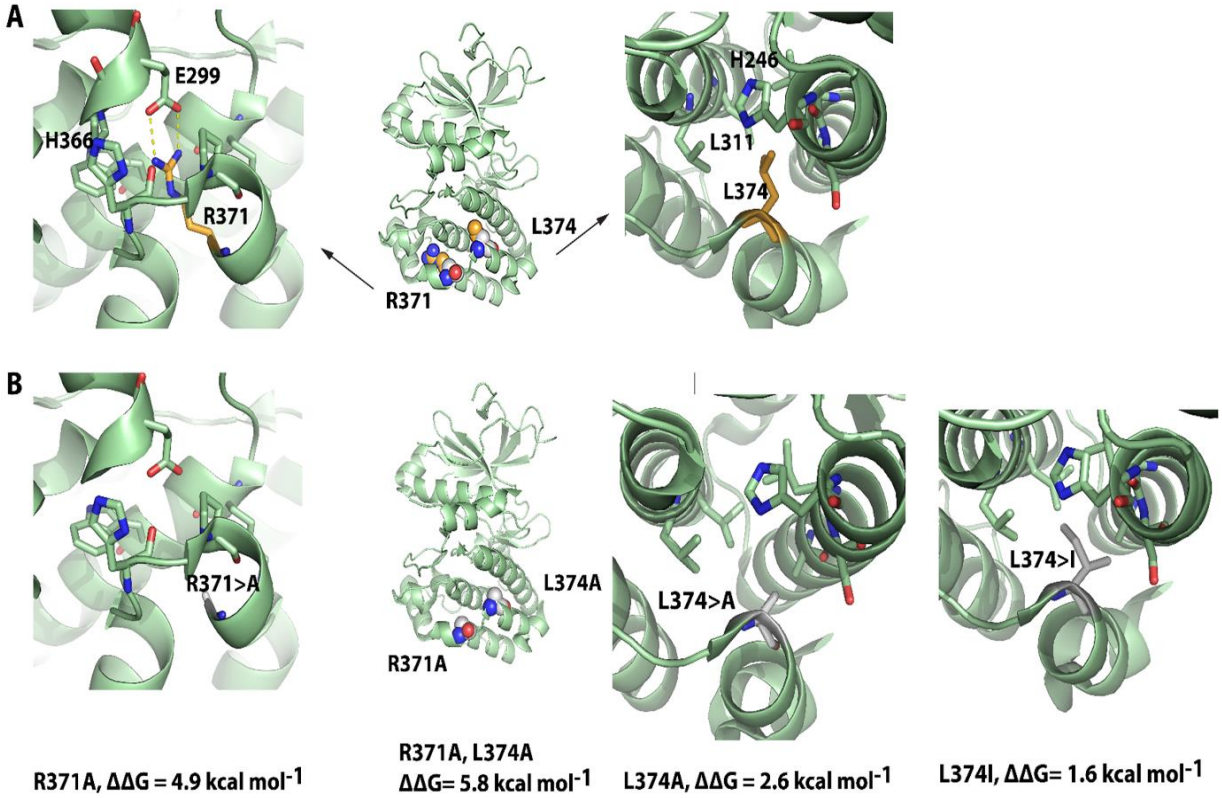

Figure 3-2 Predicting the effect of D-box mutations on the structure using PyMol and FoldX3. A) D- box is structurally buried within the kinase domain. R_{371} and conserved residue E299 interact to form salt bridge. The position of L_{374} fitted into the hydrophobic aliphatic pocket. B) Folding free energy (ΔΔG) upon each point mutations: $R_{371}A$, $L_{374}A$ >$R_{371}A$> $L_{374}A$> $L_{374}I$.

3.2.2 The effects of D-box mutations on AURKA localization

Having demonstrated the likely destabilizing effect of different D-box mutations on the structure, I then examined the effects of mutations on AURKA localization. AURKA localizes to the mitotic spindle through its interaction with TPX2 (Kufer et al., 2002). Tags on the N-terminus of AURKA reduce its degradation and interactions with proteins that are required for the localization during mitosis (Roghi et al., 1998). Therefore, I used C- terminal-tagged AURKA in my experiments. To investigate the localization of destabilizing mutants in living cells, U2OS cells were transiently transfected with Venus C- terminal-tagged AURKA mutants and were imaged 24 h after transfection. I found that wild-type AURKA localized to mitotic bipolar spindles and the signal then quickly fades **(Figure 3-3 A)**, through the protein destruction that is consistent with other reports (Crane et al., 2004a; Floyd et al., 2008; Giubettini et al., 2011; Lindon et al., 2015).

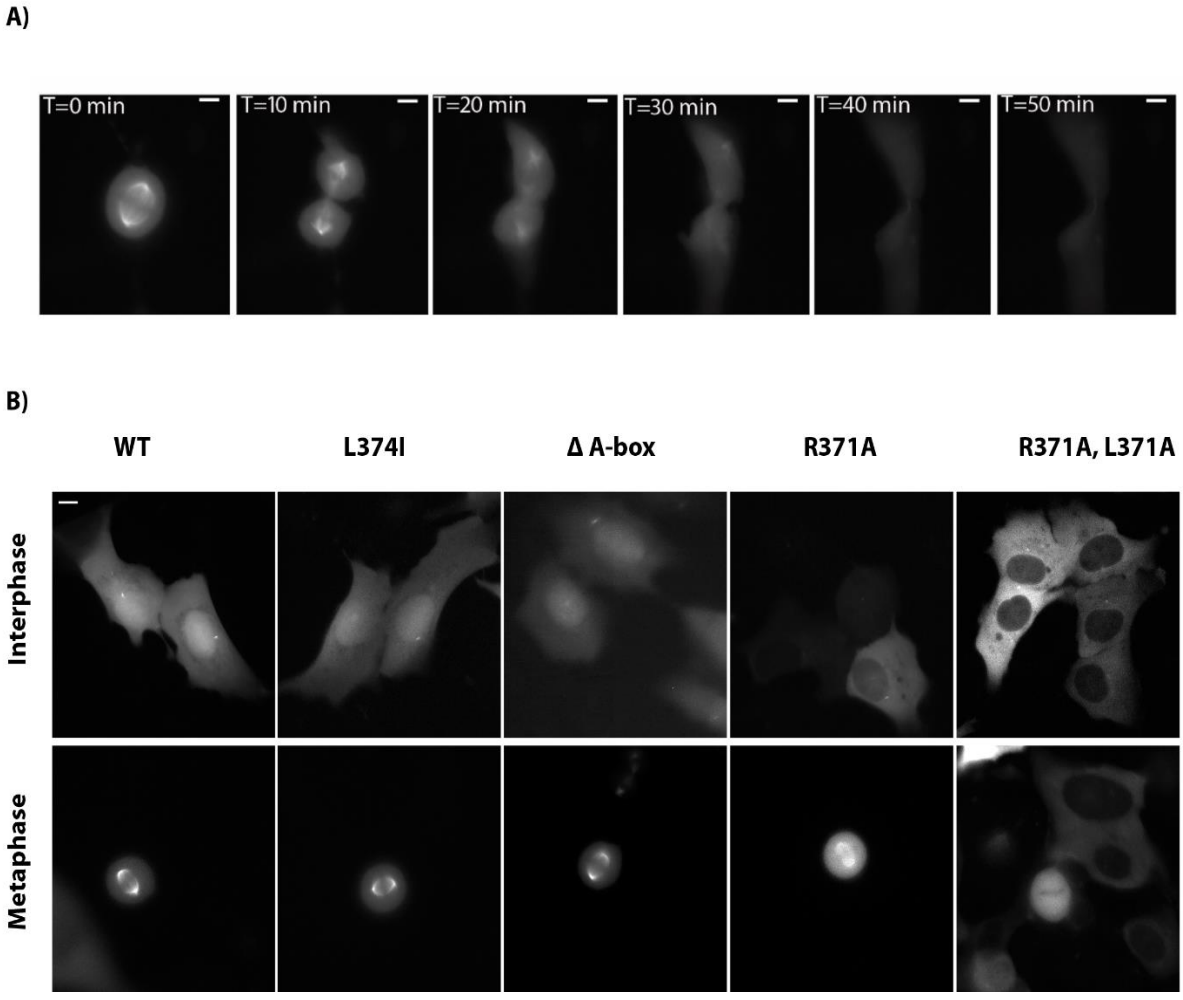

Figure 3-3 *In vivo* localization of AURKA D-box mutants. A) Time-lapse images of U2OS cells transfected with wild-type AURKA-VENUS. Images of mitotic cells were acquired every

2 min for 2 hours. Scale bar: 10 µm. B) Localization of wild-type AURKA, AURKA D-box like motif mutants, and AURKA A-box deletion during interphase and mitosis (metaphase). number of repeats n=3, Scale bar: 5 µm.

During mitosis, versions with destabilizing substitutions did not behave like the wild-type (WT) protein, being not localized or weakly localized to the bipolar mitotic spindle poles. $R_{371}A$, $L_{374}A$ double substitutions did not localize on the mitotic spindle as WT AURKA. $R_{371}A$ localized partially to the spindle. In interphase, cells expressing double point mutation $R_{371}A$, $L_{374}A$ of the D-box, and $R_{371}A$ demonstrated cytoplasmic localization compared to WT or $L_{374}I$. On the other hand, Δ A-box which is known to stop AURKA destruction does not affect AURKA localization in mitosis or interphase. This data suggests that D-box AURKA mutants are unable to localize to the nucleus because it cannot adopt the correct conformation, and consequently loses its interaction with binding partners required for its nuclear localization **(Figure 3-3 A, B)**. I concluded that mutating the D-box motif of AURKA abrogates normal localization of the protein.

3.2.3 The effects of D-box mutations on AURKA degradation

Next, I tested our panel of putative D-box substitutions for their effect on mitotic degradation of AURKA-Venus using a fluorescence time-lapse assay. Quantification of fluorescence measurements from single mitotic cells were used to generate degradation curves for AURKA mutants and fluorescence intensities were normalized to the level at anaphase onset. The $R_{371}A$, $L_{374}A$ double mutation was completely stable, like the 'non-degradable' ΔA-box version. Substitution with partial destabilizing effect on AURKA, $R_{371}A$ single substitution, showed partial resistance to mitotic degradation whilst substitution of $L_{374}I$, with the lowest ΔΔG, did not affect mitotic degradation of the protein ($R_{371}A$>$L_{374}I$, in line with ΔΔG values) **(Figure 3-4 A, B)**. Moreover, folding free energy (ΔΔG) of AURKA mutants is correlated to the degradation of the protein during mitotic exit **(Figure 3-4 C)**. I concluded that both mitotic degradation of AURKA, and its correct localization/function, are dependent on the correct folding of the C-terminal part of the kinase domain.

3.2.4 Conserved single point mutation Leucine to Isoleucine within D-box is sufficient to stop the degradation by the APC/C

Structural studies of the D-box docked to its receptor on APC/C-FZR1 (He et al., 2013) allow prediction that L>I substitution at the P4 position of a D-box should disrupt D-box

binding to the receptor site on the APC/C (Norman Davey, personal communication) and should be sufficient to stabilize substrate against APC/C-mediated degradation. I tested this prediction by making L>I substitution in the known D-box-dependent anaphase substrate of APC/C, Polo-like kinase 1 (Plk1), to ask if this is sufficient to stop its destruction during mitotic exit **(Figure 3-5)**.

A)

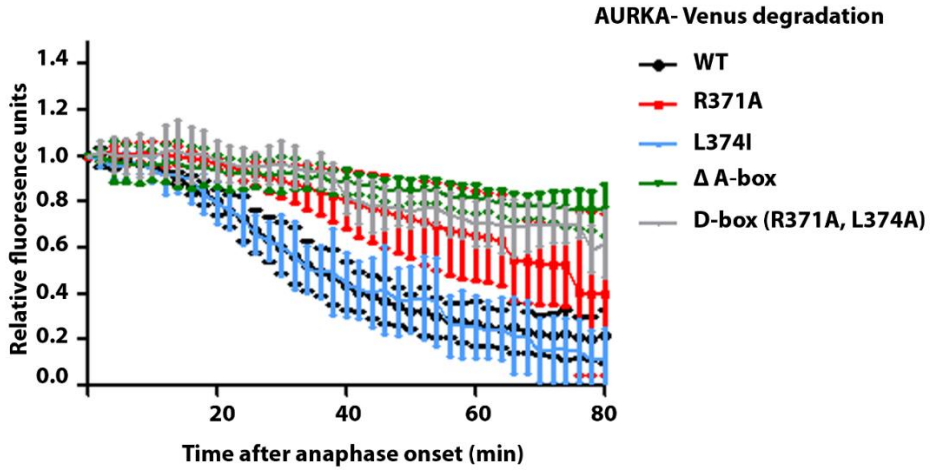

B)

Mutants	Interphase	Mitotic spindle poles	Degradation	Folding free energy (ΔΔG)
WT	Cytoplasmic and nuclear	Localized	Degraded	
L374I	Cytoplasmic and nuclear	Localized	Degraded	ΔΔG= 1.6 kcal mol^{-1}
R371A	Cytoplasmic	Partially localized	Partially degraded	ΔΔG = 4.9 kcal mol^{-1}
R371A, L374A	Cytoplasmic	Not localized	Not degraded	ΔΔG= 5.8 kcal mol^{-1}

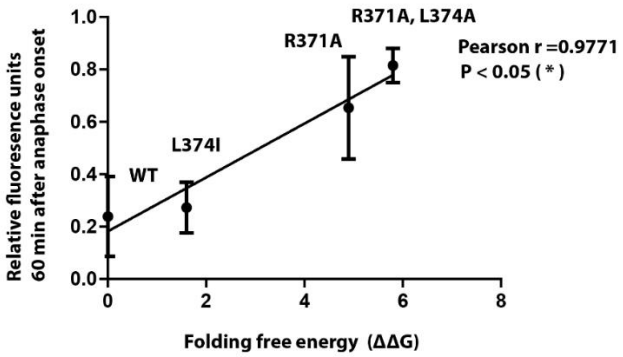

Figure 3-4 *In vivo* degradation of AURKA D-box mutants. A) Quantification of fluorescence measurements from single mitotic cells were used to generate degradation curves for AURKA mutants and fluorescence intensities were normalized to the level at anaphase onset, where n = 5 cells. B) Table indicates the localization, degradation and folding free energy (ΔΔG) of different AURKA mutants. C) Pearson correlation analysis between the degradation and folding free energy (ΔΔG) of AURKA mutants r=0.9771, P<0.05 (*). Number of repeats n=3, error bars indicate s.d.

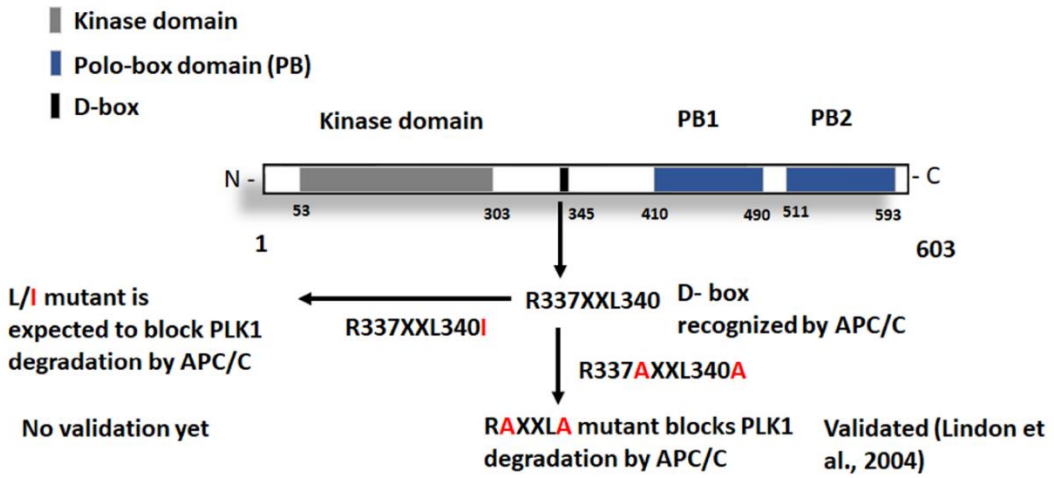

Figure 3-5 Schematic of D-box sequence of PLK1 and the previously used mutants. R337xxL340 was described as D-box regulating the destruction of PLK1 at mitotic exit.

I found that L340I substitution in the D-box of Plk1 showed the same pattern in blocking degradation of the substrate as the previously tested $R_{337}A/L_{340}A$ version (Lindon 2004), supporting the prediction that L>I substitution at P4 abrogates D-box function. The localization at the centrosome stays the same for all the mutants **(Figure 3-6 A, B)**. This result indicates that $R_{371}xxL_{374}$ of AURKA is probably not a functional D-box since the conservative substitution of the P4 residue L>I do not affect the degradation of the protein. It supports our hypothesis that the lack of degradation of $R_{371}A$, $L_{374}A$ is due instead to disruption of the protein conformation that indirectly stabilizes the protein.

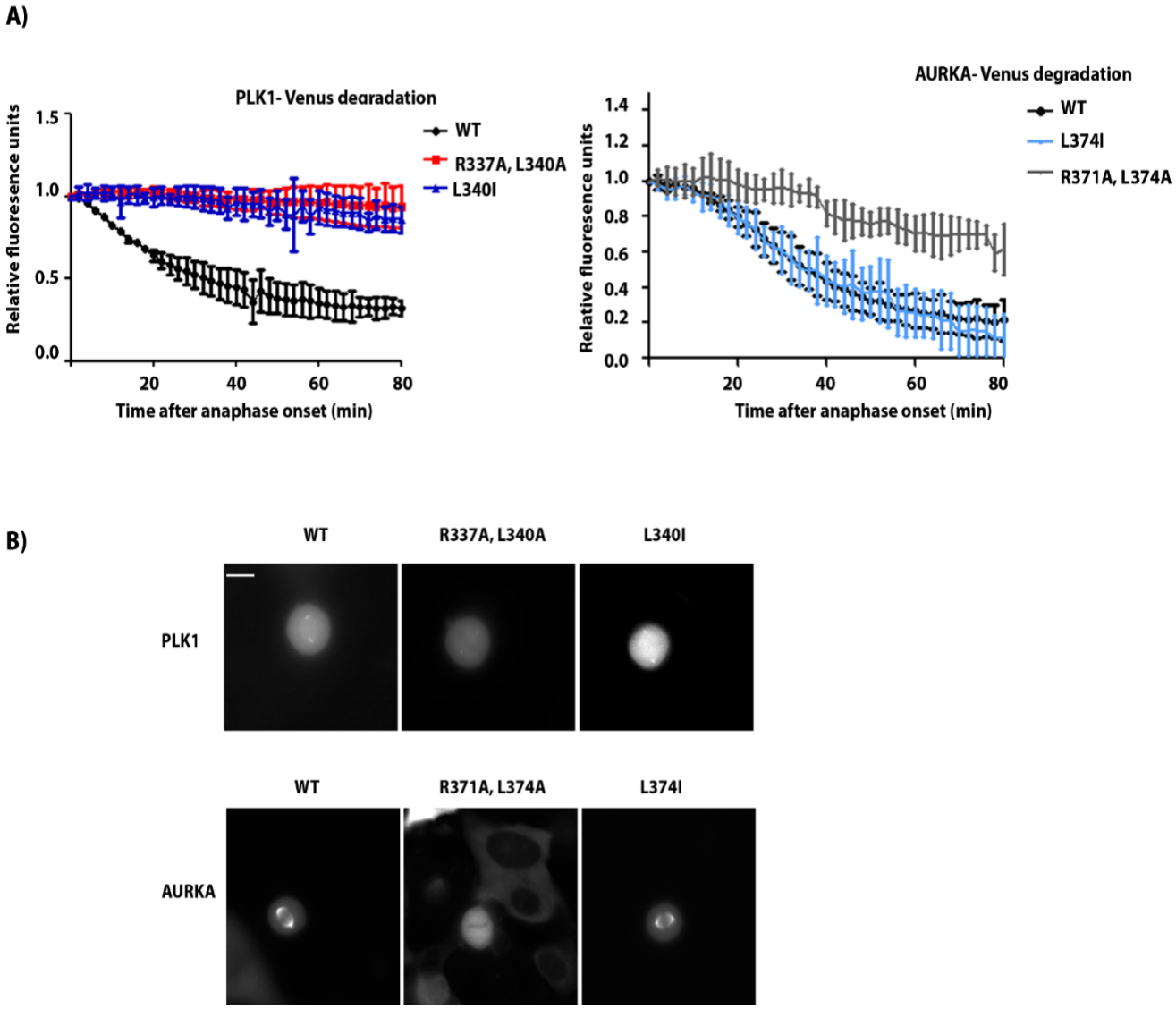

Figure 3-6 L>I substitution in the known D-box-dependent anaphase substrate of APC/C, Polo-like kinase 1 (PLK1) is enough to stop its degradation by the APC/C. U2OS were transiently transfected with WT PLK1/AURKA, and D-box like motif mutants (PLK1 $L_{340}I$ and $R_{337}A$, L340A)/ (AURKA $L_{374}I$ and $R_{371}A$, $L_{374}A$). A) Quantification of fluorescence measurements from single mitotic cells were used to generate degradation curves for PLK1 mutants and fluorescence intensities were normalized to the level at anaphase onset, where n = 6 cells. Error bars indicate s.d. B) Localization of wild-type AURKA, PLK1 and their D-box like motif mutants 2 min before anaphase onset. Number of repeats n=2, Scale bar: 5 µm.

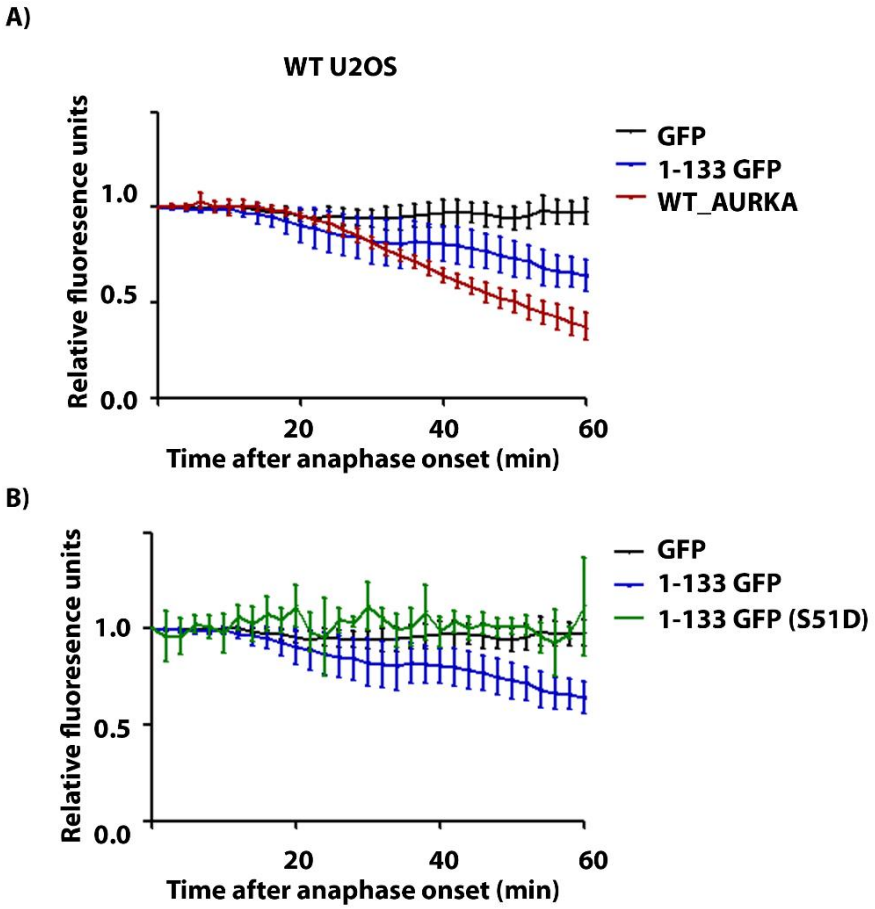

Figure 3-7 N-terminal IDR are sufficient for AURKA degradation that starts at anaphase. A) U2OS were transiently transfected with WT AURK, GFP, N-terminal AURKA tagged GFP. B) U2OS were transiently transfected with GFP, N-terminal AURKA and N-terminal AURKA tagged GFP (S51D) mutant. Quantification of fluorescence measurements from single mitotic cells were used to generate degradation curves and fluorescence intensities were normalized to the level at anaphase onset. Number of repeats n=2, Error bars indicate s.d.

3.2.5 N-terminal SLiMs are sufficient for properly regulated AURKA degradation at mitotic exit

In the absence of a known degron in the C-terminal domain of AURKA, I investigated whether the N-terminal IDR would be sufficient as well as necessary for mitotic degradation in live cell assays. I tested AURKA (1-133) fused to GFP in live cell assays using U2OS cells. I found that AURKA (1-133) was sufficient to direct anaphase-specific degradation of GFP **(Figure 3-7 A)**. Degradation was blocked by phosphomimetic substitution at Ser51, recapitulating the known phospho-regulation of the degradation of the full-length protein (Crane et al., 2004b; Lindon et al., 2015; Taguchi et al., 2002) **(Figure 3-7 B)**. These results are consistent with the report, which revealed that AURKA lacking its N-terminal domain stabilized during mitotic exit (Littlepage and Ruderman, 2002). The question arose as to

whether N-terminal IDR degradation is FZR1-dependent. To answer this question, I used the U2OS FZR1 knockout (KO) cell line that is generated in our lab by targeting the first exon of FZR1. Single-cell clones were validated for loss of FZR1 by sequencing the genomic locus, immunoblotting, and live-cell imaging of APC/C substrates (FZR1KO cell line generated by Begum Akman, Research Associate at the Department of Pharmacology, University of Cambridge, UK). U2OS FZR1KO cells were transfected with AURKA (1-133) GFP and GFP. I found that N-terminal IDR did not direct the degradation of GFP during mitotic exit in the absence of FZR1 **(Figure 3-8)**. Therefore, although the efficiency of degradation of 1-133 is reduced compared to the full-length protein, our results indicate that AURKA degron(s) present as SLiMs in its N-terminal IDR are sufficient for the protein degradation at mitotic exit. Our data also suggest that there is an additional site that helps with signalling the degradation.

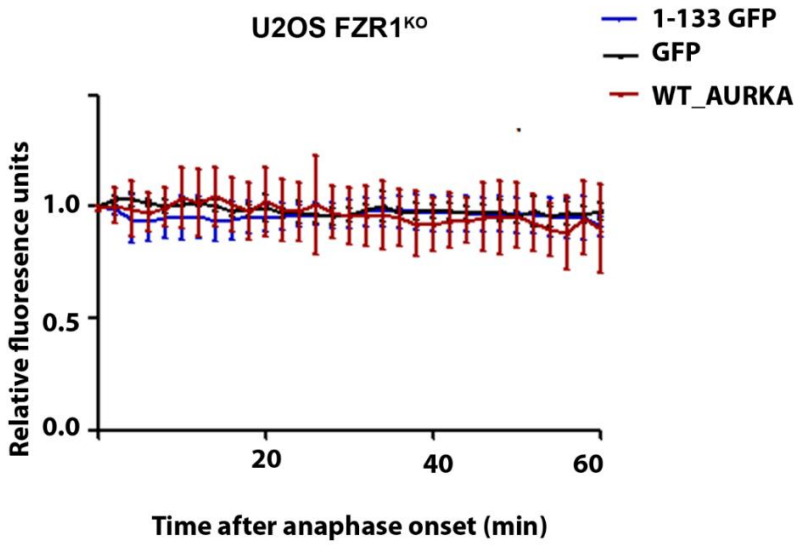

Figure 3-8 N-terminal SLiMs-dependent AURKA degradation is also FZR1 dependent. U2OS FZR1KO were transiently transfected with WT AURKA, GFP, AURKA (1-133) GFP. Quantification of fluorescence measurements from single mitotic cells were used to generate degradation curves and fluorescence intensities were normalized to the level at anaphase onset, where n = 5 cells. Number of repeats n=2, error bars indicate s.d.

3.2.6 In-silico docking of the A-box into the degron receptor sites on FZR1

Using the FlexPepDock server, in collaboration with Alessandro Paiardini lab, I used an in-silico docking approach to examine whether the atypical Q_{45}RVL degron (the A-box) might bind a known degron receptor site on FZR1. I docked the peptide Q_{45}RVLCPSNS into the sites on FZR1 (D-box, KEN, ABBA) receptors identified from the crystal structure of the

FZR1 WD40 domain bound to the pseudosubstrate domain of Acm1 (He et al., 2013) **(Figure 3-9 A)**.

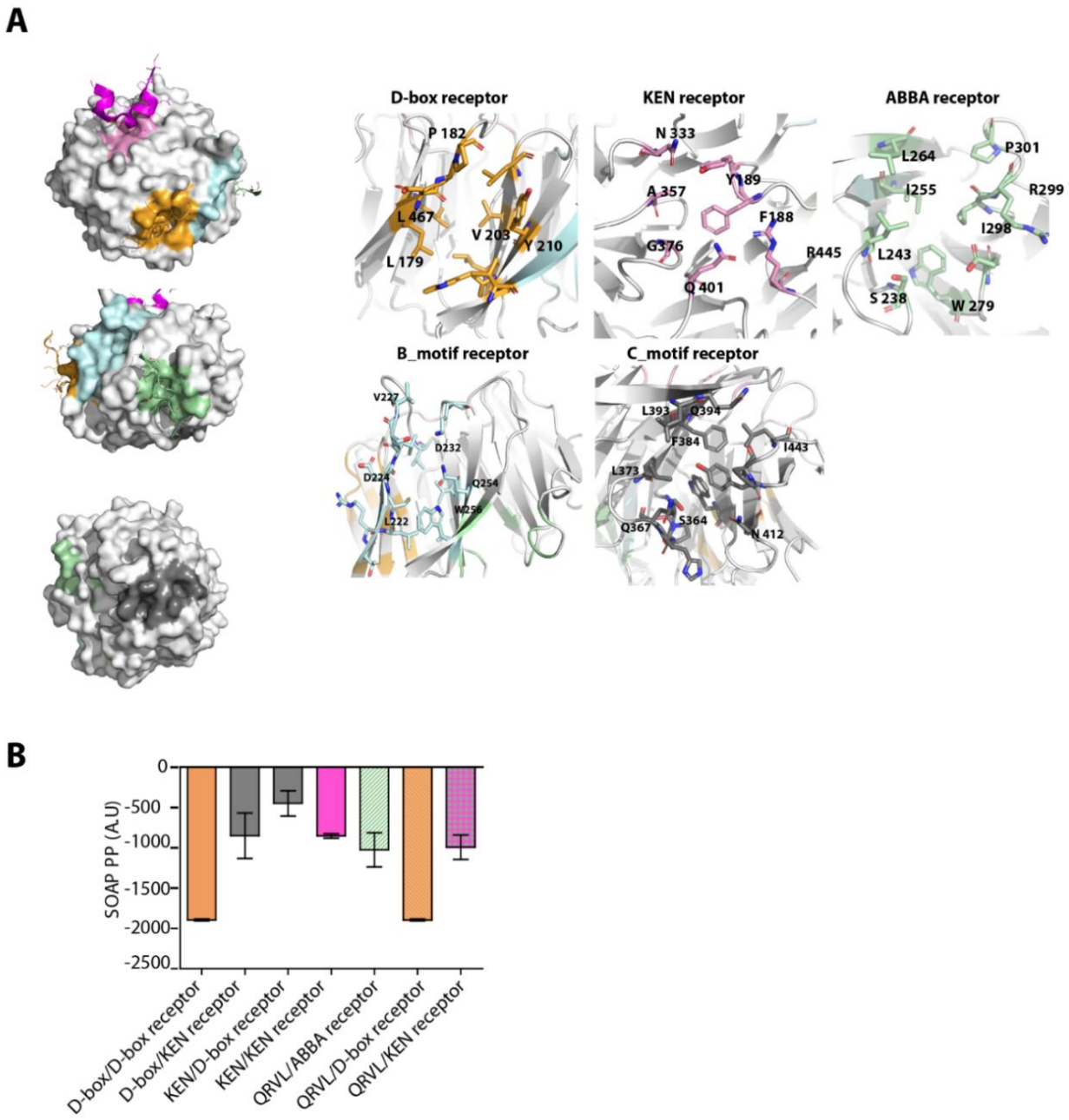

Figure 3-9 In-silico docking of A-box into the sites on FZR1 (D-box, KEN, ABBA) identified from the cryo-EM structure of FZR1 WD40 domain. A) The WD40 domain of FZR1 with the three degron-binding pockets occupied by the D box, KEN box, ABBA motif and two newly identified possible sites for A-box interaction named as B motif receptor and C motif receptor. B) Statistically Optimized Atomic Potential (SOAP) for A-box docking into the sites on FZR1 (D-box, KEN, ABBA). Error bars indicate s.d.

The statistically optimized pose at each site was compared with the binding of a cognate degron and the Statistically Optimized Atomic Potential (SOAP) (Dong et al., 2013) assigned to each

interaction. This revealed that the Q_{45}RVL peptide favoured interaction at the D-box pocket compared to other sites and docking of Q_{45}RVL at this site was energetically comparable to docking of D-box peptides **(Figure 3-9 B)**. Comparison of the A-box with a panel of D-boxes showed that it docks with an affinity within the range of known D-boxes, although with reduced affinity compared to more canonical D-boxes **(Figure 3-10)** (http://slim.ucd.ie/apc/index.php?page=instances). I note that in silico docking to FZR1 alone ignores potentially favourable contacts made with APC10 that contribute to the D-box binding pocket, and therefore I may have underestimated the likely preference of Q_{45}RVL for this receptor site.

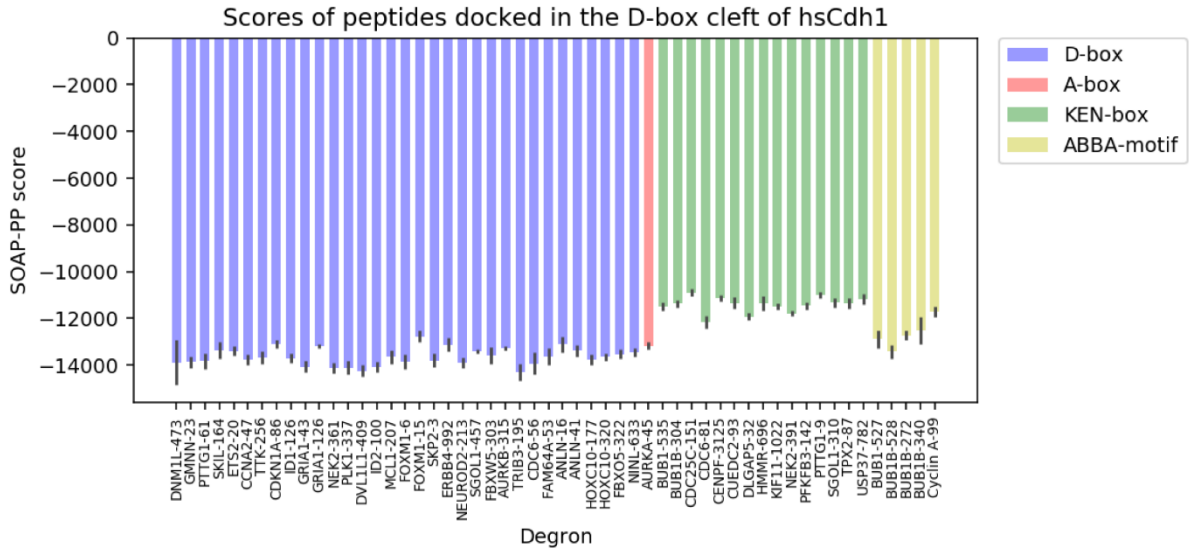

Figure 3-10 Comparison of the A-box with a panel of D-boxes into the sites on FZR1 (D-box, KEN, ABBA). Statistically Optimized Atomic Potential (SOAP) for degrons docking into on FZR1 D-box receptor. Error bars indicate s.d.

The Q_{45}RVLCPSNS peptide can be docked in a similar pose to the D-box, such that the side chain of L4 extends into the hydrophobic cleft in FZR1 identified by (He et al., 2013) **(Figure 3-11 A, B),** consistent with L at P4 being the most critical residue of the D-box. I concluded that the A-box of AURKA is likely to be a new variant of the well-characterised D-box. Indeed, a D-box variant with Q at P1 (QKPL) has previously been identified in Spo13, using D-box peptides to compete for Spo13 destruction by APC/C-FZR1(Davey and Morgan, 2016; He et al., 2013). In a scenario where the D-box consensus is 'relaxed' for FZR1 recognition, it may be that R residue at P1 is more important for FZR1 binding than Cdc20 binding: R at P2 may replace the electrostatic interactions with E465 of FZR1 seen by R at P1 in canonical D-boxes **(Figure 3-11C)**.

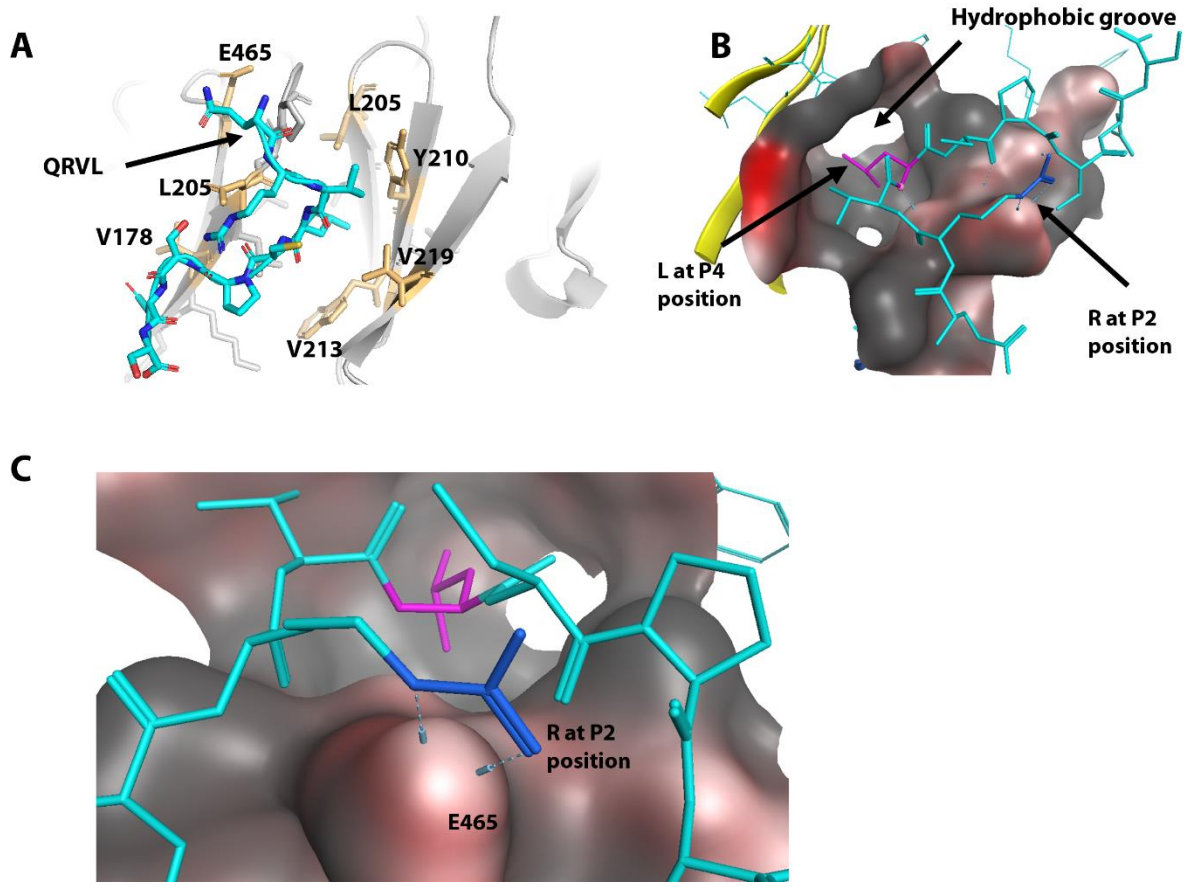

Figure 3-11 Outline of the molecular docking process of A-box docked onto D-box site. A) A-box motif binds to the D-box receptor on FZR1. B) Leucine residue (magenta colour) at P4 fits into the hydrophobic groove of the D-box receptor of FZR1. C) R (blue colour) at P2 make electrostatic interactions with E465.

3.3 Discussion

The work presented here addresses AURKA degrons within the protein sequence and evaluates their contribution to AURKA stability in live single cells. Previous work had reported that AURKA is degraded at mitotic exit in FZR1 dependent manner through two APC/C recognition signals: D-box and A-box (Floyd et al., 2008; Min et al., 2015; Pines, 2011). The $R_{371}A/L_{374}A$ double point mutation of the C-terminal D box has led to the conclusion that D-box is required for AURKA degradation because it stops AURKA destruction during mitotic exit (Castro et al., 2002; Crane et al., 2004b; Littlepage and Ruderman, 2002). I find, however, that D-box is not functional, and the effect of the D-box double point mutation can be attributed to a lack of proper folding. My in-silico studies reveal that $R_{371}A/L_{374}A$ is predicted to destabilize the structure of the protein and live cell imaging studies show it has a dramatic effect in AURKA localization. Conserved mutation of leucine to isoleucine in a known D-box-dependent substrate of APC/C is enough to stop its degradation via the APC/C. In the case of

AURKA, L374I mutation in the C- terminal D box does not block FZR1-induced destruction during mitotic exit implies that it has no essential role either in folding or in the context of a functional D-box. This novel finding agrees with the crystal structure of AURKA, which shows that D-box is buried in the kinase domain (Davey and Morgan, 2016; Lindon et al., 2015). This finding is not surprising since degrons are normally located in the IDR of cell cycle regulators.

In general APC/C substrates are recognized by more than one degron, such as Cell division cycle 6 (Cdc6), the kinase Hsl1p, and cyclin A proteins, whose APC/C-dependent degradation requires the KEN box, ABBA and the D box for degradation (Burton and Solomon, 2001; Di Fiore et al., 2015; Petersen et al., 2000; Qin et al., 2016). In those cases, a mutation in one of the recognition signal sequences alone partially affects the stability of those proteins. In contrast, a mutation in the A-box of the AURKA sequence completely stabilizes the protein (Littlepage and Ruderman, 2002; Floyd et al., 2008). I also find that N-terminal non-catalytic domain by itself, which contains KEN and A-box degrons, is degraded by APC/C and mutation of serine 51 within the A-box motif blocks its destruction. From these data, I conclude that A-box is sufficient for AURKA degradation in APC/C dependent manner. Our in-silico approaches also show that A-box can be docked in a similar pose to the D-box to the D-box receptor in FZR1. This finding suggests that the A-box of AURKA might be a new variant of the well-characterized D-box.

Chapter 4 AURKA destruction is essential to suppress interphase activity

4.1 Introduction

Aurora-A kinase (AURKA) activity is regulated by phosphorylation on T288 within the activation loop, or its interaction with different binding partners (Bayliss et al., 2003; Burgess et al., 2015; Eyers et al., 2003; Joukov et al., 2010; Littlepage et al., 2002; Richards et al., 2016). TPX2 is a well-known interactor, controls AURKA localization, activation, and stability during mitosis (Bayliss et al., 2003; Giubettini et al., 2011; Kufer et al., 2002). Interaction of TPX2 protects the autophosphorylated site pT288 from dephosphorylation by PP1 phosphatase (Bayliss et al., 2003). It also stabilizes the T-loop with or without its phosphorylation. Therefore, the dephosphorylation of pT288 may not be sufficient to eliminate the kinase activity of AURKA.

AURKA destruction at the end of mitosis and in G1 phase is controlled by the APC/C co-activator FZR1 (Lindon et al., 2015). AURKA is expressed at elevated levels in many types of cancers even in the absence of gene amplification (Gritsko et al., 2003; Jeng et al., 2004; Lai et al., 2010) suggesting that mutations that affect AURKA destruction might also lead to its stability and overactivity in cells. Although, previous studies have characterised AURKA activity in mitosis, surprisingly little attention has been paid to the regulation of the timing of its inactivation at mitotic exit. In particular the question of how AURKA activity is regulated during mitotic exit, given that AURKA also has anaphase functions (Afonso et al., 2017; Reboutier et al., 2015), and the importance of its destruction for attenuation of activity, remains unclear. In this chapter, our goal was to define the role of APC/C-mediated destruction in the timing of AURKA inactivation at mitotic exit and interphase using an FZR1 knockout cell line, pT288 AURKA antibody, and a new FRET-based biosensor for measuring AURKA activity.

4.2 Results

4.2.1 AURKA activity can be measured using an antibody specific for the phosphorylated T-loop (pT288)

I first examined whether the pT288 AURKA antibody would be a useful marker for measuring AURKA activity. To validate the pT288 AURKA antibody, a western blot

experiment was performed in mitotic-arrested U2OS cells that were treated with AURKA inhibitor MLN8237 for 3 hours at different doses. I found that total pT288 AURKA in cell extracts was abolished at 100 nM MLN8237 **(Figure 4-1 C).** Next, I examined if the pT288 signal was also sensitive to MLN8237 by immunofluorescence. U2OS cells were treated with 100 nM MLN8237 before fixation and immunostaining for pT288 AURKA, γ-Tubulin, and chromosomes (DAPI). As shown in **(Figure 4-1 A, B)**, the pT288 signal was seen localized strongly to centrosomes and spindle poles, consistent with known localization of AURKA in mitosis, and that all phospho-epitope signal on the centrosomes and spindle poles was abolished by treatment with AURKA inhibitor MLN8237. These results indicate that the centrosomal pT288 signal is specific to AURKA as expected. In contrast, the signal at the midbody (where the same antibody recognizes pT232 of AURKB) was insensitive to 100 nM MLN8237 **(Figure 4-2 A, B)**.

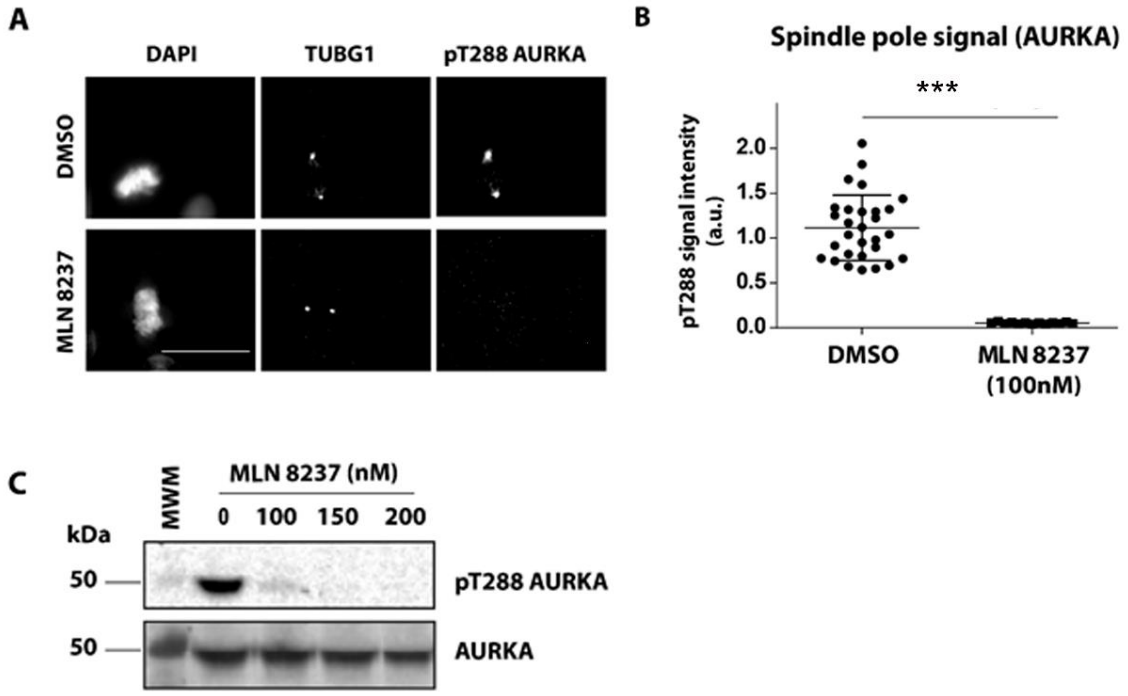

Figure 4-1 P-AURKA was not seen on mitotic centrosomes in cultures after treatment with AURKA inhibitor. A) AURKA activity is sensitive to AURKA-specific inhibitor MLN8237 by immunofluorescence on mitotic cells from a MeOH-fixed unsynchronized population. AURKA-specific pT288 signal is restricted to centrosomes and spindle pole bodies (marked by γ-Tubulin, TUBG1). Bars, 10 μm. **B)** Fluorescence intensity was significantly reduced compared with individual centrosomes in MLN8237 treated prometaphase cells. Scatter plots show distributions with mean ± S.D. *** $p < 0.0001$, Student's t-test. **C)** pT288-AURKA signals is abolished by AURKA inhibitor (MLN8237). Cell lysates were collected from STLC-arrested mitotic cells treated with MLN8237 for 3 hours at the indicated doses. Sample were collected and analysed by SDS-PAGE followed by blotting with pT288 AURKA and total AURKA. Number of repeats n=2.

I concluded that the centrosomal pT288 signal is specific to AURKA and can be used as a useful marker for the activity (Asteriti et al., 2014; de Groot et al., 2015). Since AURKA activity has been described to peak in G2/M, I also monitored the expression of AURKA level and activity during the cell cycle to further validate the pT288 antibody. U2OS cells were synchronized at distinct cell cycle phases. Cells were arrested at G0 after serum starvation for 40 h and were released into serum-containing media for 2hr to obtain G1 synchronization. For G1/S, cells were synchronized using a double thymidine block (DNA synthesis inhibitor). For S-phase, cells were prepared by releasing G1/S phase cells into serum-containing media for 5 h. For the M-phase cell population, cells were incubated with 10 μM STLC for 12 h. Mitotic cells were then collected by shake-off. AURKA activity was analysed by immunoblotting using the pT288 antibody as a marker. I found that AURKA and its activator TPX2 levels were low during the G1/S phase but rose in mitosis. However, I only observed the kinase activity (i.e., pT288 AURKA) in mitosis (**Figure 4-3**).

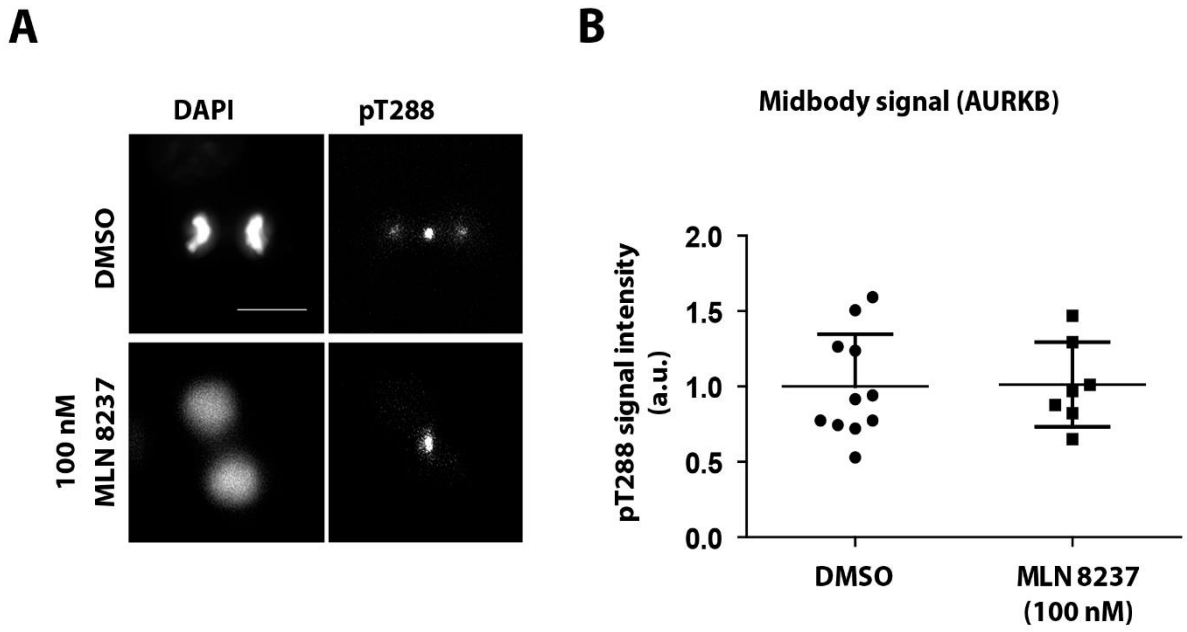

Figure 4-2 Midbody AURKB signal is not affected following MLN8237 treatment and is therefore centrosomal signal specific for AURKA activity. A) Immunofluorescence analysis of mitotic U2OS cells fixed and stained with antibody against pT288-AURKA shows signal midbody whereas midbody signal is persistent to MLN8237 inhibition and attributed to the recognition of pT232-AURKB epitope. Bar, 10 μm. **B)** Scatter plots show distributions with mean ± S.D. of pT288 signal intensity measurements at spindle pole or midbody, normalized to the mean value of the control (DMSO-treated) population. P>0.05, non-significant (n.s), Student's t-test. Number of repeats n=2.

4.2.2 Inactivation of AURKA occurs rapidly during mitotic exit

Although AURKA activity has been described to peak in G2/M at centrosomes, the description of active pT288 AURKA has not been characterised within each step of mitosis. To compare AURKA activity within each mitotic stage, U2OS cells were fixed and stained for immunofluorescence analysis (IMF) using antibody pT288 AURKA, γ-Tubulin, and chromosomes (DAPI). Fluorescence intensity associated with pT288 was quantified at different stages of mitosis and scored according to DNA morphology **(Figure 4-4 A)**. During G2, pT288 AURKA was associated with both centrosomes. Following nuclear envelope breakdown (NEB), prometaphase (PM) cells showed a strong increase in centrosome- and spindle pole-associated pT288 signal, peaking at metaphase. Moreover, the pT288 signal remained strong in anaphase cells before declining strongly in telophase cells **(Figure 4-4 B)**. I concluded that inactivation of AURKA measured as a decrease in pT288 signal occurs at approximately the time of onset of AURKA destruction, which occurs around 10 minutes after anaphase onset in human cells (Floyd et al., 2008).

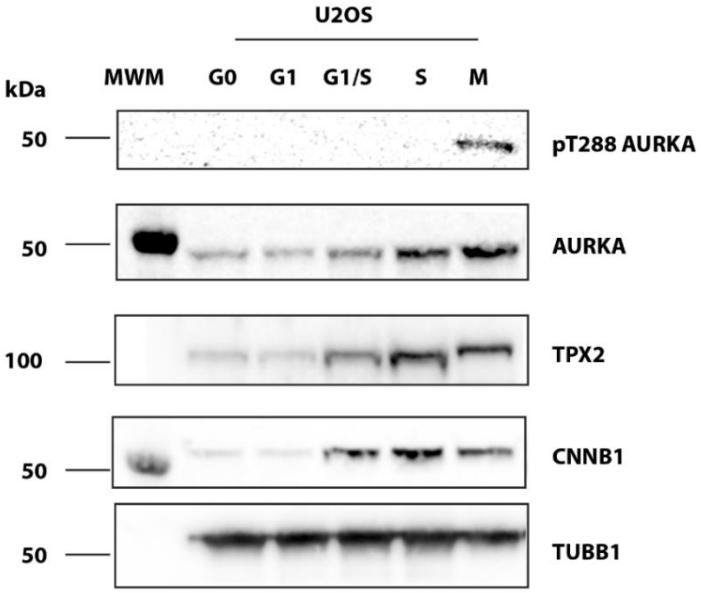

Figure 4-3 AURKA activity peaks during mitosis. pT288 antibody detects active AURKA only in mitotic cells. Cells were synchronized at different cell cycle stages. For G1, G0-arrested cells were released into serum-containing media for 2 h. For G1/S, cells were incubated with media containing 2 mM thymidine for 16 h, washed with PBS, released into regular media for 12 h, and then incubated in media containing 2 mM thymidine for 15 h. S-phase cells were prepared by releasing G1/S phase cells into regular media minus thymidine for 5 h. For M-phase cell population, cells were incubated with 10 µM STLC for 12 h. Mitotic cells were then collected by shake-off. Thirty micrograms of protein were loaded per lane, separated by SDS-PAGE and blotted with pT288, total AURKA, TUBB1 (Beta-tubulin), Cyclin B1 (CCNB1), and TPX2. Number of repeats n=2.

I next sought to determine how AURKA degradation and inactivation are related during mitotic exit. First, I compared AURKA level and activity by immunoblot analysis of extracts from cells synchronized through mitotic exit. U2OS cells were synchronized for the prometaphase enrichment by blocking with Eg5 inhibitor (5 μM STLC) to trigger the spindle assembly checkpoint (SAC), then treated with Mps1 inhibitor (10 μM AZ3146) to override SAC-mediated mitotic arrest. Cell extracts were collected at different time points and analysed by immunoblotting. Interestingly, I found that AURKA activity (i.e., pT288-AURKA) appears to drop much faster than the protein level.

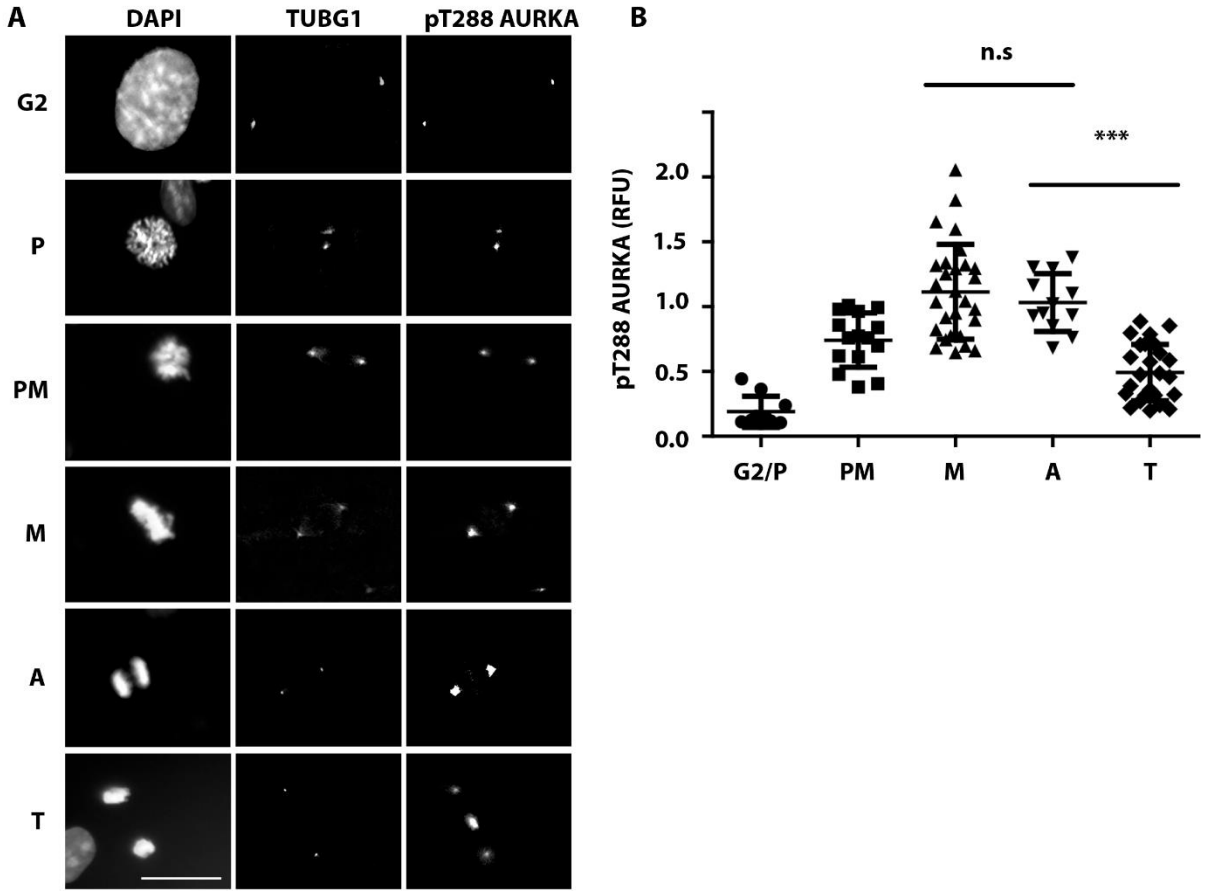

Figure 4-4 Active AURKA is associated with centrosomes and its activity at this location increases during mitosis. A) Unsynchronized cell populations were fixed MeOH-fixed. Cells were measured at different stages of mitosis according to DAPI staining and scored for mean pT288 AURKA signal measured in a fixed ROI centred on TUBG1 signal at centrosomes or spindle poles. **B)** Scatter plots show average fluorescence intensity P-AURKA staining on G2, prophase (P), prometaphase (PM), and anaphase/telophase (A/T) centrosomes. Data are normalized to mean value from two independent experiments. G2 and prophase (P), n=10; prometaphase (PM), n=15; metaphase (M), n=30; anaphase (A), n=30; and telophase (T), n=26. M vs A, not significant (n.s.); A vs T, $p < 0.0001$ (***), Students' t-test. Error bars indicate the SD. RFU, Relative Fluorescence Units. Bars, 10 μm. Number of repeats n=3.

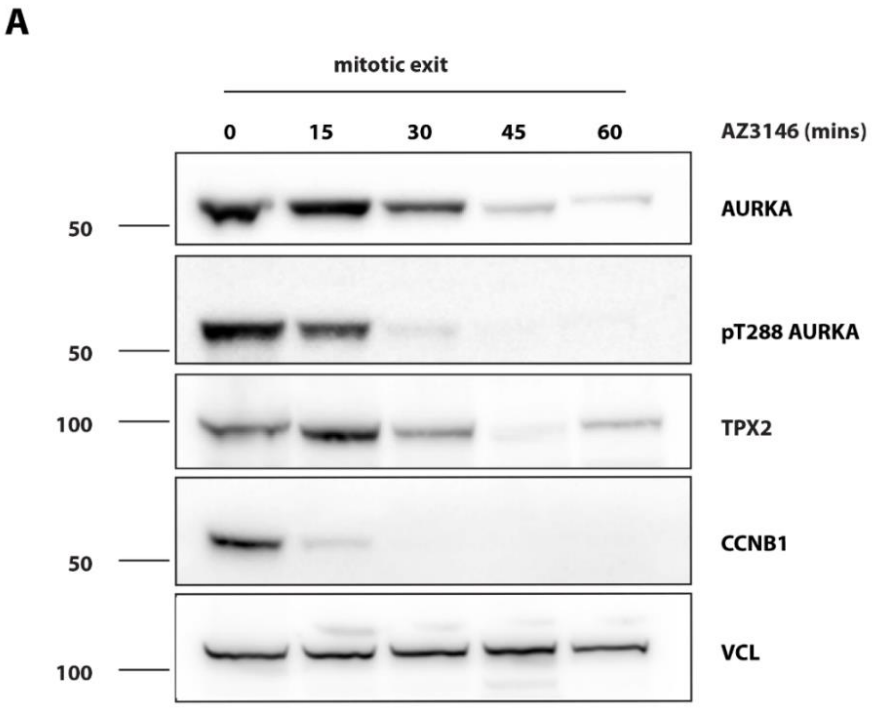

Figure 4-5 AURKA inactivation rate is faster than its degradation. Cells were synchronized in 5 μM STLC and released by checkpoint inhibition using 10 μM AZ3146, with extracts harvested at times indicated. Thirty micrograms of protein were loaded per lane, separated by SDS-PAGE and blotted with pT288, total AURKA, Vinculin (VCL), Cyclin B1 (CCNB1), and TPX2. Disappearance of Cyclin B1 (CCNB1) acts as marker for mitotic exit, level of vinculin (VCL) as loading control. Number of repeats n=2.

4.2.3 In FZR1KO cells, mitotic exit occurs without degradation of AURKA

The question arises whether AURKA destruction contributes to the fall in kinase activity at mitotic exit. Mitotic AURKA destruction is dependent on the FZR1 co-activator of APC/C. Therefore, I hypothesized that a FZR1 knockout (FZR1KO) in U2OS cells generated by CRISPR/Cas9 could be used to monitor both protein level and activity of the endogenous AURKA in the absence of its destruction at mitotic exit.

FZR1KO cells had been generated in the Lindon Lab by Dr Begum Akman, who collaborated on experiments where indicated in Figure legends. First, AURKA stability was evaluated in FZR1KO cells by monitoring the AURKA level in single-cell degradation assays. U2OS and FZR1 knockout cells were transiently transfected with Venus-tagged AURKA and were imaged 24 h after transfection. In FZR1KO cells, the AURKA protein level measured in single-cell degradation assays remained constant after anaphase onset, compared to the parental U2OS cell line **(Figure 4-6)**. This consistent with multiple reports that AURKA degradation is FZR1 dependent (reviewed in (Lindon et al., 2015)).

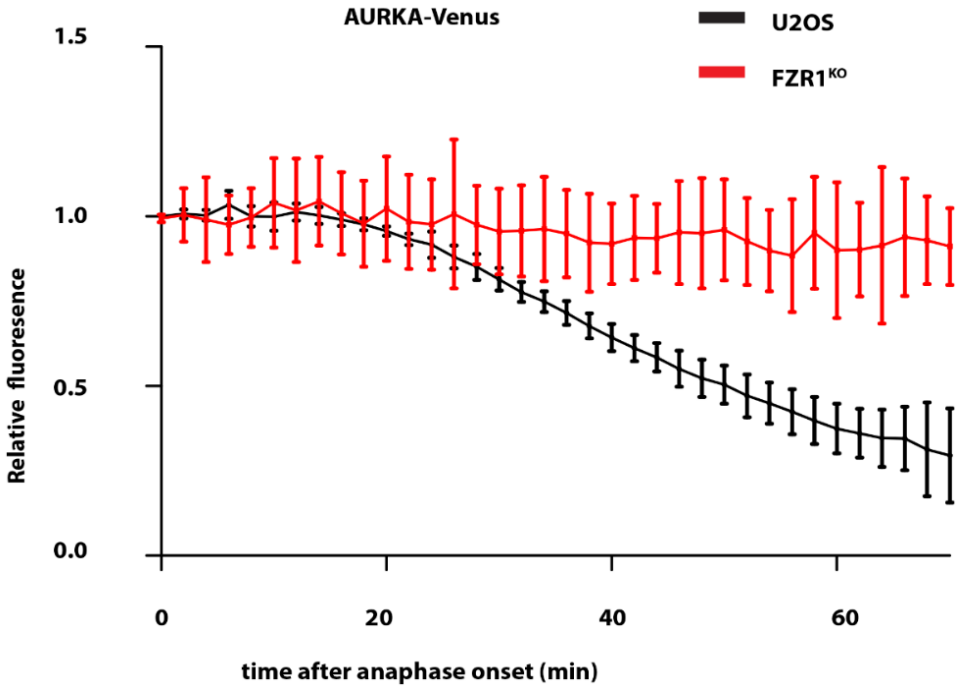

Figure 4-6 There is no destruction of AURKA in FZR1KO cells during mitotic exit. AURKA-Venus was transiently transfected into both U2OS and U2OS FZR1KO cells. Quantifications of total fluorescence measurements from single mitotic cells were used to generate degradation curves for AURKA-Venus. Fluorescence values for individual curves were normalized to the last frame before anaphase onset. n = 6 cells. Number of repeats n=3.

4.2.4 loss of pT288 AURKA at mitotic exit was identical in parental and FZR1KO cells

I next compared the loss of pT288 staining during mitotic exit between parental and FZR1KO cells. U2OS and FZR1 knockout cells were synchronized at mitosis by blocking with Eg5 inhibitor (5 μM STLC) and released by adding checkpoint inhibitor Mps1(10 μM AZ 3146). I found that the AURKA protein level remains constant in FZR1 knockout compared to the parental U2OS cell line. Surprisingly, loss of pT288 signal was identical in both cell lines despite the strong stabilization of the AURKA signal during mitotic exit in FZR1KO cells. AURKB was also stabilized over the time-course of the experiment but to a lesser extent, consistent with slower degradation of AURKB (Lindon et al., 2015). Moreover, I found that degradation of endogenous TPX2 at mitotic exits, like inactivation of AURKA, was insensitive to FZR1 knockout, and appeared more complete in FZR1KO cells. I examined Cdc20 levels in our extracts. Cdc20 is the activator of APC/C responsible for mitotic cyclin degradation that brings about mitotic exit, and itself becomes a target for APC/C-FZR1 once FZR1 is active. Cdc20 levels persist for longer during mitotic cells in FZR1KO cells, compared to the parental cells, I concluded that TPX2 level is not sensitive for FZR1 loss at mitotic exit **(Figure 4-7 A)**.

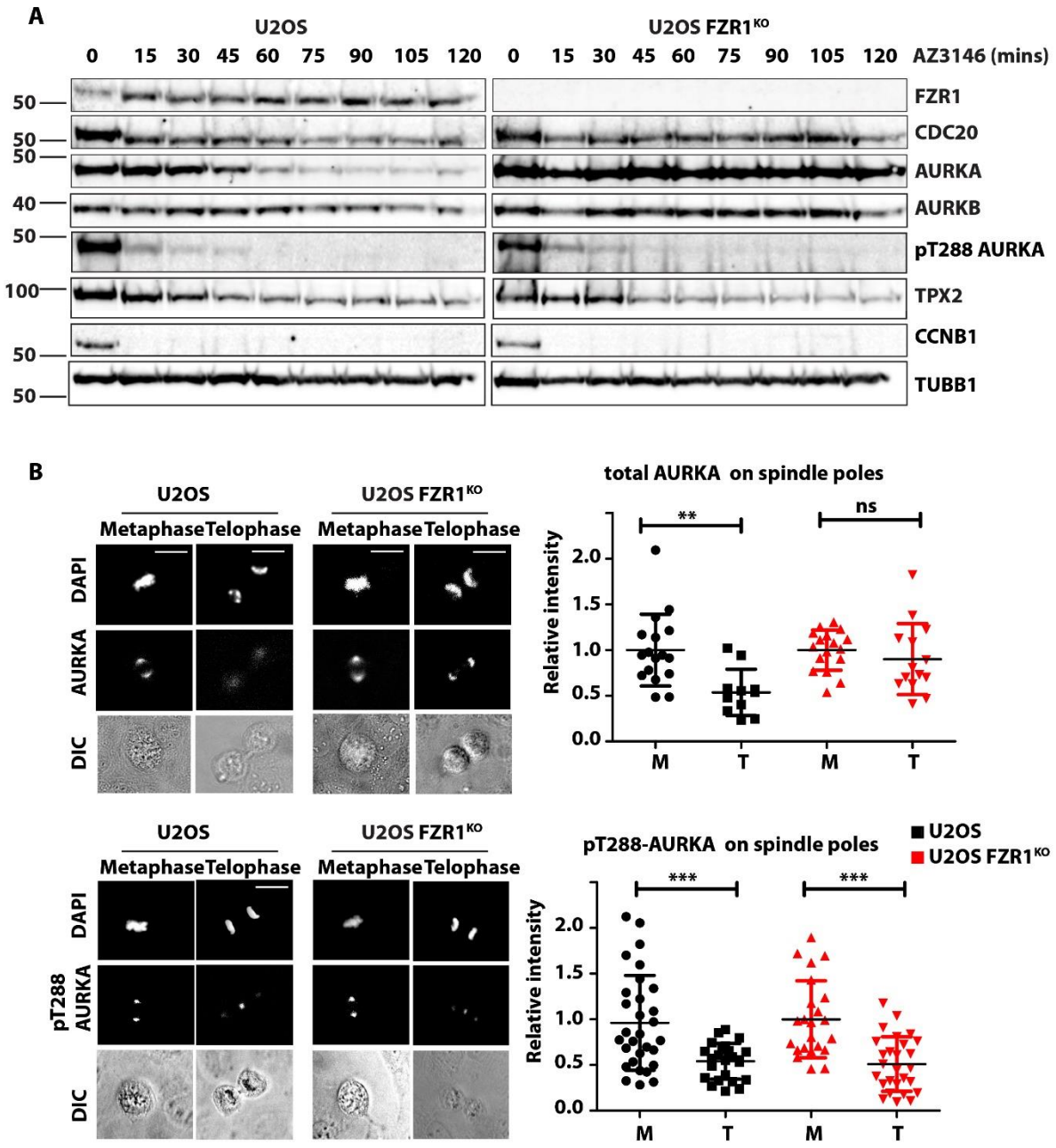

Figure 4-7 AURKA destruction is not required for pT288-AURKA down-regulation at mitotic exit. A) U2OS and FZR1KO cells were synchronized to prometaphase using 5 μM STLC and released by checkpoint inhibition using 10 μM AZ3146, with extracts harvested at times indicated. Lysates were analyzed by immunblot with antibodies against AURKA, pT288-AURKA and other mitotic regulators. **B)** pT288-AURKA and AURKA staining associated with individual centrosomes/spindle poles in metaphase (M) versus telophase (T) cells (left hand panels). Fluorescence intensity was significantly in telophase reduced compared with individual centrosomes in metaphase cells. Fluorescence values were measured and were presented as scatter plots, with mean ± S.D. indicated, for total AURKA and pT288-AURKA in both U2OS and FZR1KO. All values were normalized to the mean value from control metaphase cells. ns, non-significant; ** $p < 0.001$; *** $p < 0.0001$, Student's t-test. $n \geq 11$ from one experiment; $n \geq 23$ from two experiments. Bars, 10 μm.

Parental U2OS and FZR1KO cells were then fixed for quantitative immunofluorescence analysis of pT288-AURKA and total AURKA staining at spindle poles at metaphase and telophase. In this analysis, I found that AURKA persisted on spindle poles during mitotic exit in FZR1KO cells compared to parental U2OS **(Figure 4-7 B)**. In both cell lines, the presence of active AURKA, as measured by T-loop phosphorylation of the kinase (pT288), was strongly reduced after the onset of mitotic exit independent of the level of protein remaining **(Figure 4-7 B)**. This suggests that AURKA destruction is not required for its inactivation, and other mechanisms ensure a proper timing of AURKA inactivation.

Since the drop of AURKA kinase activity at mitotic exit was similar in the absence of its destruction, I asked whether there is any change in the duration of mitotic exit in FZR1 Knockout cells affecting our interpretation for AURKA activity? To answer this question, I first followed individual U2OS and FZR1 Knockout cells at higher magnification (40×; 2 frame/min) as they exit mitosis. In this study, I define the mitotic exit as that period between anaphase onset and the first signs of telophase (cytokinesis/membrane blebbing). I found that FZR1 Knockout does not prolong anaphase onset to cytokinesis **(Figure 4-8 A)**.

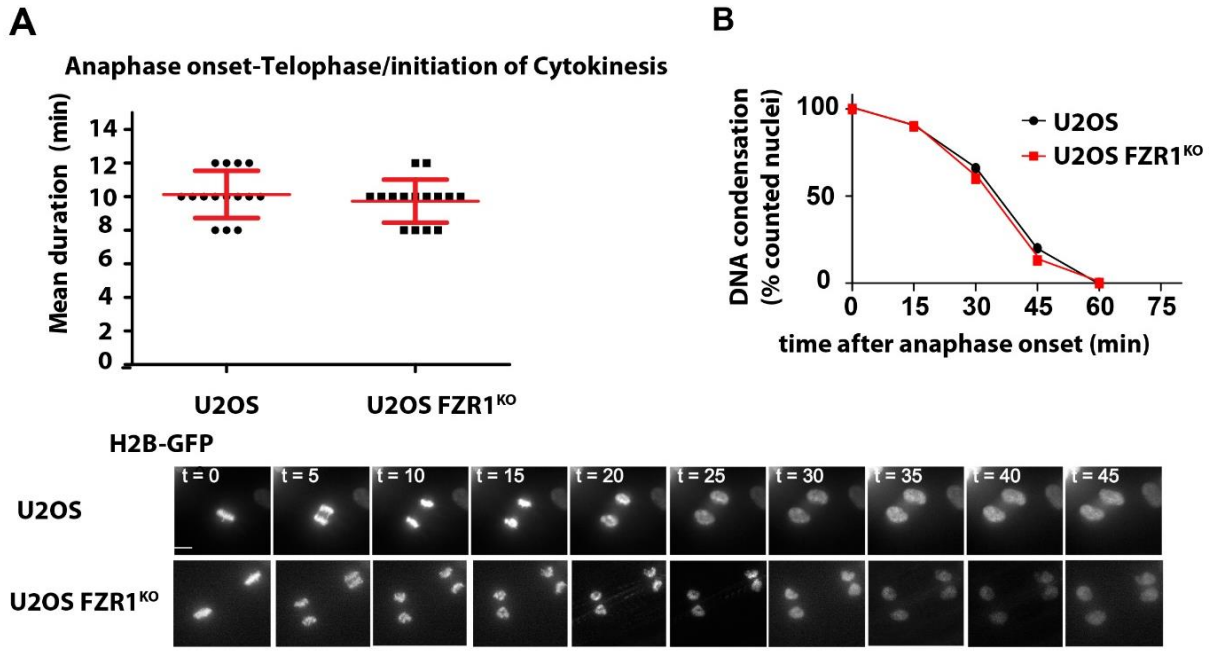

Figure 4-8 FZR1 activity is not required for timely progress through anaphase/telophase. A) Anaphase onset to telophase/cytokinesis is identical in WT U2OS and U2OS FZR1KO cells. Mean durations are presented as scatter plots, with mean ± S.D. P>0.05, non-significant (n.s), Student's t-test **B)** H2B-GFP was transiently transfected into both U2OS and U2OS FZR1KO cells. H2B-GFP fluorescence was used to score DNA as condensed or decondensed in cells undergoing mitotic exit. Images are of U2OS FZR1KO cells. Percentage of cells with condensed DNA over time was plotted as a measure of cumulative mitotic exit. P>o.o5, non-significant (n.s). n = 10 cells. Number of repeats n=2.

I next measured DNA de-condensation during unperturbed mitotic exit in parental and FZR1KO U2OS cells. Cells were transiently transfected with H2B-GFP and were imaged after 24hrs. I observed that there was no delay in mitotic exit in FZR1KO cells that could account for the stability of AURKA, measuring the elapsed time from anaphase onset to completed DNA de-condensation during unperturbed mitotic exit in parental and FZR1KO U2OS **(Figure 4-8 B)**. I concluded that mitotic exit is slightly accelerated in FZR1KO cells as previously reported using siRNA-mediated suppression of FZR1 (Floyd et al., 2008).

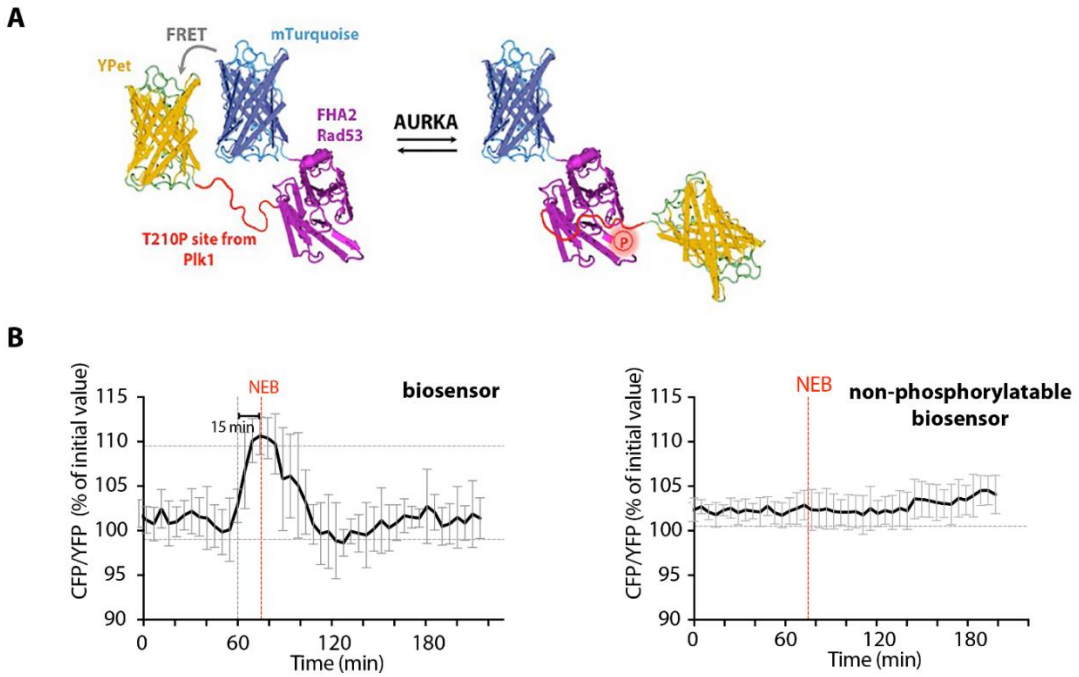

Figure 4-9 The AURKA biosensor detects AURKA activity during G2/M. A) Schematic illustration of AURKA biosensor showing high FRET (left) versus low FRET states (right). It consists of two fluorophores, a cyan fluorescent protein (mTurquoise) and yellow fluorescent protein (YPet), that are separated by the FHA2 domain (phospho-threonine binding domain) and as specific phosphorylation motif, the T210 motif from the T-loop of Plk1. **B)** Inverted FRET measurements (CFP/YFP emission) from time-lapse movies of cells expressing the biosensor, or a non-phosphorylatable version, show that the biosensor reports on mitotic phosphorylation events, $n \geq 8$. This figure prepared in collaboration with Olivier Gavet lab.

4.2.5 Validation of a new FRET AURKA biosensor for measuring its kinase activity

Several AURKA binding partners have been shown to affect the activity of AURKA, some acting independently of T-loop phosphorylation on T288, via distinct effects on its conformational dynamics (Lake et al., 2018; Ruff et al., 2018). Therefore, I used a new diffusible kinase biosensor for AURKA that was made available to me through collaboration with Dr Olivier Gavet (Institute Gustave Roussy, UMR9019-CNRS, France). The novel

biosensor was based on the well-established design of a fluorescent protein FRET pair separated by a phospho-threonine binding domain and specific phosphorylation motif (Violin et al., 2003), to provide a cell-wide readout of AURKA activity in living single cells as they progress through mitosis. It consists of two fluorophores, a cyan fluorescent protein (mTurquoise) and yellow fluorescent protein (YPet), that are separated by the FHA2 domain (phospho-threonine binding domain) and as specific phosphorylation motif, the T210 motif from the T-loop of Plk1 as a well-established target of AURKA (Macurek et al., 2008; Seki et al., 2008). When the sensor is phosphorylated by AURKA, it undergoes a conformation change that separates the cyan fluorescent protein (mTurquoise) – yellow fluorescent protein (YPet) pair and reduces the resonance energy transfer between YPet and mTurquoise **(Figure 4-9 A)**. To validate the FRET biosensor, U2OS cells were transiently transfection with the FRET AURKA biosensor and were imaged after 24hrs. I found that phosphorylation of the T210 motif in the biosensor causes reduction of FRET in mitotic cells, measured as an increase in CFP/YFP emission ratio of approximately 10%, in a manner dependent on its phosphorylation site **(Figure 4-9 B)**.

Olivier Gavet lab carried out extensive validation of the AURKA biosensor by testing its response to specific inhibitors of AURKA and AURKB. This work is recorded in Appendix 1. To determine whether AURKA inhibitors perturb AURKA FRET activity measured by the biosensor, I studied the effect of the pharmacological AURKA inhibitors MLN8237, MK51087, and AURKB inhibitor AZD1152 on FRET signal. U2OS cells were transfected with the AURKA-directed biosensor. Following the release double-thymidine block, cells were arrested in mitosis by treatment with MG132, then treated with AURKA- or AURKB-specific inhibitors. We found that the AURKA FRET signal significantly reduced to the pharmacological inhibition of the kinase activity of AURKA. We also observed some sensitivity to inhibitors of AURKB at higher doses indicating that the biosensor might not be completely specific to AURKA **(Appendix B -Figure B-1)**. This finding was not unexpected for a diffusible biosensor since some of the specificity in substrate phosphorylation by Aurora kinases is proposed to reside in the colocalization of the kinase with substrates (de Groot et al., 2015; Hegarat et al., 2011).

4.2.6 FRET-based biosensor reveals that Aurora kinase activity is independent of FZR1 at mitotic exit but becomes sensitive to FZR1 in interphase.

I next used FRET biosensor to compare AURKA activity during mitotic entry and exit in both U2OS and FZR1KO cells. To monitor the activity of AURKA in the absence of its

destruction, U2OS and FZR1KO cells were transiently transfected with FRET biosensor and were imaged 24 hrs after transfection. I found that FRET measurements in mitotic cells agreed with the analysis of pT288 staining showing that biosensor activity started to increase in late G2, peaking after NEB and decaying during mitotic exit. I also found that the increase in activity measured at mitotic entry was identical in individual U2OS and FZR1KO cells **(Figure 4-10 A, B)**: peak activity showed a small but not significant increase in FZR1KO cells. Moreover, if I normalized FRET signals to the anaphase onset value, the inactivation curves were directly superimposable **(Figure 4-10 C)**. I observed, however, that biosensor activity starts to increase again gradually in G1 in FZR1KO cells compared to parental U2OS cells and is significantly increased at 160 minutes after NEB **(Figure 4-10 B)**. I, therefore, conclude that the destruction of AURKA itself is not required for its timing of inactivation during the mitotic exit, but may be important to prevent re-activation early in the cell cycle.

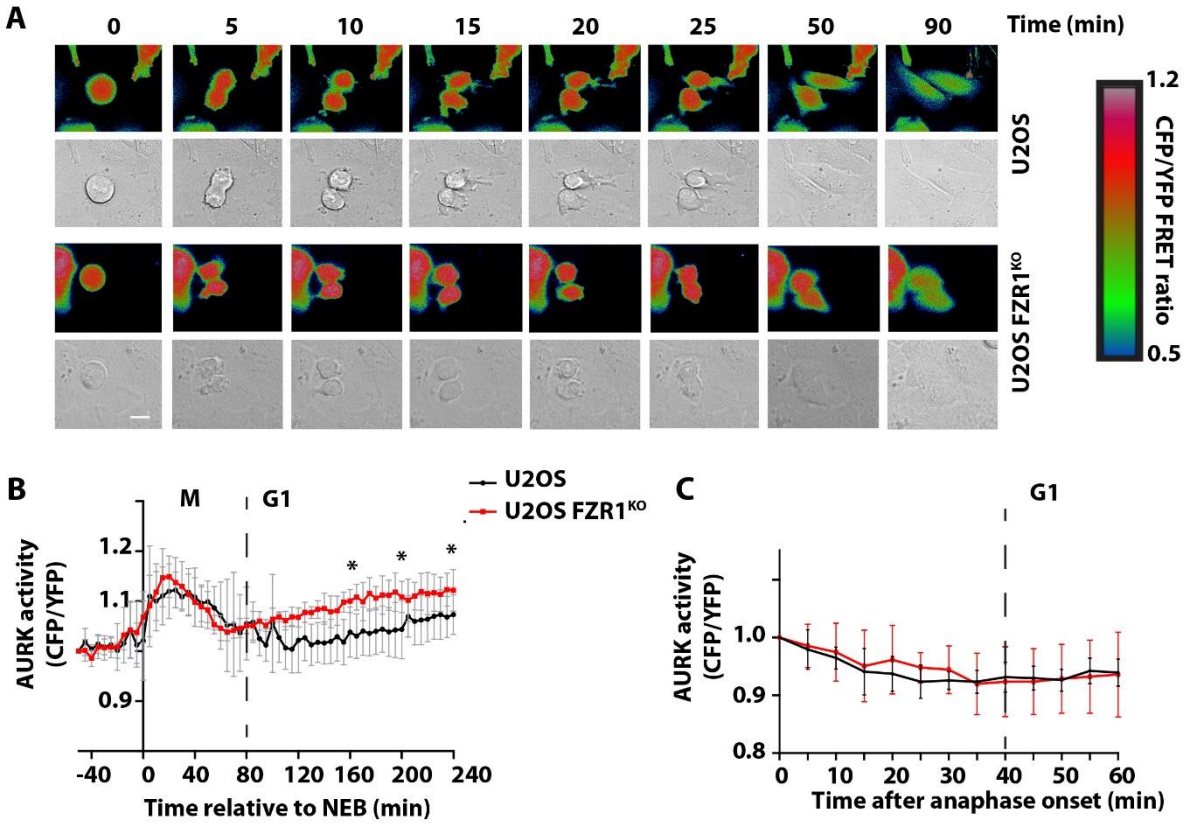

Figure 4-10 FRET-based biosensor records unaltered parameter of mitotic AURKA activation and inactivation in FZR1KO cells. **A)** Examples of inverted false-coloured FRET ratio of biosensor-expressing single U2OS and FZR1KO cells passing through mitosis: High FRET (blue) reports on non-phosphorylated state, whereas low FRET (red) reports on the phosphorylated probe. **B)** FRET ratio values measured using biosensor show AURK activity is normally regulated through mitosis in FZR1KO cells but rises again in G1 phase (*, $p < 0.05$,

Student's t-test). Curves were aligned on NEB, Data are means ± SD. **C)** FRET values normalized to anaphase onset. Data from two independent experiments.

4.2.7 TPX2 destruction is required for AURKA inactivation at mitotic exit

TPX2 has been previously shown to interact and stabilize AURKA against APC/C-FZR1-mediated degradation (Giubettini et al., 2011), and from this it was concluded that loss of interaction with TPX2 contributes to the timing of AURKA degradation in mitotic exit. Our previous result that AURKA degradation plays no role in its inactivation at mitosis led us to the hypothesis that loss of interaction with TPX2 might be directly responsible for inactivation as well as degradation of AURKA. If this were the case, then nondegraded TPX2 would cause delay in the timing of AURKA inactivation *in vivo*. To test this possibility, I used an N-terminal fragment of TPX2 (amino acids 1-43) known to be sufficient for binding and activating AURKA (Bayliss et al., 2003), but not degraded at mitotic exit. U2OS and FZR1KO cells were transiently transfected with TPX2(1-43-CFP) and AURKA activity was monitored during mitotic exit. Cells were synchronized using mitotic arrest and release protocol. I found that persistence of TPX2(1-43) through mitotic exit stabilized AURKA protein during mitotic exit in U2OS cells **(Figure 4-11 A, B)** as previously described (Giubettini et al., 2011). As expected, TPX2(1-43) showed no effect on AURKA levels in FZR1KO cells where the protein is not degraded **(Figure 4-12 A, B)**. Interestingly, I found a marked effect of TPX2(1-43) in stabilizing the pT288-AURKA signal during mitotic exit in both parental U2OS cells and FZR1KO cells **(Figure 4-11, 4-12)**. From these observations, I concluded that loss of interaction with TPX2 is the rate-limiting step in the inactivation of AURKA in mitotic exit.

4.2.8 Protein Phosphatase PP1 is required for AURKA inactivation at mitotic exit

Previous work has shown that phosphatase 1 (PP1) can negatively regulate AURKA through dephosphorylation of T288, and AURKA contains a functional PP1-binding motif within the C terminus. To confirm whether PP1 is required for AURKA inactivation in our assays where I measure AURKA inactivation through the loss of pT288. Tautomycin acid treatment was used to selectivity target PP1 at low concentrations. To examine its effect on pT288 AURKA activity at the mitotic exit, mitotic exit released U2OS cells were treated with 3nM tautomycin at different time points. I found that inhibition of the phosphatase, PP1, after mitotic exit also stabilized the pT288 signal **(Figure 4-13)**. These results demonstrated that dephosphorylation rather than destruction controls AURKA activity in mitotic exit.

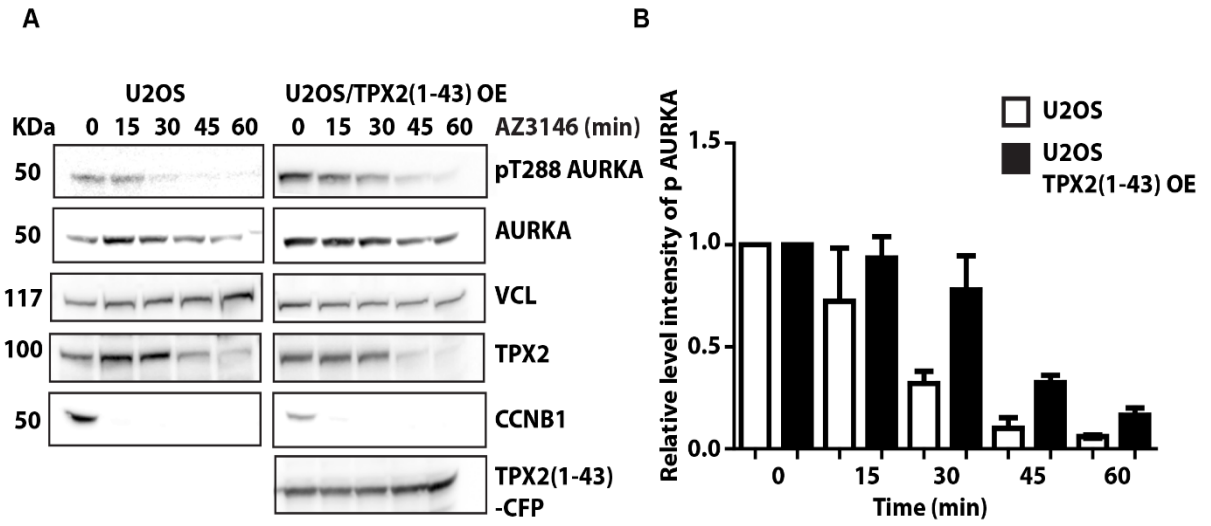

Figure 4-11 AURKA inactivation is controlled through TPX2 in U2OS cells. U2OS cells were transfected with TPX2(1-43)-CFP. Cells were synchronized at the metaphase by blocking with Eg5 inhibitor (5 μM STLC), then released by adding checkpoint inhibitor Mps1(10 μM AZ 3146) at different time points. **A)** Quantitative immunoblotting of cell lysates shows that loss of pT288-AURKA during mitotic exit is delayed in the presence of TPX2(1-43) in parental U2OS cells. Thirty micrograms of protein were loaded per lane, separated by SDS-PAGE and blotted with pT288, total AURKA, Vinculin (VCL), Cyclin B1 (CCNB1), GFP and TPX2. Cyclin B1 (CCNB1) is used as marker for mitotic exit, level of vinculin (VCL) as loading control. **B)** pT288 signal normalized against vinculin. Bar charts. Results presented are mean values from 2 independent experiments ± S.D. Number of repeats n=3.

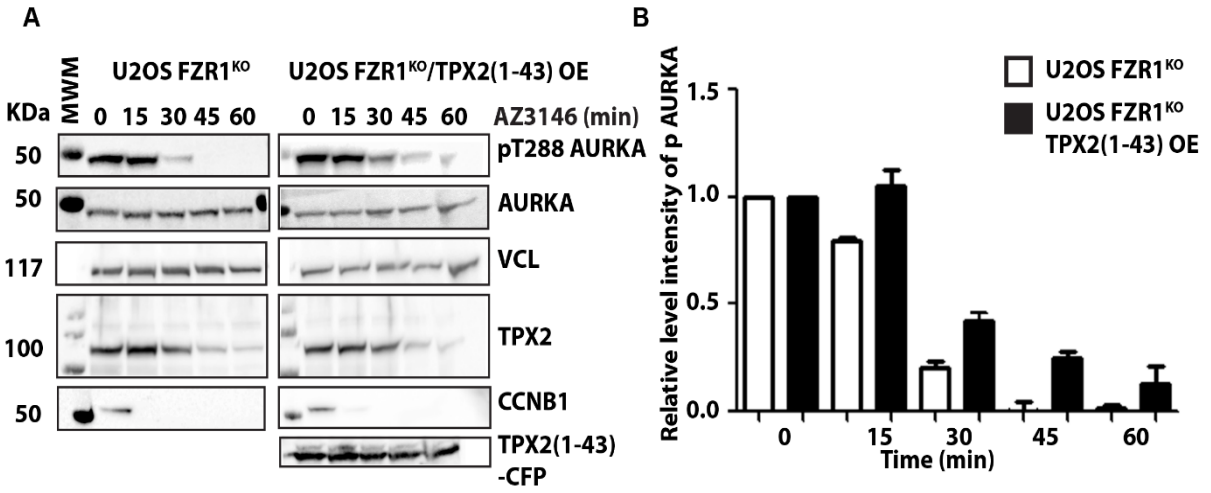

Figure 4-12 AURKA inactivation is controlled through TPX2 in FZR1KO cells. FZR1KO cells were transfected with TPX2(1-43)-CFP and synchronized through mitotic exit as described in material and methods. **A)** Quantitative immunoblotting of cell lysates shows that loss of pT288-AURKA during mitotic exit is delayed in the presence of TPX2(1-43) in FZR1KO cells. Thirty micrograms of protein were loaded per lane, separated by SDS-PAGE and blotted with pT288, total AURKA, Vinculin (VCL), Cyclin B1 (CCNB1), GFP and TPX2. Cyclin B1 (CCNB1) is used as marker for mitotic exit, level of vinculin (VCL) as loading control. **B)** pT288 signal normalized against vinculin. Bar charts. Results presented are mean values from 2 independent experiments ± S.D. Number of repeats n=3.

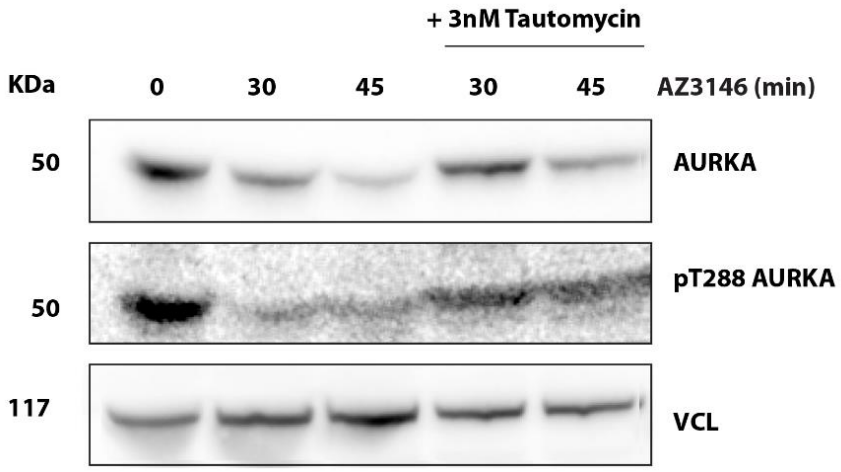

Figure 4-13 PP1 inhibition blocks AURKA inactivation at the mitotic exit. U2OS cells undergoing mitotic exit were treated with 3 nM PP1 inhibitor tautomycin 10 minutes after release of SAC arrest by AZ3146. Lysates harvested at the indicated time points after AZ3146 treatment were subject to immunoblot analysis. Thirty micrograms of protein were loaded per lane, separated by SDS-PAGE and blotted with pT288, total AURKA, and Vinculin (VCL). Number of repeats n=2.

4.2.9 AURKA inactivation in G1 depends on its destruction

If AURKA destruction at mitotic exit is not required to inactivate the kinase, then what is it for? I had observed a small but significant increase in the accumulation of Aurora kinase biosensor activity following mitotic exit in FZR1KO cells **(Figure 4-10B)**. I further examined whether FZR1-mediated destruction of AURKA is required for its inactivation during interphase. Using both AURKA and AURKB biosensors (Fuller et al., 2008) and pT288 staining, I examined Aurora kinases activity in cells arrested at the G1/S boundary. U2OS and FZR1KO cells were transiently transfected either with AURKA or AURKB biosensor, then cells were synchronized in G1/S by double thymidine block. I found that Aurora kinase activity measured by the AURKA-specific biosensor was increased in FZR1KO cells compared to the parental cells. This increase was abolished by treatment with MLN8237 **(Figure 4-14A)**. The AURKB-specific sensor was insensitive to MLN8237 at the dose used **(Figure 4-14B)**, indicating that our AURKA biosensor indeed measures increased AURKA activity at interphase in FZR1KO cells. I also fixed parental U2OS and FZR1KO cells synchronized in G1/S for quantitative immunofluorescence analysis of pT288-AURKA and γ-Tubulin. Consistent with our biosensor data, I found that pT288 stained centrosomes in interphase FZR1KO cells but not parental U2OS **(Figure 4-14C)**.

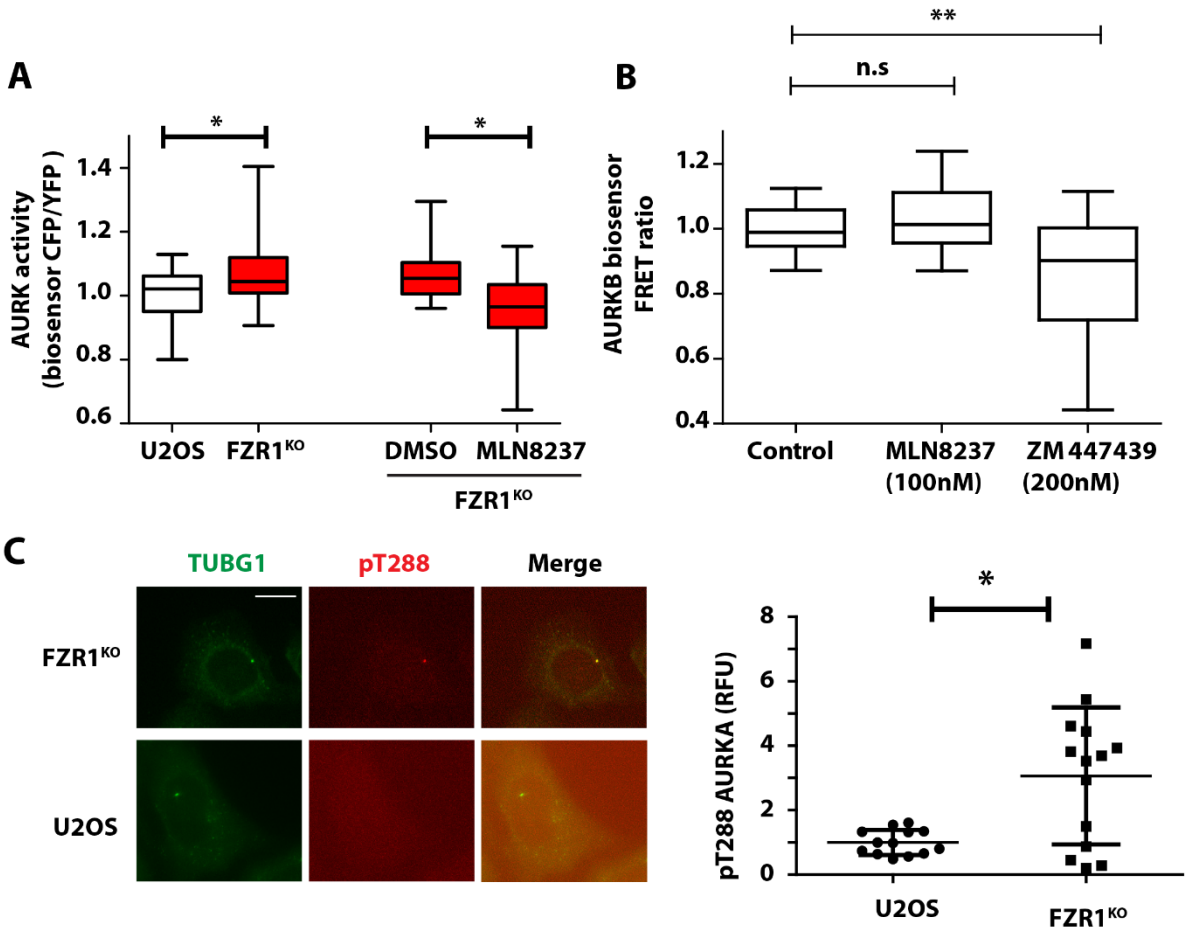

Figure 4-14 Destruction of AURKA by APC/C/FZR1 is required to inhibit interphase activity of AURKA. A) FRET biosensor reveals increased Aurora kinase activity in interphase FZR1KO cells. Cells were synchronized in G1/S using double thymidine block and treated with/without 100 nM AURKA inhibitor MLN8237 for 3 hours. Scatter plots show CFP/YFP emission ratios with mean ± S.D. from individual cells in U2OS and FZR1KO populations (n = 20; $p < 0.05$, Student's t-test) and are representative of two independent experiments. **B)** Activity of AURKB-directed biosensor in interphase FZR1KO cells is insensitive to 100 nM AURKA inhibitor MLN8237 that is sufficient to inhibit activity of an AURKA-directed sensor. FZR1KO cells were arrested at G1/S by double thymidine block and treated with MLN8237 and ZM447439 for 3 hours at indicated doses. FRET values calculated for individual cells and normalized against the population mean are shown as scatter plots with mean ± S.D. indicated for each condition. **, $p < 0.001$, Mann-Whitney U-test. **C)** pT288 staining in fixed cells synchronized at G1/S, and scatter plots show that pT288 can be detected at centrosomes of G1/S FZR1KO cells, but not at centrosomes of parental U2OS cells. ***, $p \leq 0.0001$, $n \geq 21$, Student's t-Test. RFU, Relative Fluorescence Units. Number of repeats n=2.

4.3 Discussion

In this study, I investigated the contribution of AURKA degradation to the timing of its inactivation during mitotic exit and interphase. AURKA activity increases during mitosis in parallel with the protein level and both drop during mitotic exit (Afonso et al., 2017; Floyd et al., 2008). I observed, however, that AURKA inactivation proceeds much faster than the

destruction of the protein during mitotic exit. Despite the expectation that non-degradable AURKA might retain some activity during mitotic exit, I find that the kinase activity in FZR1KO cells decreased at end of mitosis as rapidly as in parental cells. Moreover, the FRET biosensor revealed that FZR1 instead suppresses AURKA activity in late G1. Therefore, I concluded that AURKA degradation is not required for its inactivation in late mitosis but required in interphase. Our finding implies that there must be an additional mechanism regulating the timing of AURKA inactivation during mitotic exit.

The microtubule-binding protein TPX2 has been previously shown to regulate AURKA localization and activity protecting it from the action of PP1 phosphatase (Bayliss et al., 2017; Bayliss et al., 2003) during mitosis. Our result showed that TPX2 was degraded normally in FZR1KO cells as compared to the parental cells, suggesting that TPX2 degradation may play a role in the timing of AURKA inactivation. Importantly, I find that overexpression of an N-terminal TPX2 fragment sufficient for AURKA binding, but not degraded at mitotic exit, caused a delay in AURKA inactivation, which I showed to be a PP1-dependent event, as expected. Our results are consistent other reports that TPX2 is a substrate for APC/C at mitotic exit (Min et al., 2014; Singh et al., 2014) a conclusion that implies that TPX2 destruction plays a critical role in the release of AURKA to be accessible for PP1-mediated inactivation (Bayliss et al., 2003). Therefore, I suggest that AURKA inactivation in mitotic exit is determined not by its destruction, but by the degradation of its activator TPX2 and therefore likely dependent on Cdc20 rather than FZR1.

Our studies also revealed that APC/C-FZR1-mediated destruction of AURKA is critical for suppression of its activity at interphase. A growing body of literature in recent years has started to reveal the importance of interphase roles of AURKA in both healthy and cancer cells (Bertolin and Tramier, 2020; Damodaran et al., 2017; Nikonova et al., 2013), and experiments I carried out to explore one of these are described in the following chapter. Identifying these physiological consequences will further clarify AURKA oncogenic activity associated with various types of cancer in the absence of gene amplification.

Chapter 5 Regulation of mitochondrial morphology by control of AURKA stability

5.1 Introduction

In the previous chapter, I have identified that AURKA destruction is required to regulate its kinase activity at interphase. AURKA was originally reported as a mitotic regulator, however, additional nonmitotic functions have been identified throughout interphase and at different organelles (Pugacheva et al., 2007; Wu et al., 2016). One of its pivotal functions is the promotion of mitochondrial fragmentation. Mitochondria is a highly dynamic organelle that undergoes fission and fusion. During mitosis, mitochondria are fragmented into smaller subunits and are segregated between the daughter cells to ensure their viability. AURKA acts as an upstream regulator to direct the activity of CDK1/cyclin B to activate DRP1, and therefore achieve mitochondrial fragmentation (Kashatus et al., 2011). But that work does not address how AURKA destruction influences mitochondria reassembly after cell division. Imbalances in the signaling pathways governing mitochondrial fission and fusion are commonly associated with tumor development to control the adoption of distinct metabolic programs. For example, mitochondrial fragmentation in various types of cancer (Serasinghe et al., 2015) augments glycolysis to provide energy supply, a phenomenon termed as “the Warburg effect” (Wai and Langer, 2016). Given that AURKA influences mitochondrial morphology and the well-documented overexpression of AURKA in tumors, I examined whether the AURKA level correlates with the mitochondrial fragmentation in different cancer cell lines. I also investigated the contribution of the AURKA N-terminal domain in regulating mitochondrial fragmentation. Finally, in order to define the physiological consequences of endogenous nondegradable AURKA on mitochondrial fragmentation, I analysed changes in mitochondrial morphology in FZR1KO at G1.

5.2 Results

5.2.1 Assessing the correlation between AURKA level and mitochondrial fragmentation in different breast cancer cells.

Previous work in the lab had shown that AURKA activity promotes mitochondrial fragmentation (Grant et al., 2018). Fragmented mitochondrial networks are a characteristic of

cancer cells. Whether AURKA overexpression in cancer would be a cause of mitochondrial fragmentation seen in cancer cells is not clear yet. Therefore, I examined if there was a correlation between AURKA level and mitochondrial phenotype in different cancer cells. To address this question, different breast cancer cells were stained with 100nm MitoTracker CMXRos for 15 min and were imaged live using epifluorescence microscopy. Breast cancer cell lines showed different mitochondrial length **(Figure 5-1 A)**. The differential expression level of AURKA and its activator TPX2 was then analysed by immunoblotting in unsynchronized cells. I found that MCF10A (non-transformed cell line) contains a highly interconnected mitochondria network and a low AURKA level. An epithelial transformed cell line, MDA-MB-157, showed a highly interconnected mitochondrial network and higher expression of AURKA relative to the non-transformed MCF10A. Others, like T47D cells and HCC1143, contain highly fragment mitochondria and a low level of AURKA.

These observations indicate that the level of AURKA in the tested cancer cell line does not show an apparent correlation to the fragmented mitochondria **(Figure 5-1 B, C, D).** Strikingly, the HCC1143 cell line which displays highly fragmented mitochondria accompanied by high levels of TPX2 **(Figure 5-1 D)**. I cannot exclude that AURKA activity may correlate with the mitochondrial morphology. It is possible that the requirement of AURKA interphase activity may be dependent on other activators. Another possibility would consider that the correlation may be dependent on AURKA mitochondrial pool. Therefore, AURKA FRET biosensor targeted to the mitochondria would be a useful tool to verify association between AURKA and mitochondrial fragmentation in cancer cells.

5.2.2 AURKA modulates mitochondrial morphology.

I selected two cell lines, MCF10A, and HCC1143 with different mitochondrial phenotypes, expressing an endogenous low and high level of AURKA, respectively. I tested whether the mitochondrial phenotype is affected when AURKA is overexpressed or inhibited. To answer this question, MCF10A cells were transiently transfected with AURKA-Venus or Venus only and stained with MitoTracker Red CMXRos for live imaging after 24hrs **(Figure 5-2 A)**. An analysis of mitochondrial length revealed that MCF10A cells overexpressing AURKA-Venus have a shorter mitochondrial length compared to the control **(Figure 5-2 B)**, indicating that AURKA promotes mitochondrial fragmentation.

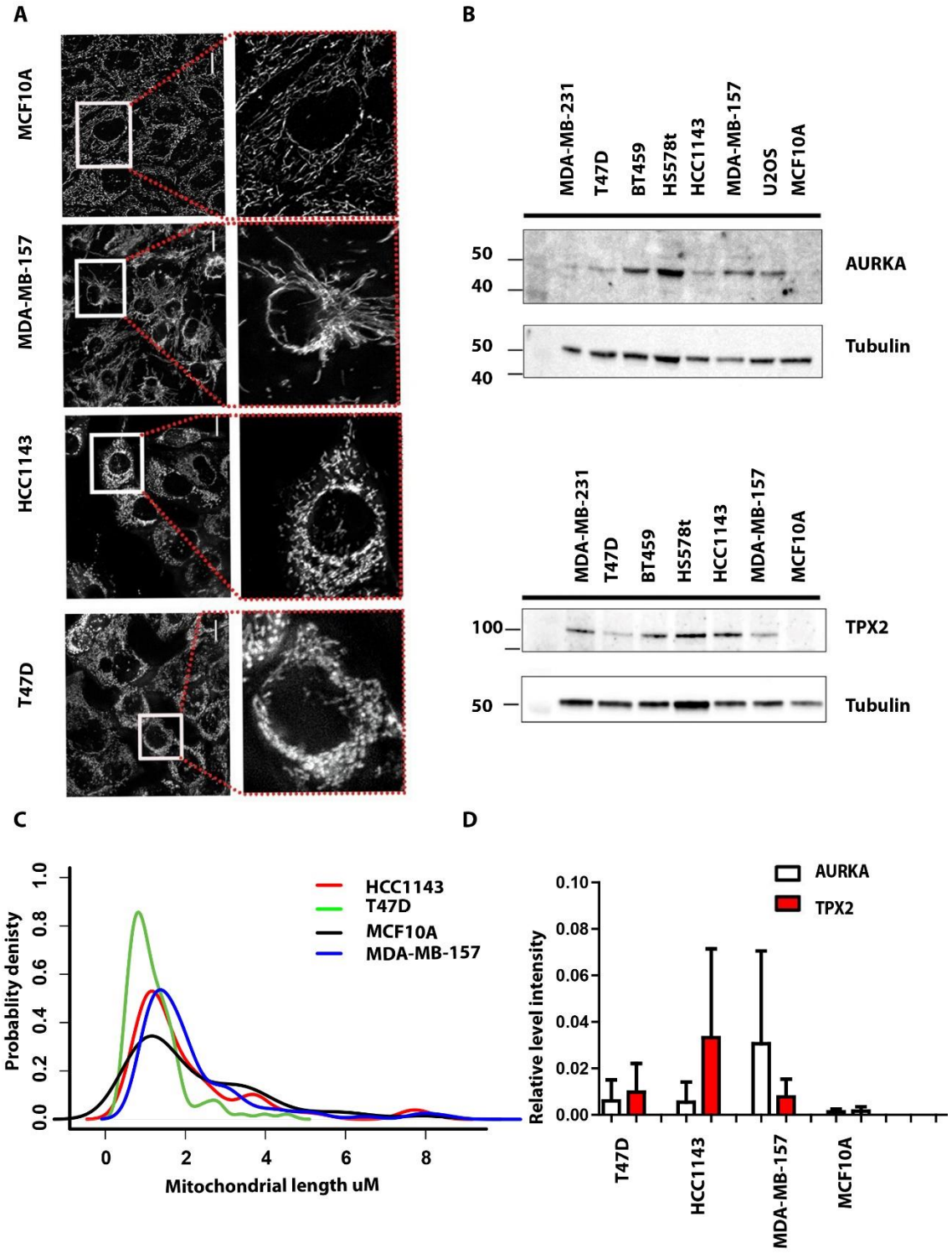

Figure 5-1 AURKA level shows no correlation with mitochondrial phenotype in cancer cells. A) Representative live images of Mitochondria in various cancer cell lines stained with 100nm MitoTracker CMXRos segmented using Micro-P software. **B)** Western blots of AURKA and its activator TPX2 in various cancer cell lines. Cell lysates were collected from different cell lines. Samples were analyzed by SDS-PAGE followed by immunoblotting of AURKA, TPX2, and alpha-tubulin. **C)** Kernel density plot of Micro-P mitochondria length quantification measurements. Scale bar: 25 µm. **D)** Quantification of the western blots in cancer cell lines relative to tubulin. Number of repeats n=3.

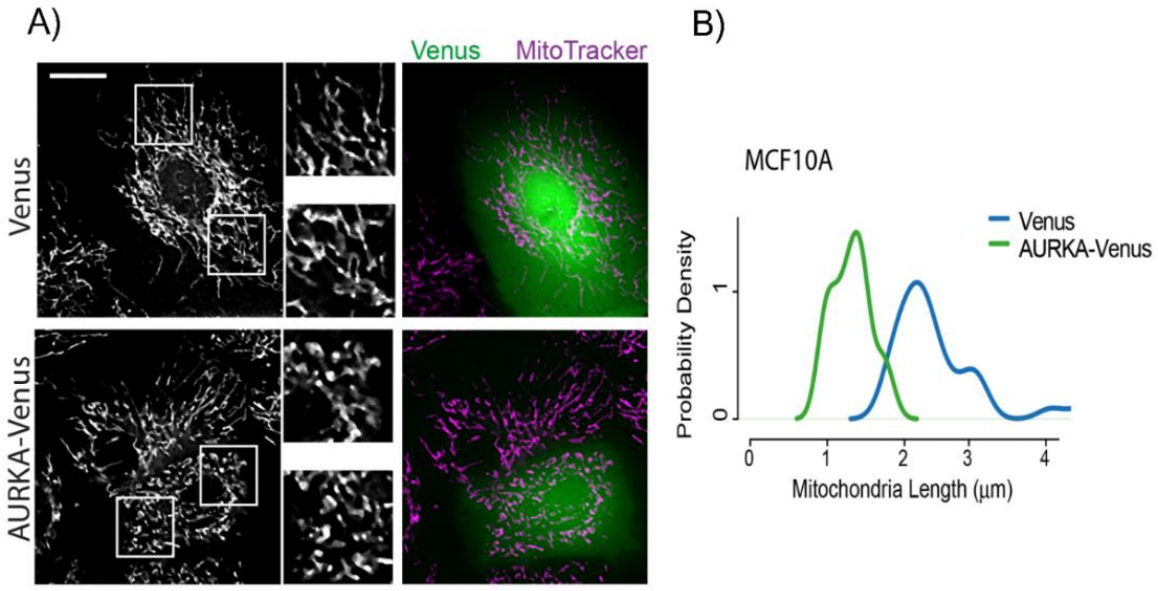

Figure 5-2 AURKA overexpression induces mitochondrial fragmentation. A) MCF10A were transiently transfected with a plasmid expressing AURKA-Venus or Venus only, and stained with MitoTracker Red CMXRos for live imaging after 24hr from transfection. **B)** Mitochondrial tubular length measurements are measured using micro-P and plotted as probability density curves (***) $P<0.001$ for maximal deviation $D=0.45$, Kolmogorov-Smirnov test (K-S). Scale bars 10 μm. Number of repeats n=2.

To determine the effect of AURKA inhibition on mitochondrial fission, I treated the HCC1143 cancer cell line that has highly fragmented mitochondria with AURKA inhibitor (100nM MLN8237), or DMSO as a control for 3 hrs before staining with MitoTracker Red CMXRos for live imaging **(Figure 5-3 A)**. I found that the mitochondrial length was longer in the presence of AURKA inhibitor (MLN8237), as compared to the control **(Figure 5-3 B)**. From these novel data, I conclude that AURKA activity is required for mitochondrial fragmentation.

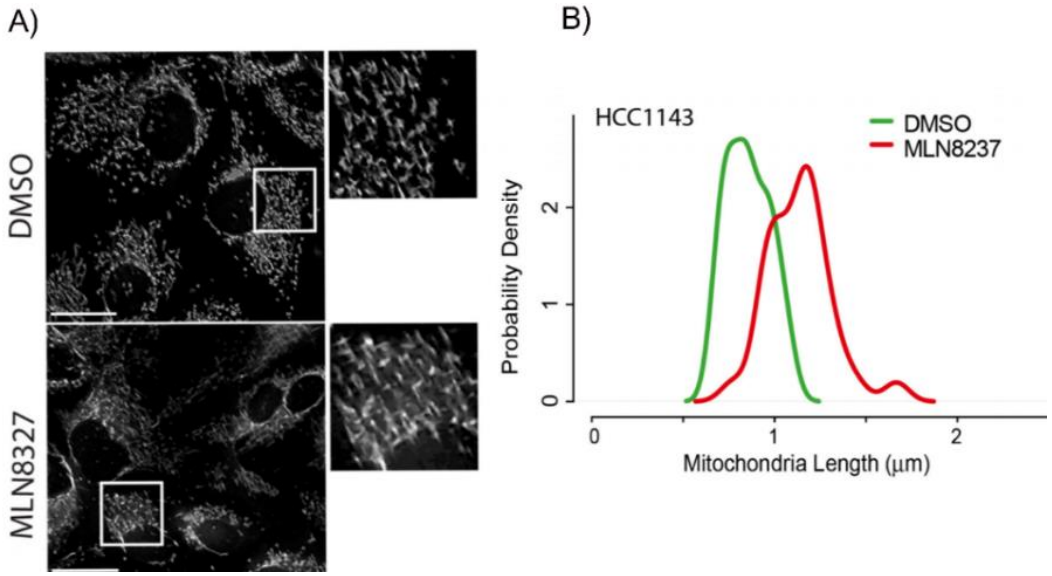

Figure 5-3 AURKA inhibition blocks mitochondrial fragmentation in the HCC1143 cancer cell line. A) HCC1143 cells with highly fragmented mitochondria were treated with 100nM MLN8237, or DMSO control treatment, for 2hrs before staining with MitoTracker Red CMXRos for live imaging. B) Mitochondrial tubular length measurements are measured using micro-P and plotted as probability density curves (***) $P<0.001$ for maximal deviation $D=0.21$, K-S test. Scale bars 10 μm. Number of repeats n=3.

5.2.3 APC/C-FZR1 regulates AURKA-dependent changes in mitochondrial morphology during interphase.

Work from Horn and co-authors has demonstrated that APC/C-FZR1 regulates mitochondrial reassembly at G1. They concluded that this effect may depend on the ability to target Drp1, a known regulator of the mitochondria fragmentation, for degradation. However, our previous work had showed that AURKA regulates mitochondrial morphology, and that whereas AURKA is a target of FZR1, our lab unpublished mass spectroscopy data indicate that Drp1 levels are unaffected in FZR1KO cells (Begum Akman, unpublished data). In previous chapter, I showed that the destruction of AURKA by APC/C-FZR1 is required for kinase inactivation during interphase, but not at the mitotic exit. Therefore, I asked whether alteration of AURKA activity in the interphase contributes to the changes in the mitochondrial morphology mediated by APC/C-FZR1. The mitochondrial morphology was compared between FZR1KO and parental U2OS cells. During the G1/S border in the cell cycle, mitochondria normally form an interconnected long network. Therefore, FZR1KO and parental U2OS were synchronized at G1/S by double thymidine treatment and stained with MitoTracker Red CMXRos for live imaging **(Figure 5-4 A)**. I found that FZR1KO cells have highly fragmented mitochondria in comparison to the parental U2OS **(Figure 5-4 A, B)**. Mitochondria morphology was then classified into two subtypes: fragmented globules, and tubular.

Morphological subtyping of mitochondria showed a significant increase in the percentage of fragmented globules and a significantly reduced tubular in FZR1KO cells **(Figure 5-4 C)**.

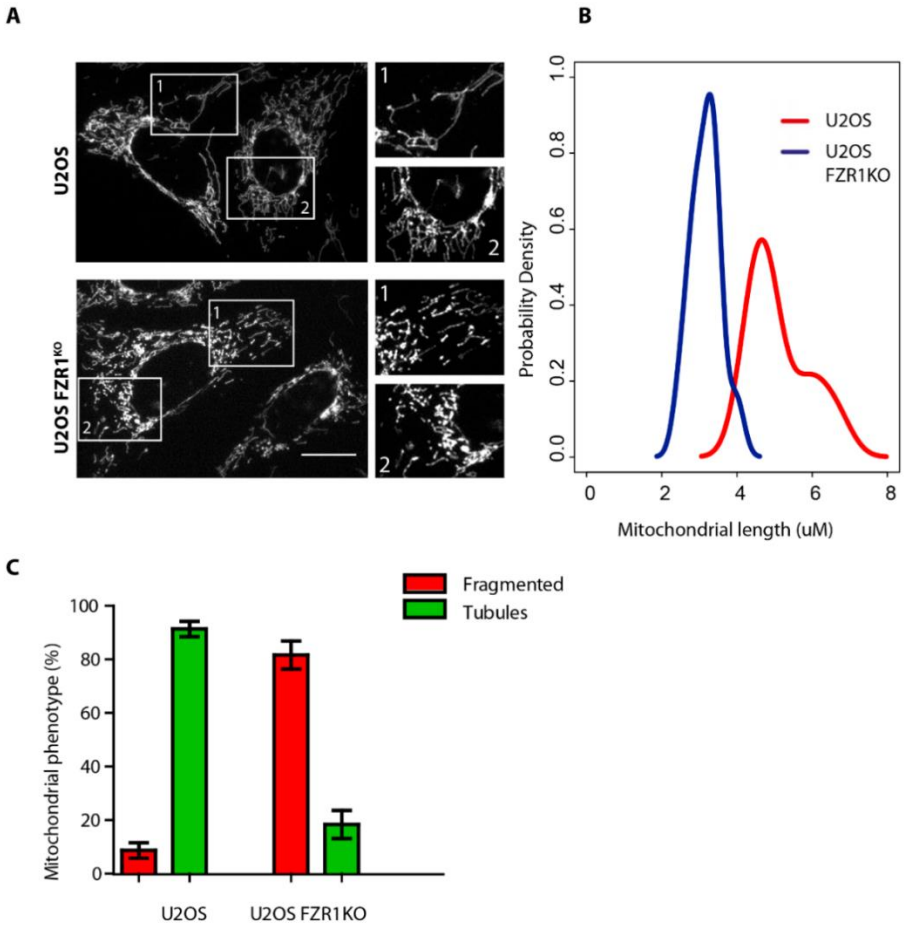

Figure 5-4 Mitochondria are over-fragmented in interphase FZR1KO cells. A) U2OS and FZR1KO cells were synchronized in G1/S then stained with MitoTracker® and imaged live B) Mitochondrial tubular length are measured using micro-P and are plotted as probability density curves (***) P<0.0001 for maximal deviation D=1, K-S test. Scale bars 10 μm. Number of repeats n=2.

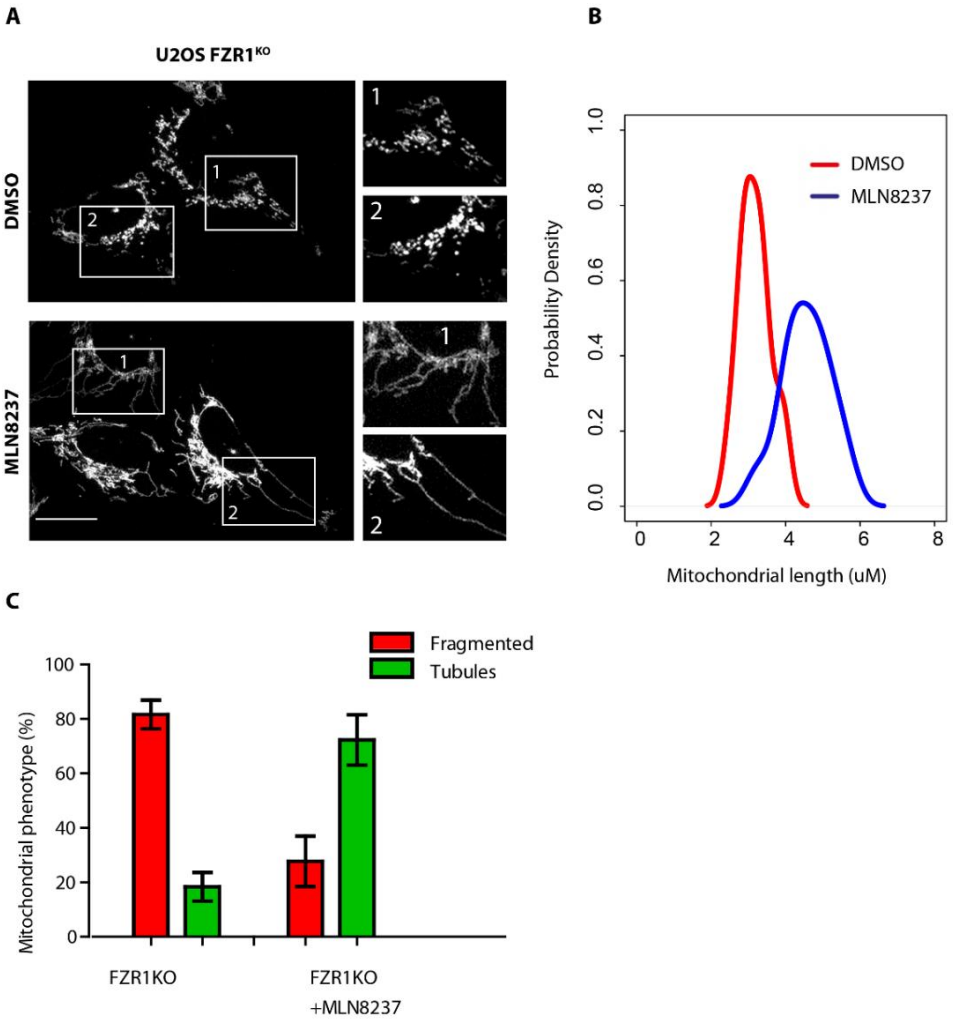

Figure 5-5 Mitochondria are over-fragmented in interphase FZR1KO cells in an AURKA-sensitive manner. A) U2OS and FZR1KO cells were synchronized in G1/S then stained with MitoTracker® and imaged live. FZR1KO cells were treated with DMSO or 100nM MLN8237 for 3 hours Scale bars, 10 μm. B) Mitochondrial tubular length measurements are plotted as probability density curves (***) P<0.0001 for maximal deviation D=0.866, K-S test. Scale bars 10 μm. Number of repeats n=2.

Based on our observation that knockout of FZR1 increases AURKA protein level and activity in interphase, I tested whether the observed effect of FZR1 on mitochondrial morphology is AURKA dependent. To address this question, the mitochondrial morphology was examined in FZR1KO cells arrested at G1/S. FZR1KO cells were treated with AURKA inhibitor 100nM MLN8237, or DMSO as a control for 3 hrs prior to staining with MitoTracker CMXRos for live imaging **(Figure 5-5 A)**.

Interestingly, I found that inhibition of AURKA activity completely rescued mitochondrial length and morphology in FZR1KO cells **(Figure 5-5 A, B, C)**, consistent with data showing AURKA to be an upstream regulator of DRP1 (Bertolin et al., 2018; Kashatus et al., 2011).

Since FZR1KO stabilizes AURKB as well as AURKA. Moreover, MLN8237 can inhibit AURKB at higher concentrations. I next examined whether AURKB also contributes to the regulation of mitochondrial morphology in FZR1KO cells. To answer this question, FZR1KO cells were synchronized in G1/S by double thymidine block and treated with an AURKB-specific inhibitor (ZM447439). I found that the treatment of FZR1KO cells with an AURKB-specific inhibitor did not affect mitochondrial morphology **(Figure 5-6 A, B)**. Therefore, I conclude that the regulation of mitochondrial morphology by APC/C-FZR1 is dependent on AURKA.

5.2.4 APC/C-FZR1 regulates AURKA levels, but not DRP1.

Since increasing the stability of DRP1 may cause mitochondrial fragmentation, I wondered whether the DRP1 level increases in FZR1KO cells at G1/S. To answer this question, I synchronized FZR1KO cells at G1/S by double thymidine treatment. AURKA and DRP1 levels were analysed by immunoblotting. I found no alteration in DRP1 levels in FZR1KO cells as compared to the parental cells **(Figure 5-7 A)**.

APC/C substrates are usually degraded at mitotic exit. To determine whether DRP1 is an APC/C substrate and degraded in U2OS cells exiting from mitosis. U2OS cells were synchronized for prometaphase with Eg5 inhibitor (5 μM STLC), then treated with Mps1 inhibitor (10 μM AZ3146) to override SAC-mediated mitotic arrest. I observed a drop in the DRP1 level during mitotic exit in parental cells **(Figure 5-7 B)**. This suggests that it could be a substrate for APC/CCdc20, or another ubiquitin ligase. I concluded that APC/C-FZR1 regulates mitochondrial dynamics by preventing AURKA reactivation in interphase, independent of DRP1.

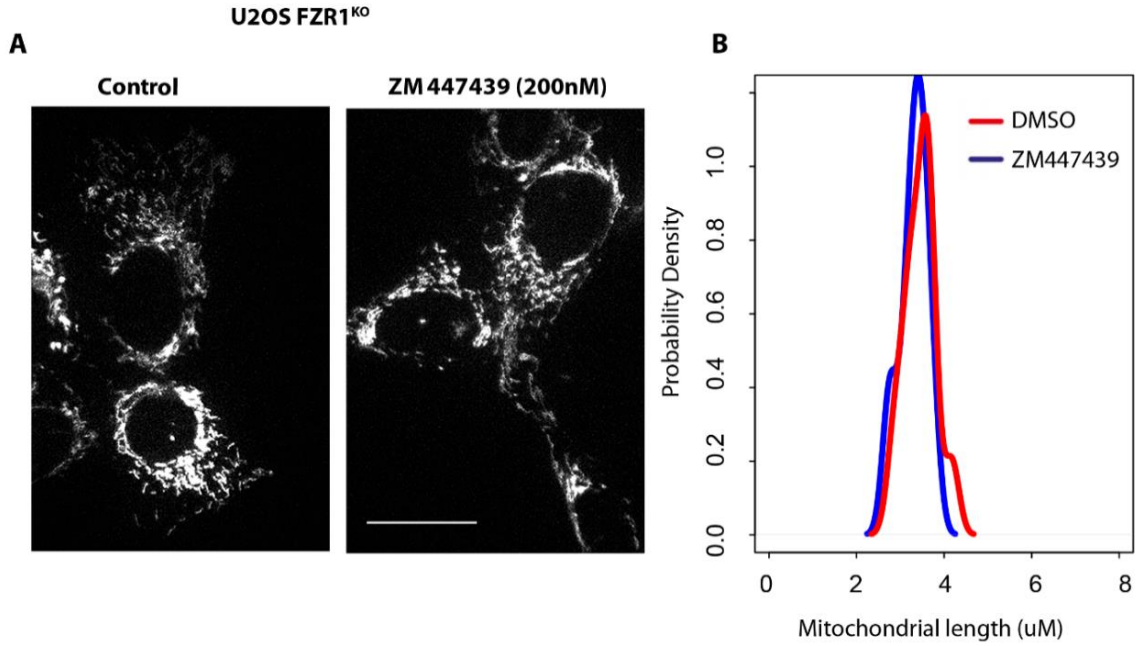

Figure 5-6 Fragmented mitochondria in interphase FZR1KO cells is not affected by AURKB inhibition. A) U2OS and FZR1KO cells were synchronized in G1/S then stained with MitoTracker® and imaged live. FZR1KO cells were treated with DMSO or 100nM MLN8237 for 3 hours Scale bars, 10 μm. B) Mitochondrial tubular length measurements are plotted as probability density curves P>0.84 for maximal deviation D=0.25, K-S test. Scale bars 10 μm. Number of repeats n=2.

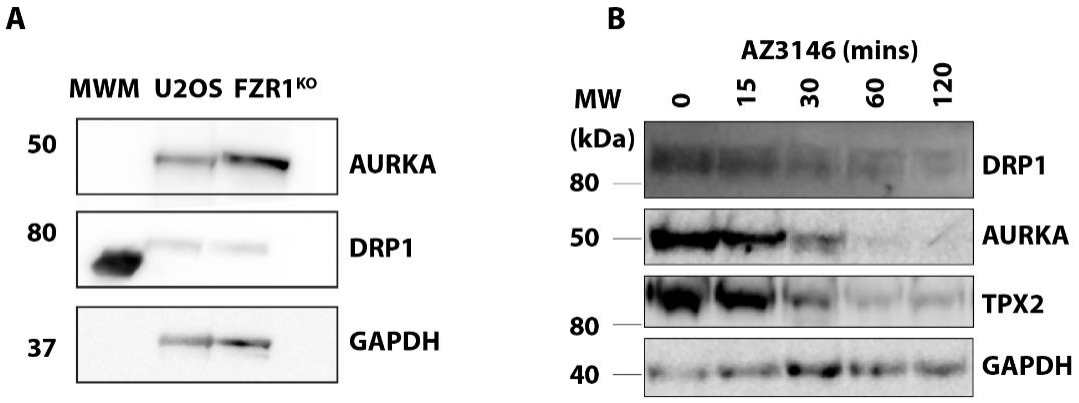

Figure 5-7. FZR1 regulates AURKA level but not DRP1 in G1. A) Levels of the DRP1 at G1/S boundary. U2OS were arrested at G1/S by double thymidine treatment. Immunoblotting U2OS and FZR1KO cells shows that DRP1 levels, unlike those of AURKA, are not altered in FZR1KO cells. Thirty micrograms of protein were loaded per lane, separated by SDS-PAGE and blotted with DRP1, AURKA, and GAPDH B) DRP1 undergoes modest degradation during mitotic exit. U2OS cells were synchronized in 5 μM STLC and released by checkpoint inhibition using 10 μM AZ3146, with extracts harvested at times indicated. Thirty micrograms of protein were loaded per lane, separated by SDS-PAGE and blotted with DRP1, AURKA, TPX2, and GAPDH. Number of repeats n=2.

5.3 Discussion

Mitochondria are dynamic organelles that change shape through the balance between fission and fusion events. Changes in the balance of fission-fusion enable cells to modulate mitochondrial size and adopt distinct metabolic activities that are required for cellular functions (Tilokani et al., 2018). The rate of mitochondrial fission increases in order to form smaller subunits during mitosis, and these subunits are equally distributed between daughter cells (Chen and Chan, 2017). Previous reports have shown that mitochondrial fragmentation in the mother cell occurs in response to the activation of AURKA during mitosis (Bertolin et al., 2018; Kashatus et al., 2011). I find that AURKA also modulates mitochondrial dynamics in interphase (Grant et al., 2018). Overexpression of AURKA causes mitochondria fragmentation in immortalized cells MCF10A, while inhibition of AURKA promotes mitochondria elongation in HCC1143 cancer cell line. Furthermore, I showed that N-terminal (1-31) is required to function in the mitochondrial fragmentation.

Abundant evidence indicates that APC/C-FZR1 is critical to the link between the bioenergetic profile and regulation of cell proliferation (Almeida et al., 2010; Colombo et al., 2010). I find as others have, that knocking out FZR1 leads to an elevated mitochondrial fragmentation (Horn et al., 2011). In some studies, this mitochondrial fragmentation has been attributed to the stability of DRP1. However, our live-cell studies reveal that when AURKA is inhibited, FZR1KO cells restores mitochondrial length as parental cells. In FZR1KO, I do show significant downregulation of DRP1 at G1 while the AURKA level was stabilized. During G1, non-degraded AURKA delays reassembly of the mitochondrial fragments after cell division. My results provide new evidence that excess AURKA is active in interphase, and therefore would also cause fragmentation of mitochondrial morphology and prevent mitochondrial reassembly after cell division. This mechanism may operate in cells to ensure that mitochondrial function is tightly controlled in both cell growth and proliferation. The elucidation of the connections between AURKA's effect on mitochondrial dynamics and metabolic changes during tumor development and metastasis will surely come from future research.

Chapter 6 Evaluation the role of AURKA SLiMs within the N-terminal IDR

6.1 Introduction

Aurora kinase family has two structural domains, one conserved C- terminal catalytic domain, the other is the N-terminal non-catalytic domain that varies in size and sequence. The N-terminal of AURKA is the longest intrinsic disorder region (IDR) within the family member (Willems et al., 2018). IDR contains short linear motifs (SLiMs) that thought to facilitate diverse post-translational modification and provide specificity for the recognition of binding partners (Fuxreiter et al., 2007). They also serve as localisation signal to target the catalytic activity to restricted sites during cell cycle progression (Davey et al., 2017). The non-catalytic IDR of AURKA kinase is involved in three functions *in vivo*: to regulate the kinase activity, to regulate degradation, and to localize the protein to centrosome, and mitochondria.

Norman Davey's lab generated an interactive bioinformatics tool called ProViz for identifying important functional regions through mapping SLiM of proteins (Jehl et al., 2016). The bioinformatic analysis of AURKA revealed the highly conserved degron A-box (centred on Q_{45}RVL), which have undoubted functional significance. A number of papers from the Golemis lab (Plotnikova et al., 2012; Plotnikova et al., 2010), described the finding that AURKA activity is regulated through the binding of Ca2+/calmodulin (CaM) to the IDR containing A-box degron. CaM binds preferentially to IDR carrying auto-phosphorylated serines that include S51. S51A shows attenuated binding to CaM (Plotnikova et al., 2010).

The same degron has been reported to mediate AURKA degradation in APC/C-FZR1 dependent manner (Lindon et al., 2015; Littlepage and Ruderman, 2002). S51D blocks degradation but S51A does not, giving rise to the hypothesis that FZR1 and CaM binding would be mutually exclusive, and that therefore AURKA degradation could be under the control of Ca2+ signaling. In this chapter, I have investigated further the role of SLiMs present in the N-terminal IDR, including testing the hypothesis that CaM protect AURKA from degradation. I also identified new SLiM within the N-terminal non-catalytic domain and examined its role in AURKA activation and degradation.

6.2 Results

6.2.1 Bioinformatic analysis of SLiMs within the N-terminal AURKA

I investigated the potential SLiMs within IDR of AURKA. Three characteristics can be used to identify SLiMs. Firstly, SLiMs are located in the disorder regions of the proteins that generally have the ability to fold and bind with the binding partners pockets (Fuxreiter et al., 2007; Sugase et al., 2007). Secondly, they are highly conserved (Davey et al., 2012). Thirdly, the evolution of SLiMs causing the protein to acquire new function (Davey et al., 2012; Nguyen Ba et al., 2012). ProViz bioinformatics search tool was used to discover unidentified SLiM in AURKA. I found two major conserved SLiMs in AURKA IDR —one which is previously known as A- box (R_{46}VL), while the other K_{23}RV is an unidentified SLiM **(Figure 6-1)**. I further provide a more complete characterization of A-box and K_{23}RV SLiMs.

6.2.2 Investigation of Ca2+ signaling through the R_{46}VL SLiM

Recent studies have shown that Ca2+ signaling leads to CaM interaction with the N-terminal domain of AURKA, leading to its activation of the kinase through binding to a SLiM centred on R_{46}VL (Plotnikova et al., 2012; Plotnikova et al., 2010). This SLiM had previously been characterized as the A-box motif that controls AURKA degradation (Lindon et al., 2015; Littlepage and Ruderman, 2002). How the activation and degradation of AURKA might be achieved through a single motif remained an open question, and I hypothesized that CaM and FZR1 compete for binding to the A-box. According to this hypothesis, FZR1 interaction with A-box, and therefore AURKA degradation, could be regulated by Ca2+ /CaM signaling. To test this hypothesis, I used thapsigargin, a drug that increases intracellular calcium by blocking the recycling of cytoplasmic Ca2+ into ER stores. Cell-permeable dyes are widely employed to detect the calcium changes within cells. Fluo-4 is a sensitive non-ratiometric dye making it ideal for temporal measurements of calcium. I first tested the activity of thapsigargin in U2OS cells by staining with Fluor-4 for 15 min, then using time-lapse imaging microscopy to monitor temporal changes in intracellular calcium after the addition of thapsigargin. As expected, I confirmed that thapsigargin causes an increase in intracellular calcium concentration in both mitotic and interphase cells **(Figure 6-2)**.

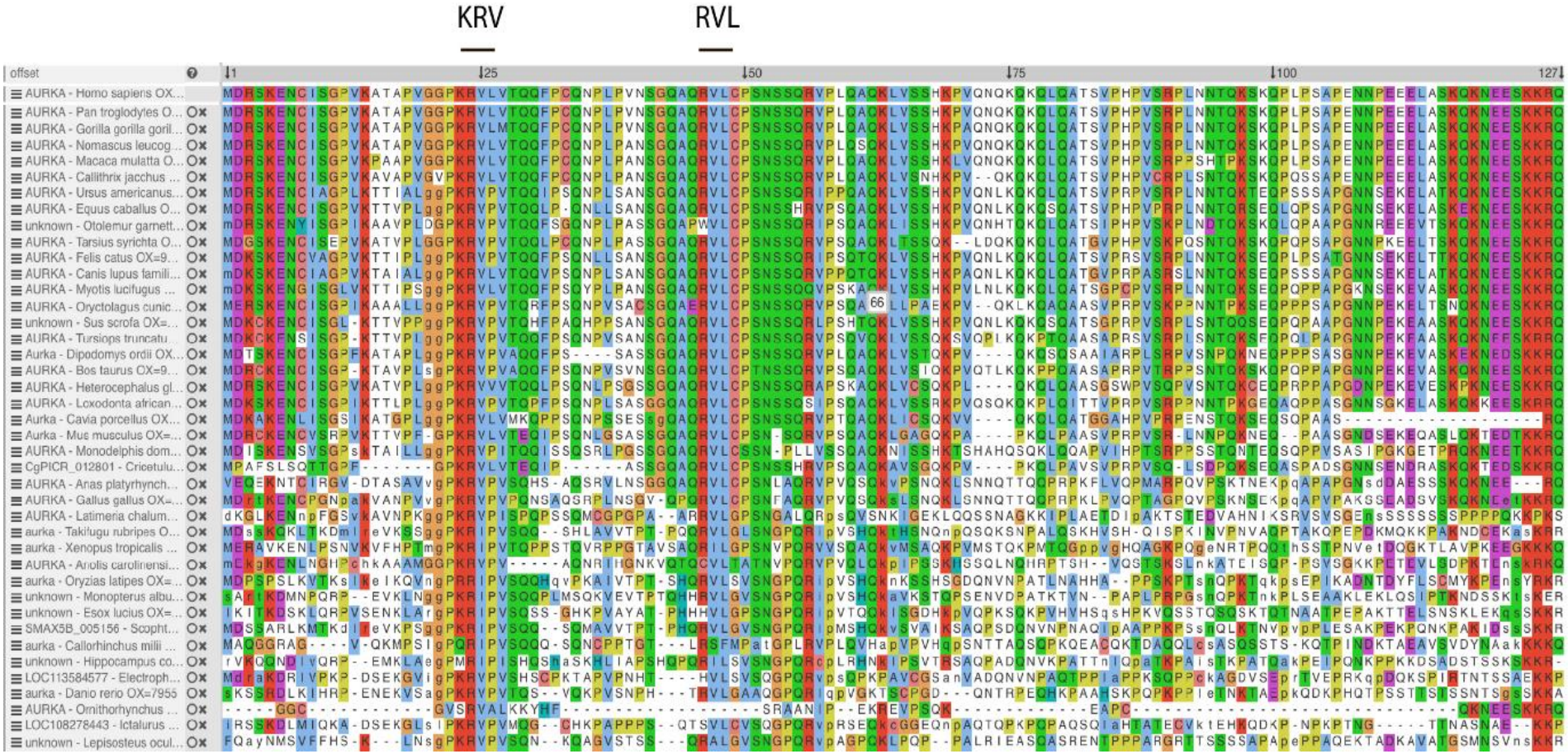

Figure 6-1 ProViz visualization for the IDR of AURKA showing a GeneTree alignment of AURKA orthologues. Key aspects of the visualization are showed: Protein name and species; data information sidebar; protein sequence data. The visualization in the example can be viewed at http://proviz.ucd.ie/proviz.php?uniprot acc=P38936. $K_{23}RV$ and $R_{46}VL$ are the most conserved SliMs in AURKA IDR.

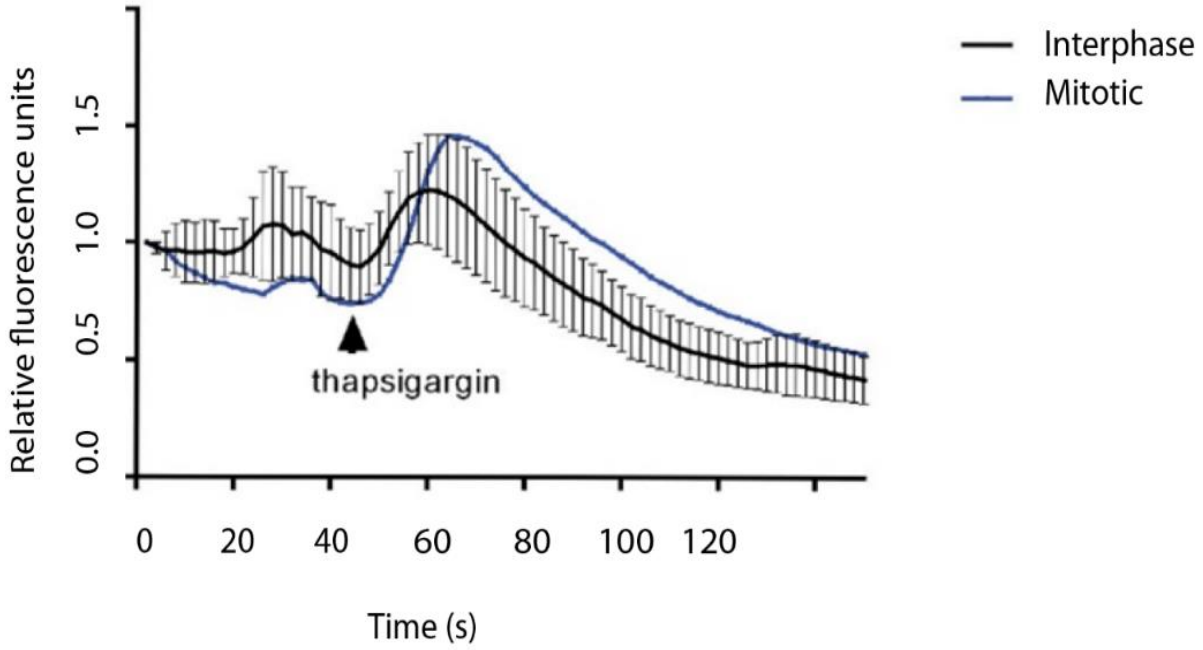

Figure 6-2 Thapsigargin-induced ER Ca 2+ release in U2OS cells. Cells were stained with Fluo-4 for 15 min and were imaged by using time-lapse fluorescence video microscopy, and the relative intensity of fluorescence, reflecting intracellular calcium levels, was plotted versus time. The arrowhead indicates the time of adding 200 nM thapsigargin. Error bars indicate s.d.

I then tested whether the perturbation of intracellular Ca2+ signaling affects AURKA degradation. U2OS cells were transiently transfected with Venus-tagged AURKA and were imaged 24 h after transfection. Mitotic cells were treated with thapsigargin at the indicated dose. AURKA protein level in single-cell degradation assays was then measured at the mitotic exit. I found that the degradation of AURKA was insensitive to calcium influx **(Figure 6-3 A, B)**.

In a few cells, degradation did stop but in these cells, there was an unusual telophase arrest probably preceding cell death **(Figure 6-3 A, B)**. I inferred that these cells might have received the highest doses of thapsigargin (which was added directly to the culture medium rather than through perfusion). Therefore, this may be indicating that there is some regulation of mitotic exit that high levels of Ca2+ are interfering with, pointing to interesting questions for the future. However, from these data, I concluded that Ca2+ signalling does not directly affect the AURKA degradation profile at mitotic exit. Therefore, there is no competition between Ca2+ signaling and FZR1 in the manner predicted by our hypothesis.

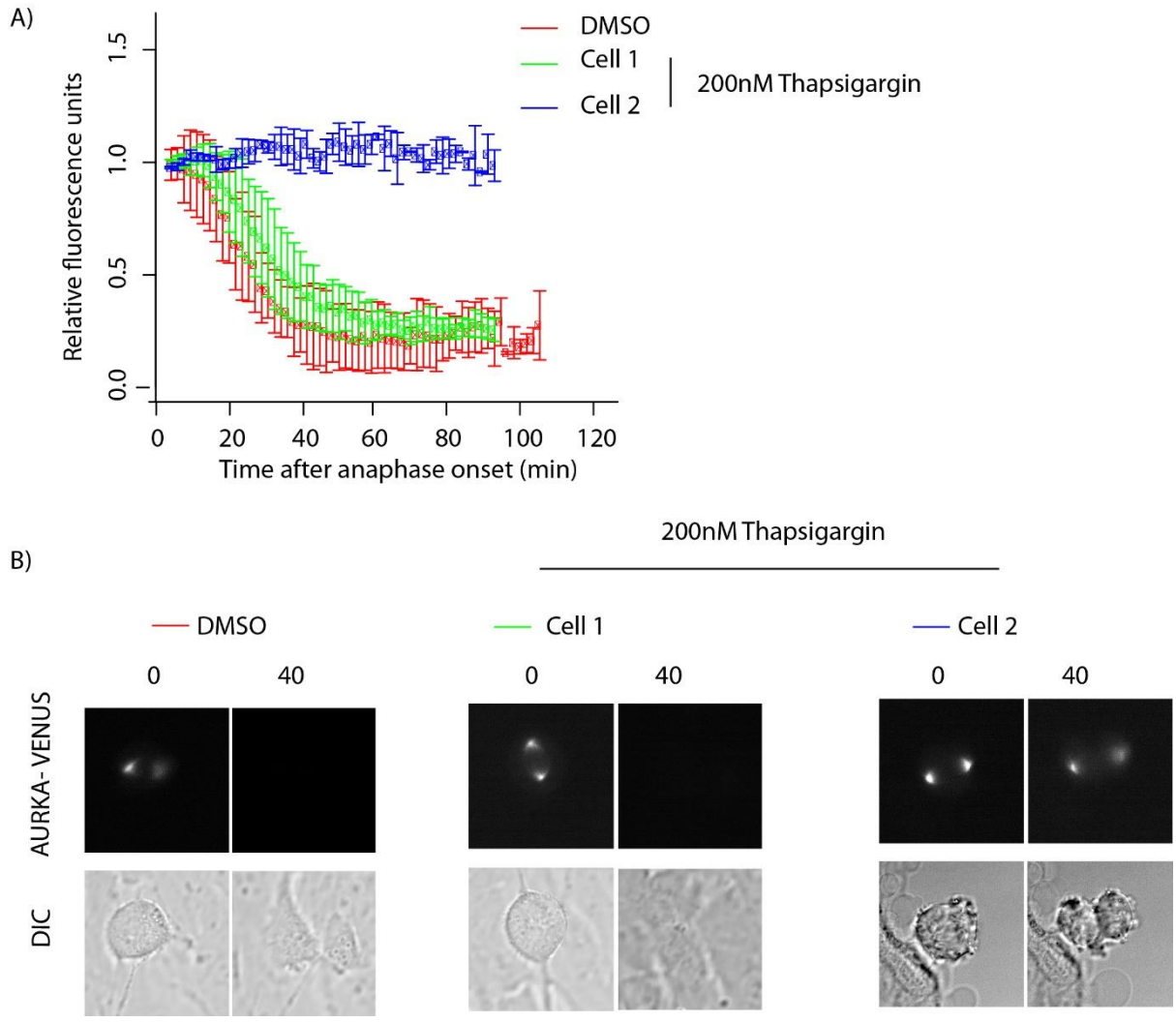

Figure 6-3 Ca2+ does not affect AURKA degradation profile at the mitotic exit. U2OS were transiently transfected with WT AURKA-Venus. A) Quantification of fluorescence measurements from single mitotic cells treated with thapsigargin were used to generate degradation curves for AURKA and fluorescence intensities were normalized to the level at anaphase onset. B) Frames from a time-lapse sequence of untreated and thapsigargin treatment proceeding through mitotic exit. Cell 1 refers to cells exiting mitosis. Cell 2 refers to telophase arrest cells. n=10 Error bars indicate s.d. Number of repeats n=3.

Since thapsigargin modulation of Ca2+ had no effect on AURKA degradation, I tested whether direct inhibtion of CaM binding affects AURKA degradation. To answer this question, U2OS cells were transiently transfected with Venus-tagged AURKA and were imaged 24 h after transfection. Mitotic cells were treated 5 μM Calmidazolium (Calmodulin inhibitor). AURKA level was monitored in single-cell degradation assays at mitotic exit. I found that Calmodulin inhibition did not affect AURKA degradation profile **(Figure 6-4)**.

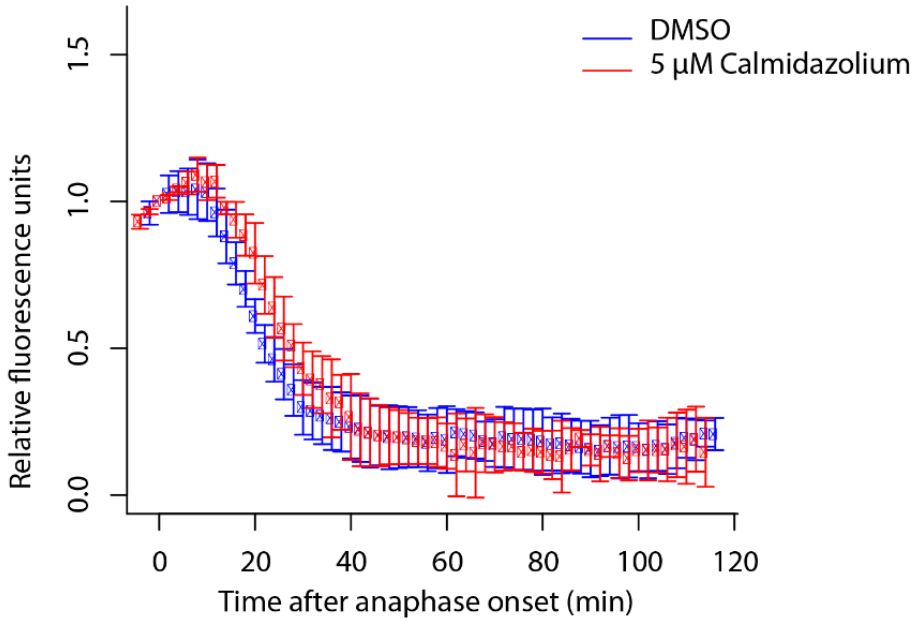

Figure 6-4 Calmodulin does not affect AURKA degradation profile at the mitotic exit. Quantification of fluorescence measurements from single mitotic cells treated with calmidazolium were used to generate degradation curves for AURKA and fluorescence intensities were normalized to the level at anaphase onset, where n = 6 cells. Error bars indicate s.d. Number of repeats n=2.

6.2.2.1 Ca2+ signaling does not affect pT288 AURKA

Western blot approach has led Golemis group (Plotnikova et al., 2010) to conclude that CaM signaling induces pT288AURKA activation. Because I was unable to find any evidence for our hypothesis that CaM influences AURKA degradation, I decided to confirm the Ca2+/CaM regulation of AURKA, by repeating the finding published in (Plotnikova et al., 2012; Plotnikova et al., 2010), where it is shown that Ca2+ signaling causes activation of AURKA as measured by pT288 epitope. Unsynchronized hTERT-RPE1 cells were treated with 500nM ionomycin (a Ca2+ ionophore), 200 nM thapsigargin, or 5 µM calmidazolium for 5 minutes. Cell lysates were then analysed by immunoblotting experiments using the pT288 AURKA antibody as a marker for the activity. I found that neither Ca2+ increasing drugs nor calmodulin inhibitor affected the pT288AURKA level detected on endogenous AURKA **(Figure 6-5 A)**. To increase the sensitivity of the assay I further tested with overexpressed AURKA. U2OS cells were transiently transfected with Venus-tagged AURKA and were treated with Ca2+ drugs and a calmodulin inhibitor for 5 min. I found no change in pT288 AURKA of the overexpressed AURKA **(Figure 6-5 B)**. Since many of the experiments carried out in Plotnikova et., al 2010 used HEK293 cells, I also tested Ca2+ drugs on AURKA activity using HEK293 **(Figure 6-5 C)**.

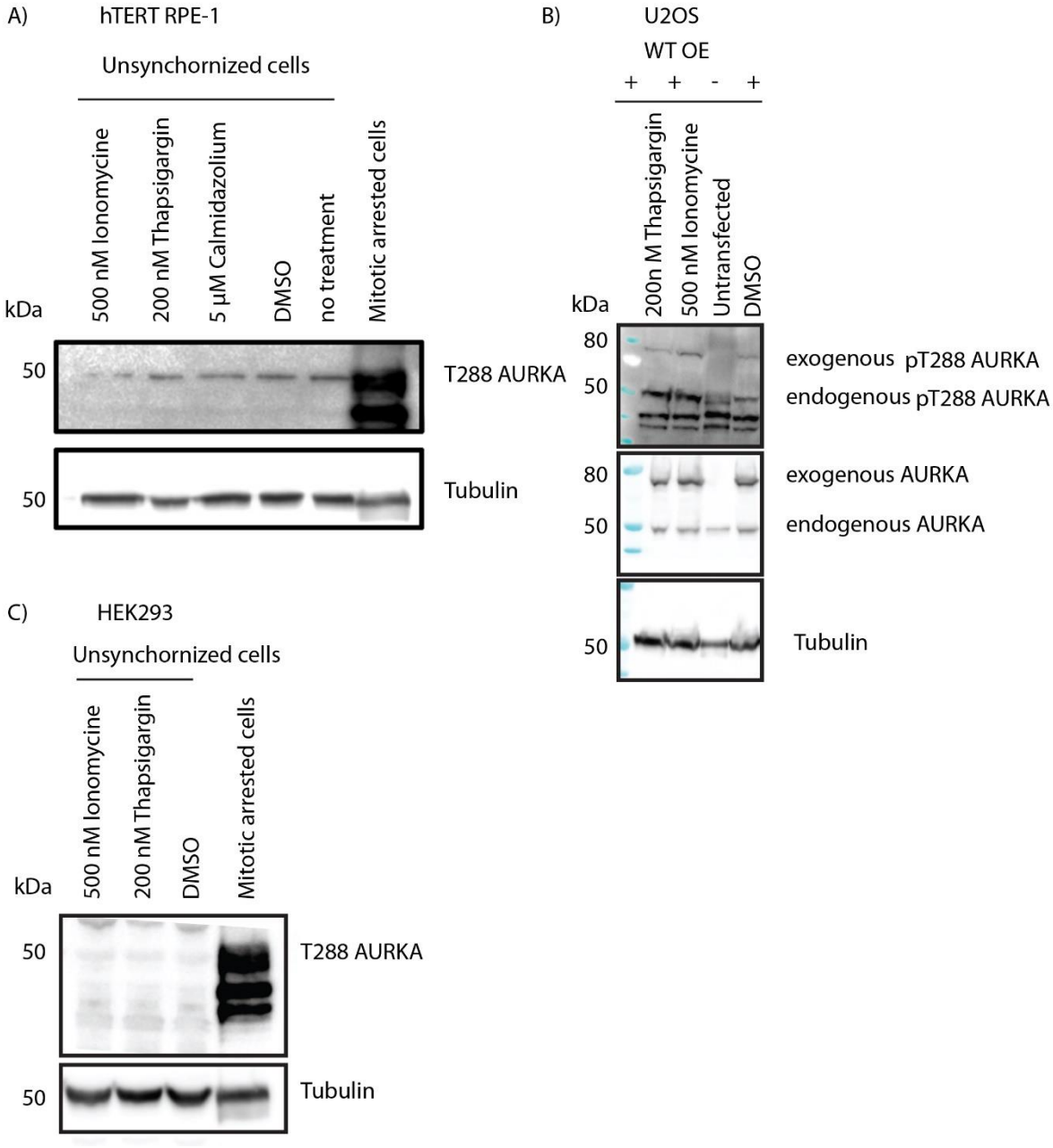

Figure 6-5 Perturbation of intracellular calcium level didn't affect AURKA activation. A) RPE1 cells were incubated for 5 minutes with 200 nM thapsigargin, 550nM ionomycin, 5 µM Calmidazolium or DMSO. B) U2OS cells were transiently transfected with AURKA venus. Cells were synchronized into mitosis using 5 µM STLC and were incubated for 5 minutes with 200 nM thapsigargin, 550 nM ionomycin. C) HEK 293 cells were incubated for 5 minutes with 200 nM thapsigargin, 0.5 µM ionomycin (Ion). Cells were lysed and analyzed by western blot using AURKA pT288, and tubulin antibody. Unit of molecular weight is kilodalton. Number of repeats n=2.

pT288 was undetectable in these cells unless they were pre-arrested in mitosis. I suggest that our pT288 antibody did not have the same affinity for its epitope as the antibody used by the Golemis Lab. Since I was not able to reproduce the results of Plotnikova et al.,2010, I could not conclude by this method that calcium signaling affects AURKA activation. Therefore, I decided

to test this question using the AURKA FRET sensor that I had previously characterized (Chapter 4) as a more sensitive way to monitor AURKA activity in real time.

6.2.2.2 Ca2+ may induce AURKA FRET activity at interphase but not in mitosis

Since the western blotting approach to study AURKA activation by Ca2+ signaling did not lead to conclusive results, I investigated AURKA activation using FRET imaging. U2OS cells were transiently transfected with the AURKA FRET biosensor and imaged after 24hrs. Cells were synchronized in mitosis by Eg5 inhibitor (5 μM STLC), then treated with 200 nM thapsigargin. AURKA FRET activity was measured in prometaphase arrested cells and interphase cells. I found that thapsigargin treatment causes a rapid increase in levels of AURKA FRET activity at interphase but not mitosis **(Figure 6-6A, B)**. I conclude that calcium signaling may activate AURKA at interphase. Although there may be some effect of Ca2+ on AURKA activity in interphase cells, I concluded that Ca2+ signalling is not the switch that determines the onset of AURKA degradation at mitotic exit.

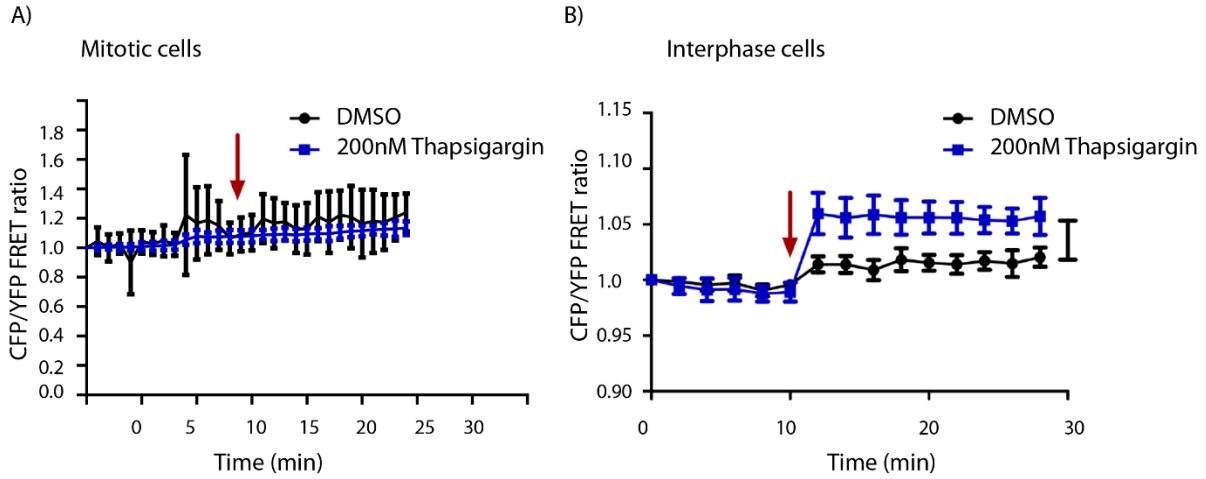

Figure 6-6. Perturbation of intracellular calcium level may affect AURKA activation in interphase. A) U2OS cells were transiently transfected with AURKA venus and synchronize into mitosis using 5 μM STLC. A) Mitotic arrested cells were incubated for 5 minutes with 5 μM thapsigargin. Arrows indicate the timing of thapsigargin addition. B) Interphase cells were incubated for 5 minutes with 200 nM thapsigargin. Arrows indicate the timing of thapsigargin addition. Error bars indicate s.d. Number of repeats n=3.

6.2.3 Investigation of role of K_{23}RVL SLiM

6.2.3.1 K_{23}RVL motif does not affect degradation

I next examined if the newly identified K_{23}RVL SLiM plays any role in AURKA stability. Since none of our experiments to identify AURKA degrons (Chapter 3) had explained why

AURKA was a specific target for FZR1 (and not Cdc20), it was possible there were further degrons to identify in the N-terminal IDR. I also considered the hypothesis that the strong conservation of this SLiM reflected the role of K23 as a ubiquitination site. To answer these questions, I generated K_{23}RVL/AAAA (to test degron function) and K23R (to test for ubiquitination site) AURKA mutants. U2OS cells were transiently transfected with Venus-tagged AURKA mutants and were imaged 24 h after transfection. I find that neither mutation in the K_{23}RVL motif affected the localization and the degradation of the protein **(Figure 6-7 A, B)**. From these data, I conclude that the K_{23}RVL motif is not required for AURKA degradation.

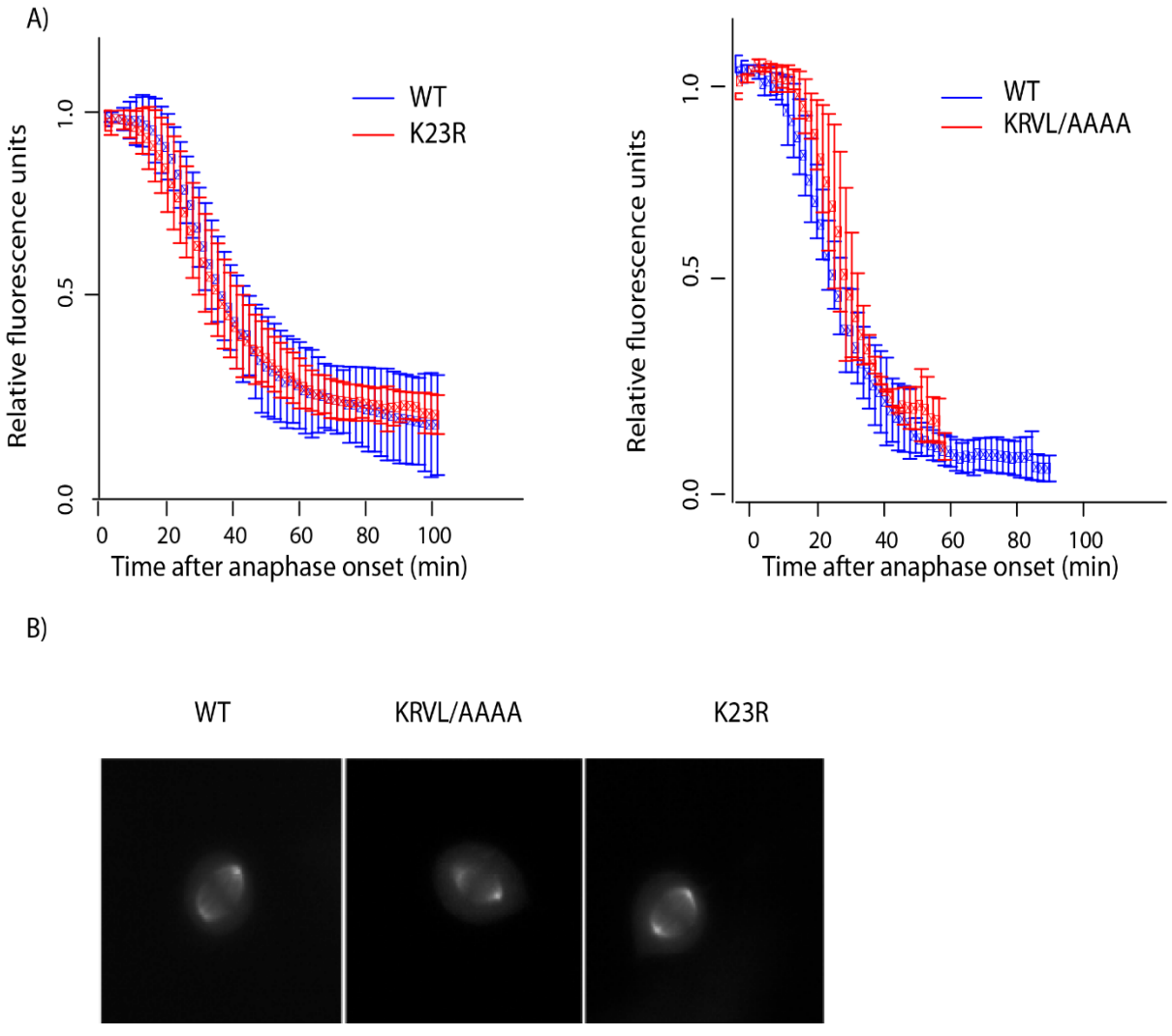

Figure 6-7 K23RVL motif does not affect the degradation profile at the mitotic exit. U2OS were transiently transfected with WT AURKA, K23R and K23RVL/AAAA mutants**.** A) Quantification of fluorescence measurements from single mitotic cells were used to generate degradation curves for AURKA mutants and fluorescence intensities were normalized to the level at anaphase onset, where n = 6 cells. B) Mitotic localization of WT AURKA-Venus and mutants. Error bars indicate s.d. Number of repeats n=2.

6.2.3.2 K_{23}RVL motif may affect AURKA activity during mitosis

Since, unlike the other SLiMs identified in the N-terminal IDR, K_{23}RVL is not involved in controlling degradation of AURKA, I asked if instead it might be involved in regulating the activity of the kinase. Two studies have reported that the N-terminal IDR may regulate the kinase activity through its intramolecular inhibitory interaction with the C-terminal catalytic domain (Zhang et al., 2007). A further study showed that lysine residues (K99 and K119) within the N terminal domain are required for the inhibitory interaction (Bai et al., 2014). Therefore, I investigated whether the K_{23}RVL motif has any regulatory effect on the kinase activity of AURKA. U2OS cells were transiently transfected with Venus-tagged AURKA wildtype and K23R mutant and synchronized for the prometaphase enrichment by Eg5 inhibitor (5 μM STLC). Cell extracts were collected and analysed by immunoblotting with the pT288 AURKA antibody. I find that there is an increase in the exogenous AURKA T288 signal but not the exogenous WT **(Figure 6-8)**. These results suggest that the K_{23}RVL of AURKA may negatively regulate AURKA.

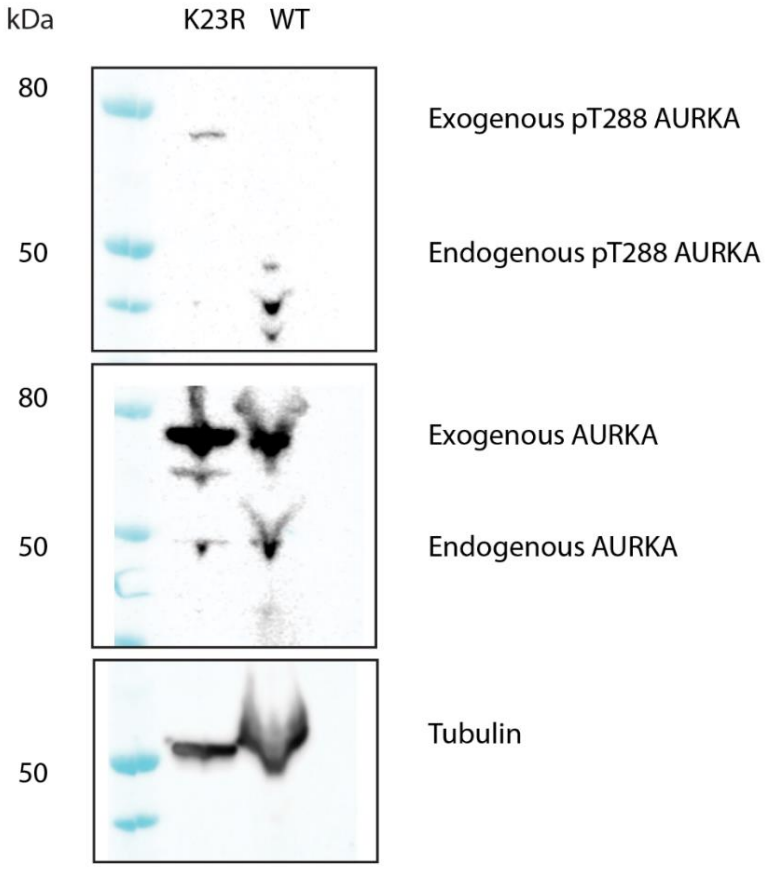

Figure 6-8 K_{23}RVL of AURKA may have inhibitory regulation of AURKA. U2OS cells were transiently transfected with WT AURKA-Venus and K_{23}R mutant. Cells were

synchronized into mitosis using 5 µM STLC. Cells were lysed and analyzed by western blot using pT288AURKA, AURKA and tubulin antibody. Results from one experiment.

Our finding is consistent with the proposed model, suggesting that when cells are not stimulated, N- terminal IDR of AURKA plays a critical role in AURKA autoinhibition. Upon stimulation of AURKA activity, the activator protein interacts with the N-terminal IDR, which opens the inhibitory conformation, and AURKA becomes active. Our preliminary data suggest that the highly conserved K_{23}RVL could be mediating the autoinhibition of AURKA presumably through interacting with the active loop of the kinase domain **(Figure 6-9)**. Our data pave the way for a better understanding of the molecular mechanism involved in the AURKA activation.

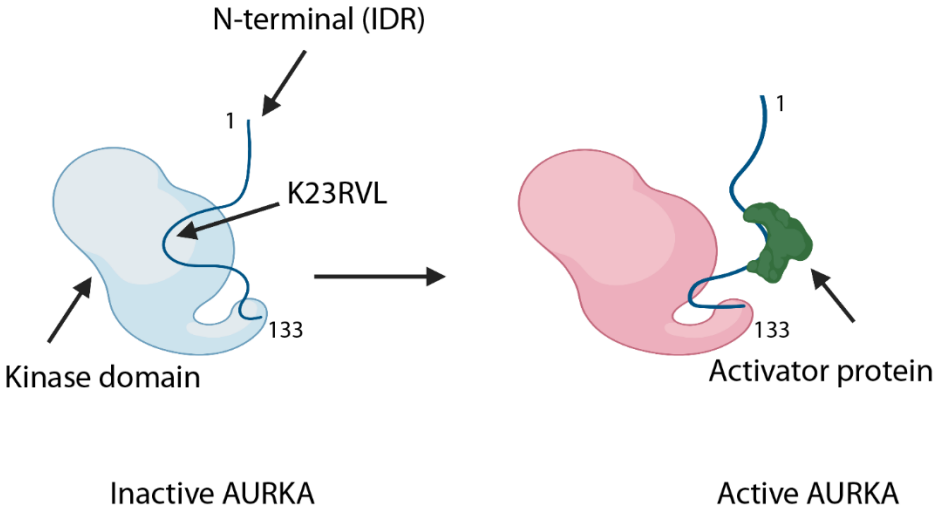

Figure 6-9 Schematic model of the proposed model for the role of K_{23}RVL of autoinhibited conformation of AURKA. In inhibitory conditions, K_{23}RVL binds to the active loop of the kinase domain. Upon stimulation of AURKA activity, the activator interacts with the IDR to switch into AURKA active conformation.

6.3 Discussion

In this chapter, I described my initial work to determine the role of AURKA SLiMs in regulating its activity and stability. Here I have investigated two conserved SLiMs within IDR of AURKA, K_{23}RVL, and Q_{45}RVL (A-box). Earlier work had described that Q_{45}RVL (A-box) is required for AURKA degradation in FZR1 dependent manner **(**Lindon et al., 2015**;** Littlepage and Ruderman, 2002**)**. A previous study claimed that CaM transiently activates AURKA by preferentially binding to the A-box motif. The binding with calmodulin is dependent on several serines, including phosphorylation of S51 that blocks AURKA degradation (Plotnikova et al.,

2010). These results suggested to us that CaM may compete with FZR1. I find that Ca2+/CaM signaling does not affect AURKA degradation. Moreover, Ca2+ signaling may activate AURKA in interphase but not in mitosis. Our finding suggests that there is no competition between CaM and FZR1 for A- box binding during mitotic exit.

The N-terminal domain of AURKA has been previously shown to regulate AURKA activity by acting as an inhibitory domain (Bai et al., 2014; Zhang et al., 2007). I conducted a preliminary study to determine if K23RVL may affect AURKA activity. Interestingly, I found that K23R increases the activity of AURKA while the stability remains similar to the wild type at mitotic exit. Therefore, K23 located within the N-terminal domain may have an inhibitory role. Understanding the function AURKA's SLiMs within N-terminus may help to organize known and future AURKA substrates into a more cohesive picture.

Chapter 7 Discussion and future perspective

Discussion

AURKA is a major mitotic serine/threonine kinase responsible for the onset and progression of mitosis as well as additional non-mitotic functions including cilia disassembly and mitochondrial fragmentation (Bertolin and Tramier, 2020; Grant et al., 2018). Overexpression or gene amplification of AURKA is associated with tumor formation and invasion (D'Assoro et al., 2015). The protein level of AURKA is cell cycle regulated, it accumulates at mitosis and is degraded at the end of mitosis. AURKA is mainly targeted for degradation by E3 ligase APC/C-FZR1. Based on *in vitro* assays, AURKA degradation depends on an A-Box and D-box (Lindon et al., 2015; Littlepage and Ruderman, 2002).

In the present study, I have challenged the accepted dogma in AURKA destruction pathway that $R_{371}xxL_{374}$ is a functional D-box to advance our understanding of AURKA regulation. I have shown that the previously reported AURKA D-box mutant $R_{371}AXXL_{374}A$ does not localize at the mitotic spindles *in vivo*. Structurally, D-box like motif is buried within the C-terminal domain that makes it inaccessible for APC/C-FZR1. In D-box dependent substrates such as PLK1 and Cyclin B1, the conserved point mutation leucine to isoleucine is sufficient to disrupt the degradation by APC/C. However, the same conserved mutation in AURKA D-box like motif $R_{371}XXL_{374}I$ is degraded at a rate similar to the wild type protein without affecting its localization. Together these data argue that D-box like motif has no functional role in AURKA degradation, and that the effect of double point mutation $R_{371}AXXL_{374}A$ within D-box like-motif can be attributed to a lack of proper folding. Several reports have shown that FZR1 localizes to the spindle pole during anaphase at mitotic exit (Meghini et al., 2016; Schindler and Schultz, 2009). One possible explanation would be that $R_{371}XXL_{374}$ localizes AURKA to the spindle pole making it accessible to APC/C-FZR1 for degradation. D or KEN box-containing peptides are observed in 70% human proteins, but most of them are not accessible to the APC/C (Davey et al., 2017). There are other examples of proposed APC/C degrons in the literature that appear to be structurally buried, such as the D boxes of Ski-like protein (SKIL), and the KEN box of 6-phosphofructo-2-kinase/fructose-2,6-bisphosphatase 3 (PFKFB3) (Davey and Morgan, 2016; Davey et al., 2017). My findings

regarding the AURKA D-Box suggests that these degrons still need more careful characterisation.

The characterisation of the highly conserved A-box SLiM located within the N-terminal IDR has revealed that it is sufficient to drive the protein degradation in APC/C-FZR1 dependent manner. Mutation to introduce a phosphomimetic amino acid at serine 51 located within the A-box motif blocked AURKA degradation, suggesting that phosphorylation might protect AURKA from destruction during mitosis. This finding is consistent with other reports and with the idea that IDRs contain SLiMs required for degradation of the target proteins (Littlepage and Ruderman, 2002; Van Roey et al., 2014). Our in-silico model suggests that the A-box motif can be docked in a similar pose to the D-box on the D-box receptor in FZR1, which raises the possibility that A-box is a noncanonical version of D-box. Variability in the key residues of the D-box degron is likely to create major differences in specificity, affinity, and type of ubiquitin modification received (Alfieri et al., 2017; Chang and Barford, 2014). Therefore, degradation kinetics of APC/C substrates vary at anaphase onset, including PLK1, KIFC1, AURKA, and AURKB.

Targeting mitotic substrates for degradation is necessary for mitotic progression. Cyclin A and cyclin B provide the best-understood examples for how deregulation of mitotic kinases stability affects mitotic exit. Stabilization of Cyclin B leads to constitutive activation of Cdk1 and blocks mitotic exit (Lindqvist et al., 2009). Non-degradable Cyclin A delays chromosome alignment and sister chromatid segregation (Gong and Ferrell, 2010). The non-degradable AURKA perturbs spindle midzone at mitotic exit (Floyd et al., 2008). Any modest increase in AURKA level rapidly promotes tumorigenesis, likely through interacting with activators, or downstream targets. The lack of clinical efficiency of Aurora-A kinase inhibitors may be due to unexpected roles of AURKA independent of its kinase activity. For example, AURKA protects N-Myc from FBXW7-mediated degradation in neuroblastoma (Otto et al., 2009). AURKA may act as a coactivator for hnRNPK and FOXM1 at the nucleus in a kinase-independent manner to enhance the proliferation of breast cancer cells (Yang et al., 2017; Zheng et al., 2016). Therefore, AURKA destruction is crucial for the fidelity of the mitotic process and protects from its oncogenic activity.

Several studies have shown that AURKA activity and level peak in preparation for mitosis, and both gradually decrease at the end of mitosis. AURKA inactivation can be regulated either by dephosphorylation or presumably through destruction. I observed that AURKA activity

decreases faster than the degradation of the protein at the mitotic exit. AURKA level is stabilized by knocking out the APC/C co-activator FZR1, while the timing of its inactivation is not affected, as measured using pT288-AURKA antibody (which detects active AURKA) reactivity or an AURKA FRET biosensor. These findings indicate that AURKA degradation is not required for its inactivation at mitotic exit. I also found that FZR1 inhibits the activity of AURKA at interphase, suggesting that APC/C-FZR1 mediated degradation of AURKA might function to regulate its interphase functions.

AURKA is activated by binding partners even in the absence of autophosphorylation, such as TPX2 (Burgess et al., 2015; Reboutier et al., 2012). The binding of TPX2 to AURKA protects it from dephosphorylation by phosphatase 1 (PP1) (Bayliss et al., 2003; Eyers et al., 2003; Katayama et al., 2001; Tsai et al., 2003). PP1 acts only on AURKA free molecules through its interaction with two motifs in AURKA: the catalytic lysine residue (K_{169}VLF) and (K_{350}VEF). On the other hand, PP6 binds to the AURKA-TPX2 complex to maintain the hypoactive form of AURKA activity during spindle assembly (Zeng et al., 2010). I find that overexpression of the non-degradable TPX2 (1-43) peptide which is sufficient to activate AURKA, also delays the timing of kinase inactivation. These results reveal that the TPX2 degradation at mitotic exit could act as the first step for pT288 dephosphorylation by PP1. Our results also demonstrate that the destruction of TPX2 by APC/CCdc20 is required to make AURKA accessible to PP1-mediated inactivation. However, this result does not exclude the possibility that the ubiquitination of TPX2 could be the first step for loss of interaction with AURKA **(Figure 7-1)**. These data are consistent with the idea that the early degradation of TPX2 is dependent on APC/C at mitotic exit (Min et al., 2014; Singh et al., 2014).

Our model suggests that Cdc20 promotes the inactivation of AURKA through the degradation of its activator TPX2 to ensure the fidelity of mitotic exit. In embryonic cells, AURKA is not degraded because the FZR1 is not expressed; Instead, these embryonic cells regulate AURKA by periodic activation and inactivation during the cell cycle (Littlepage and Ruderman, 2002). This evidence implies that during evolution, AURKA destruction has always been decoupled from its mitotic activity. Therefore, I infer that the APC/C regulates a pool of AURK activities that are associated with interphase functions.

There is evidence that AURKA regulates mitochondrial fragmentation events during mitosis (Bertolin et al., 2018; Kashatus et al., 2011). Mitochondria are cytoplasmic organelles that generate energy in order to support cell functions. During mitosis, mitochondria are

fragmented into smaller subunits and are distributed to the two daughter cells. I observed that excess AURKA in interphase is active. The phenotypic change I detected during the interphase in response to inhibiting AURKA degradation was that it impedes the mitochondrial reassembly after cell division. Mitochondrial dynamics play a central role in metabolic adaptation and are essential sources of metabolic activity (Wai and Langer, 2016). Previous studies have shown that mitochondrial fusion induces supercomplexes of the electron transport chain (ETC) and enhances oxidative phosphorylation (OXPHOS) activity (Mishra et al., 2014), while mitochondrial fragmentation augments glycolysis (Serasinghe et al., 2015). Deregulation of mitochondrial dynamics has been linked to tumorigenesis and metastasis (Ferreira-da-Silva et al., 2015; Zhao et al., 2013). This led us to speculate that AURKA's oncogenic activity might be attributed, at least in part, to its effect on mitochondrial dynamics.

The N-terminal IDR of AURKA participates in a broad functional mitotic control such as setting the timing of the G2/M transition, and proper alignment of chromosomes. It is also involved in regulating AURKA activity and stability. However, the molecular mechanisms for these regulations are poorly understood. Work from Golemis lab claimed that Ca2+/ CaM signaling activates AURKA through interacting with the N-terminal region that contains A-box motif, the same motif that is necessary for AURKA degradation (Plotnikova et al., 2012; Plotnikova et al., 2010). This data led us to ask whether Ca2+/ CaM competes with APC/C FZR1 for the same motif to protect AURKA from degradation during mitosis. I showed that Ca2+/CaM activates AURKA at interphase and does not affect the degradation at the mitotic exit, which implies that there is no competition between the two pathways.

Using ProViz bioinformatics tool, I identified K_{23}RVL as a potential SLiM in the N-terminal AURKA. I find that mutating K_{23}RVL increases AURKA activity, implies that it might be mediating the autoinhibitory effect of the N-terminal IDR of AURKA. These results are consistent with recent observations that the N-terminal AURKA acts as an autoinhibitory region that negatively regulates the kinase activity (Bai et al., 2014; Zhang et al., 2007). During normal state, the N-terminal domain has been proposed to have an inhibitory effect on the kinase activity, which is achieved via its intramolecular interaction with the catalytic domain to modulate the kinase activity and function at various subcellular locations. Upon stimulation, the activator interacts with the N-terminal domain and induces conformational changes to regulate the kinase activity. These results provide us with a molecular explanation for the inhibitory role of the N-terminal domain of AURKA. Identifying and characterizing SLiMs is

a good route for understanding protein structure-function relationships. It will be fascinating to further investigate K_{23}RVL and to understand whether it contributes to AURKA overactivity in tumors, a direction with clear clinical implications on future cancer treatment.

Future perspective

Recent discoveries have begun to shed light on novel functions of AURKA at interphase, and several future questions remain unanswered. For example, the possible relationship between AURKA and mitochondria and that this relationship is governed by the stability of AURKA in interphase provides a new direction to understand its oncogenic activity. It will be interesting to examine whether AURKA controls the adoption of distinct metabolic programs in cancer cells. In the meantime, it might be meaningful to explore the contributions of AURKA binding partners (TPX2, FOXM1, and Myc) to the adoption of metabolic changes. An important goal is defining the molecular mechanisms that regulate AURKA activity and stability at different subcellular locations. Our understanding of the molecular mechanisms underlying AURKA regulation and functions will provide key insight for drug design in cancer therapy.

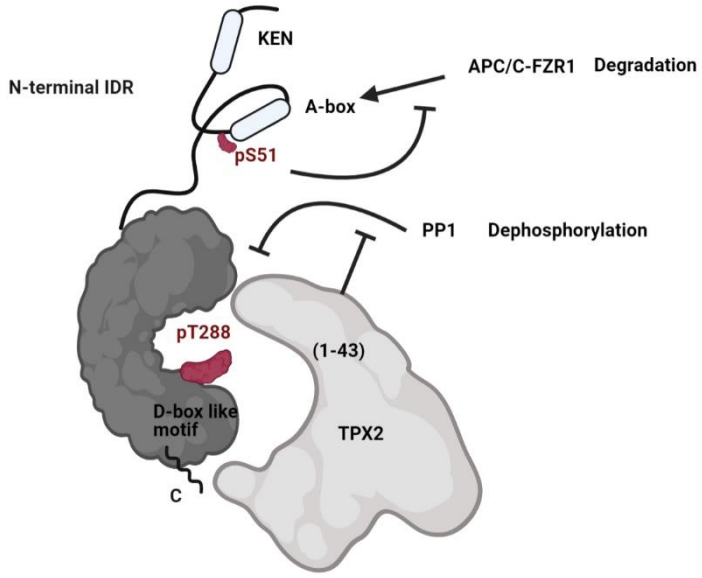

Figure 7-1 Schematic model of AURKA inactivation and degradation during mitotic exit. TPX2 degradation or loss of interaction with AURKA at mitotic exit could act as the first step for pT288 dephosphorylation by PP1. AURKA is mainly targeted for degradation by E3 ligase APC/C-FZR1. pS51 version of the A-box may block AURKA destruction at mitotic exit.

Appendix A Publications arising from this thesis

Ahmed Abdelbaki, Camilla Ascanelli, Catherine Lindon. The Destruction-box of AURKA resides in its N-terminus where its accessibility is sensitive to a conformation dependent on C-terminal sequences. Under preparation.

Ahmed Abdelbaki, Begum Akman**.** First person interview-Journal of cell Science 2020 133: jcs249649 doi: 10.1242/jcs.249649 Published 22 June 2020.

Ahmed Abdelbaki, Begum Akman, Marion Poteau, Olivier Gavet, Giulia Guarguaglini and Catherine Lindon. AURKA destruction is decoupled from its inactivation during mitotic exit and required instead to suppress interphase activity. Journal of Cell Science 2020: jcs.243071 doi: 10.1242/jcs.243071. Featured for interview to speak about our findings.

Rhys Grant, **Ahmed Abdelbaki**, Alessia Bertoldi, Maria P. Gavilan, Jörg Mansfeld, David M. Glover, Catherine Lindon. Constitutive regulation of mitochondrial morphology by Aurora A kinase depends on a predicted cryptic targeting sequence at the N-terminus. OPEN BIOLOGY. Published 13 June 2018. DOI: 10.1098/rsob.170272.

Appendix B Supplementary figures

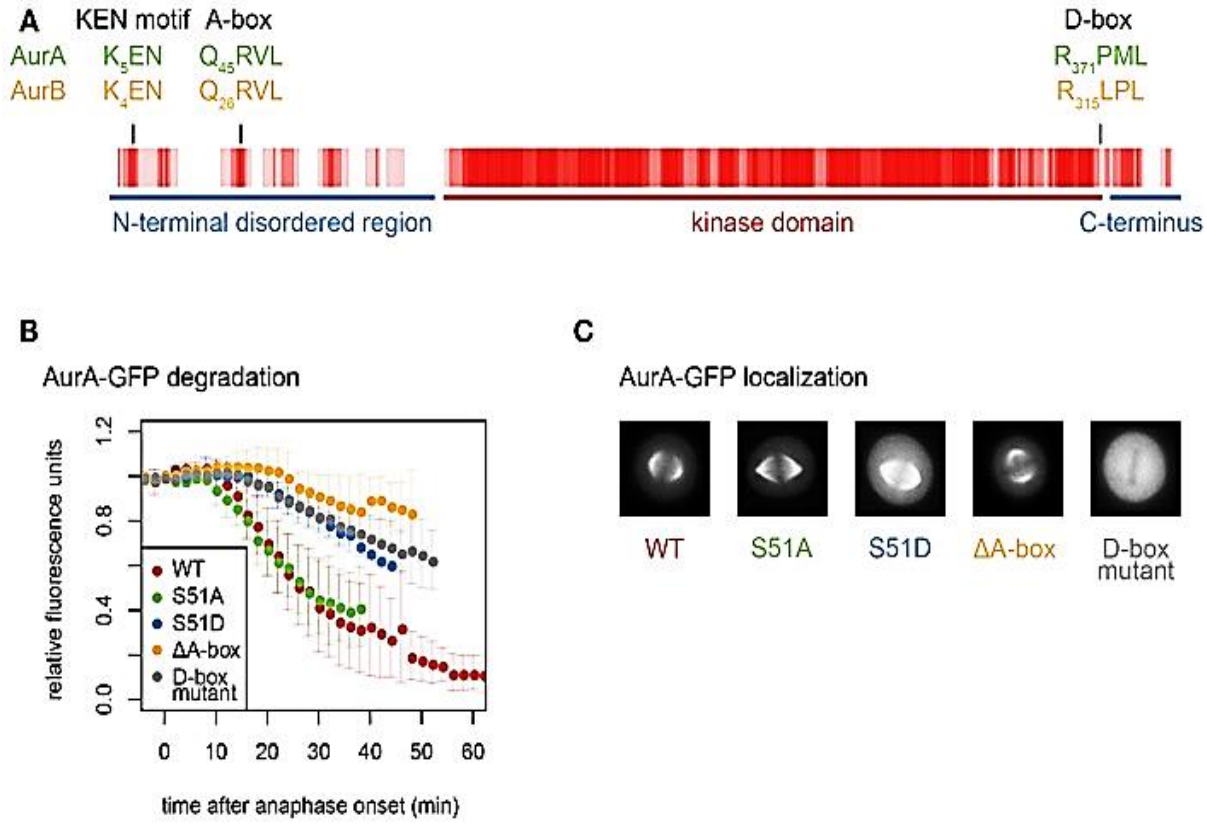

Figure B-1 Conserved degrons in Aurora kinases. A) Conserved degrons are required for AURKA and AURKB degradation. The sequence alignment of AURKA and AURKB was converted to a vector of values corresponding to conservation at each position (from 4 for fully conserved position to 0 for no conservation). Rolling averages of a five-residue window across the whole alignment is presented as a heat map. Therefore, the shade of red indicates residue conservation between the two paralogs. B) Quantification of fluorescence measurements from single mitotic cells were used to generate degradation curves for A-box- (including S51-) and D-box-mutated versions of AURKA-GFP. Fluorescence levels measured over time in single cells exiting mitosis are normalized to anaphase onset. ΔA-box = Δ31–66; D-box mutant = R371A, L374A. C) Mitotic localization of wild-type AURKA, and AURKA mutants, showing loss of functional localization of the D-box mutant. This figure is taken from (Lindon et al., 2015).

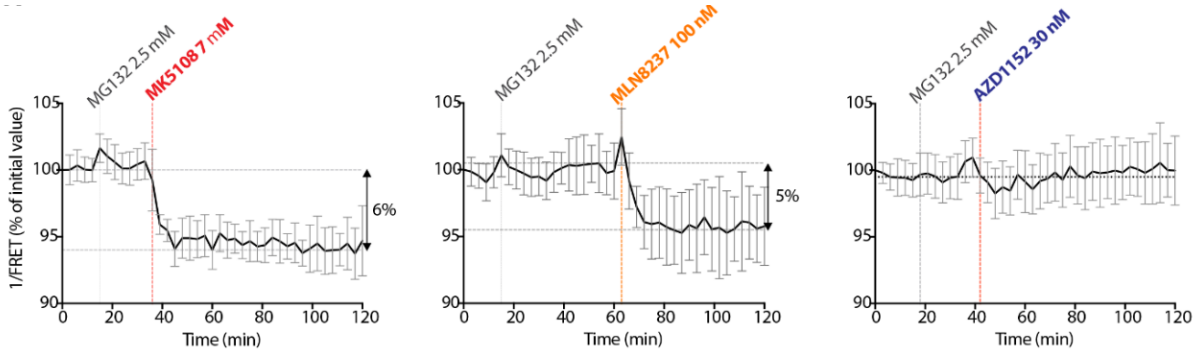

	[inhibitor]	mitotic activity inhibition	number of cells analysed
AURKA inhibitor	MK5108 7 µM	6%	13
	MLN8237 200nM	6%	16
	MLN8237 100 nM	5%	13
AURKB inhibitor	ZM447439 2 µM	2%	12
	AZD1152 500 nM	2%	22
	AZD1152 30 nM	< 1%	18

Figure B-2 Measuring Aurora kinase activity with a FRET-based biosensor. U2OS cells transfected with the AURKA-directed biosensor from a population synchronized by release from double thymidine block were arrested in mitosis by treatment with MG132, then treated with AURKA- or AURKB-specific inhibitors. Mean activity values FRET for mitotic cells undergoing different drug treatments are shown in the traces (upper panels) and results from a number of different experiments summarized in the table below. Biosensor activity was strongly inhibited by treatment with MLN8237 or MK5108, specific inhibitors of AURKA, and partially inhibited by two inhibitors of AURKB, AZD1152 and ZM447439. This figure done in collaboration with Olivier Gavet lab.

Figure B-3 Schematic showing guide RNAs used to target the first exon of FZR1 and generate CRISPR- Cas9 Knockout of FZR1.

References

Acquaviva, C., and Pines, J. (2006). The anaphase-promoting complex/cyclosome: APC/C. J Cell Sci 119, 2401-2404.

Afonso, O., Figueiredo, A.C., and Maiato, H. (2017). Late mitotic functions of Aurora kinases. Chromosoma 126, 93-103.

Alfieri, C., Zhang, S., and Barford, D. (2017). Visualizing the complex functions and mechanisms of the anaphase promoting complex/cyclosome (APC/C). Open Biol 7.

Almeida, A., Bolanos, J.P., and Moncada, S. (2010). E3 ubiquitin ligase APC/C-Cdh1 accounts for the Warburg effect by linking glycolysis to cell proliferation. Proc Natl Acad Sci U S A 107, 738-741.

Andresson, T., and Ruderman, J.V. (1998). The kinase Eg2 is a component of the Xenopus oocyte progesterone-activated signaling pathway. EMBO J 17, 5627-5637.

Arnoult, D. (2007). Mitochondrial fragmentation in apoptosis. Trends Cell Biol 17, 6-12.

Asteriti, I.A., De Mattia, F., and Guarguaglini, G. (2015). Cross-Talk between AURKA and Plk1 in Mitotic Entry and Spindle Assembly. Front Oncol 5, 283.

Asteriti, I.A., Di Cesare, E., De Mattia, F., Hilsenstein, V., Neumann, B., Cundari, E., Lavia, P., and Guarguaglini, G. (2014). The Aurora-A inhibitor MLN8237 affects multiple mitotic processes and induces dose-dependent mitotic abnormalities and aneuploidy. Oncotarget 5, 6229-6242.

Asteriti, I.A., Rensen, W.M., Lindon, C., Lavia, P., and Guarguaglini, G. (2010). The Aurora-A/TPX2 complex: a novel oncogenic holoenzyme? Biochim Biophys Acta 1806, 230-239.

Bai, M., Ni, J., Shen, S., Wu, J., Huang, Q., Le, Y., and Yu, L. (2014). Two newly identified sites in the N-terminal regulatory domain of Aurora-A are essential for auto-inhibition. Biotechnol Lett 36, 1595-1604.

Barford, D. (2011). Structural insights into anaphase-promoting complex function and mechanism. Philos Trans R Soc Lond B Biol Sci 366, 3605-3624.

Barford, D. (2019). A MAD way to regulate mitosis. Nat Rev Mol Cell Biol 20, 135.

Barr, A.R., and Gergely, F. (2007). Aurora-A: the maker and breaker of spindle poles. J Cell Sci 120, 2987-2996.

Bassermann, F., Eichner, R., and Pagano, M. (2014). The ubiquitin proteasome system - implications for cell cycle control and the targeted treatment of cancer. Biochimica et biophysica acta 1843, 150-162.

Bayliss, R., Burgess, S.G., and McIntyre, P.J. (2017). Switching Aurora-A kinase on and off at an allosteric site. FEBS J 284, 2947-2954.

Bayliss, R., Sardon, T., Vernos, I., and Conti, E. (2003). Structural basis of Aurora-A activation by TPX2 at the mitotic spindle. Mol Cell 12, 851-862.

Beltran, H. (2014). The N-myc Oncogene: Maximizing its Targets, Regulation, and Therapeutic Potential. Mol Cancer Res 12, 815-822.

Bertolin, G., Bulteau, A.L., Alves-Guerra, M.C., Burel, A., Lavault, M.T., Gavard, O., Le Bras, S., Gagne, J.P., Poirier, G.G., Le Borgne, R., et al. (2018). Aurora kinase A localises to mitochondria to control organelle dynamics and energy production. Elife 7.

Bertolin, G., and Tramier, M. (2020). Insights into the non-mitotic functions of Aurora kinase A: more than just cell division. Cell Mol Life Sci 77, 1031-1047.

Bertran-Alamillo, J., Cattan, V., Schoumacher, M., Codony-Servat, J., Gimenez-Capitan, A., Cantero, F., Burbridge, M., Rodriguez, S., Teixido, C., Roman, R., et al. (2019). AURKB as a target in non-small cell lung cancer with acquired resistance to anti-EGFR therapy. Nat Commun 10, 1812.

Bischoff, J.R., Anderson, L., Zhu, Y., Mossie, K., Ng, L., Souza, B., Schryver, B., Flanagan, P., Clairvoyant, F., Ginther, C., et al. (1998). A homologue of Drosophila aurora kinase is oncogenic and amplified in human colorectal cancers. EMBO J 17, 3052-3065.

Brockmann, M., Poon, E., Berry, T., Carstensen, A., Deubzer, H.E., Rycak, L., Jamin, Y., Thway, K., Robinson, S.P., Roels, F., et al. (2013). Small molecule inhibitors of aurora-a induce proteasomal degradation of N-myc in childhood neuroblastoma. Cancer Cell 24, 75-89.

Burgess, S.G., Peset, I., Joseph, N., Cavazza, T., Vernos, I., Pfuhl, M., Gergely, F., and Bayliss, R. (2015). Aurora-A-Dependent Control of TACC3 Influences the Rate of Mitotic Spindle Assembly. PLoS Genet 11, e1005345.

Burton, J.L., and Solomon, M.J. (2001). D box and KEN box motifs in budding yeast Hsl1p are required for APC-mediated degradation and direct binding to Cdc20p and Cdh1p. Genes Dev 15, 2381-2395.

Cao, Q., and Richter, J.D. (2002). Dissolution of the maskin-eIF4E complex by cytoplasmic polyadenylation and poly(A)-binding protein controls cyclin B1 mRNA translation and oocyte maturation. EMBO J 21, 3852-3862.

Carmena, M., and Earnshaw, W.C. (2003). The cellular geography of aurora kinases. Nat Rev Mol Cell Biol 4, 842-854.

Carmena, M., Ruchaud, S., and Earnshaw, W.C. (2009). Making the Auroras glow: regulation of Aurora A and B kinase function by interacting proteins. Curr Opin Cell Biol 21, 796-805.

Carmena, M., Wheelock, M., Funabiki, H., and Earnshaw, W.C. (2012). The chromosomal passenger complex (CPC): from easy rider to the godfather of mitosis. Nat Rev Mol Cell Biol 13, 789-803.

Castaneda, C.A., Dixon, E.K., Walker, O., Chaturvedi, A., Nakasone, M.A., Curtis, J.E., Reed, M.R., Krueger, S., Cropp, T.A., and Fushman, D. (2016). Linkage via K27 Bestows Ubiquitin Chains with Unique Properties among Polyubiquitins. Structure 24, 423-436.

Castro, A., Arlot-Bonnemains, Y., Vigneron, S., Labbe, J.C., Prigent, C., and Lorca, T. (2002). APC/Fizzy-Related targets Aurora-A kinase for proteolysis. EMBO Rep 3, 457-462.

Chan, E.H., Santamaria, A., Sillje, H.H., and Nigg, E.A. (2008). Plk1 regulates mitotic Aurora A function through betaTrCP-dependent degradation of hBora. Chromosoma 117, 457-469.

Chang, L., and Barford, D. (2014). Insights into the anaphase-promoting complex: a molecular machine that regulates mitosis. Curr Opin Struct Biol 29, 1-9.

Chang, L., Zhang, Z., Yang, J., McLaughlin, S.H., and Barford, D. (2015). Atomic structure of the APC/C and its mechanism of protein ubiquitination. Nature 522, 450-454.

Chang, S.S., Yamaguchi, H., Xia, W., Lim, S.O., Khotskaya, Y., Wu, Y., Chang, W.C., Liu, Q., and Hung, M.C. (2017). Aurora A kinase activates YAP signaling in triple-negative breast cancer. Oncogene 36, 1265-1275.

Chen, H., and Chan, D.C. (2017). Mitochondrial Dynamics in Regulating the Unique Phenotypes of Cancer and Stem Cells. Cell Metab 26, 39-48.

Ciechanover, A., Heller, H., Elias, S., Haas, A.L., and Hershko, A. (1980). ATP-dependent conjugation of reticulocyte proteins with the polypeptide required for protein degradation. Proc Natl Acad Sci U S A 77, 1365-1368.

Clijsters, L., Ogink, J., and Wolthuis, R. (2013). The spindle checkpoint, APC/C(Cdc20), and APC/C(Cdh1) play distinct roles in connecting mitosis to S phase. J Cell Biol 201, 1013-1026.

Cohen-Fix, O., Peters, J.M., Kirschner, M.W., and Koshland, D. (1996). Anaphase initiation in Saccharomyces cerevisiae is controlled by the APC-dependent degradation of the anaphase inhibitor Pds1p. Genes Dev 10, 3081-3093.

Colombo, S.L., Palacios-Callender, M., Frakich, N., De Leon, J., Schmitt, C.A., Boorn, L., Davis, N., and Moncada, S. (2010). Anaphase-promoting complex/cyclosome-Cdh1 coordinates glycolysis and glutaminolysis with transition to S phase in human T lymphocytes. Proc Natl Acad Sci U S A 107, 18868-18873.

Courtheoux, T., Diallo, A., Damodaran, A.P., Reboutier, D., Watrin, E., and Prigent, C. (2018). Aurora A kinase activity is required to maintain an active spindle assembly checkpoint during prometaphase. J Cell Sci 131.

Crane, R., Gadea, B., Littlepage, L., Wu, H., and Ruderman, J.V. (2004a). Aurora A, meiosis and mitosis. Biol Cell 96, 215-229.

Crane, R., Kloepfer, A., and Ruderman, J.V. (2004b). Requirements for the destruction of human Aurora-A. J Cell Sci 117, 5975-5983.

D'Assoro, A.B., Haddad, T., and Galanis, E. (2015). Aurora-A Kinase as a Promising Therapeutic Target in Cancer. Front Oncol 5, 295.

Damodaran, A.P., Vaufrey, L., Gavard, O., and Prigent, C. (2017). Aurora A Kinase Is a Priority Pharmaceutical Target for the Treatment of Cancers. Trends Pharmacol Sci 38, 687-700.

Darling, A.L., and Uversky, V.N. (2018). Intrinsic Disorder and Posttranslational Modifications: The Darker Side of the Biological Dark Matter. Front Genet 9, 158.

Davey, N.E., Cyert, M.S., and Moses, A.M. (2015). Short linear motifs - ex nihilo evolution of protein regulation. Cell Commun Signal 13, 43.

Davey, N.E., and Morgan, D.O. (2016). Building a Regulatory Network with Short Linear Sequence Motifs: Lessons from the Degrons of the Anaphase-Promoting Complex. Mol Cell 64, 12-23.

Davey, N.E., Seo, M.H., Yadav, V.K., Jeon, J., Nim, S., Krystkowiak, I., Blikstad, C., Dong, D., Markova, N., Kim, P.M., et al. (2017). Discovery of short linear motif-mediated interactions through phage display of intrinsically disordered regions of the human proteome. FEBS J 284, 485-498.

Davey, N.E., Van Roey, K., Weatheritt, R.J., Toedt, G., Uyar, B., Altenberg, B., Budd, A., Diella, F., Dinkel, H., and Gibson, T.J. (2012). Attributes of short linear motifs. Mol Biosyst 8, 268-281.

de Groot, C.O., Hsia, J.E., Anzola, J.V., Motamedi, A., Yoon, M., Wong, Y.L., Jenkins, D., Lee, H.J., Martinez, M.B., Davis, R.L., et al. (2015). A Cell Biologist's Field Guide to Aurora Kinase Inhibitors. Front Oncol 5, 285.

De Souza, C.P., Ellem, K.A., and Gabrielli, B.G. (2000). Centrosomal and cytoplasmic Cdc2/cyclin B1 activation precedes nuclear mitotic events. Exp Cell Res 257, 11-21.

Deribe, Y.L., Pawson, T., and Dikic, I. (2010). Post-translational modifications in signal integration. Nat Struct Mol Biol 17, 666-672.

Di Fiore, B., Davey, N.E., Hagting, A., Izawa, D., Mansfeld, J., Gibson, T.J., and Pines, J. (2015). The ABBA motif binds APC/C activators and is shared by APC/C substrates and regulators. Dev Cell 32, 358-372.

Di Fiore, B., Wurzenberger, C., Davey, N.E., and Pines, J. (2016). The Mitotic Checkpoint Complex Requires an Evolutionary Conserved Cassette to Bind and Inhibit Active APC/C. Mol Cell 64, 1144-1153.

Dodson, C.A., and Bayliss, R. (2012). Activation of Aurora-A kinase by protein partner binding and phosphorylation are independent and synergistic. J Biol Chem 287, 1150-1157.

Dong, G.Q., Fan, H., Schneidman-Duhovny, D., Webb, B., and Sali, A. (2013). Optimized atomic statistical potentials: assessment of protein interfaces and loops. Bioinformatics 29, 3158-3166.

Dutertre, S., Cazales, M., Quaranta, M., Froment, C., Trabut, V., Dozier, C., Mirey, G., Bouche, J.P., Theis-Febvre, N., Schmitt, E., et al. (2004). Phosphorylation of CDC25B by Aurora-A at the centrosome contributes to the G2-M transition. J Cell Sci 117, 2523-2531.

Eyers, P.A., Erikson, E., Chen, L.G., and Maller, J.L. (2003). A novel mechanism for activation of the protein kinase Aurora A. Curr Biol 13, 691-697.

Ferrari, S., Marin, O., Pagano, M.A., Meggio, F., Hess, D., El-Shemerly, M., Krystyniak, A., and Pinna, L.A. (2005). Aurora-A site specificity: a study with synthetic peptide substrates. The Biochemical journal 390, 293-302.

Ferreira-da-Silva, A., Valacca, C., Rios, E., Populo, H., Soares, P., Sobrinho-Simoes, M., Scorrano, L., Maximo, V., and Campello, S. (2015). Mitochondrial dynamics protein Drp1 is overexpressed in oncocytic thyroid tumors and regulates cancer cell migration. PLoS One 10, e0122308.

Fiskin, E., Bhogaraju, S., Herhaus, L., Kalayil, S., Hahn, M., and Dikic, I. (2017). Structural basis for the recognition and degradation of host TRIM proteins by Salmonella effector SopA. Nature communications 8, 14004.

Floyd, S., Pines, J., and Lindon, C. (2008). APC/C Cdh1 targets aurora kinase to control reorganization of the mitotic spindle at anaphase. Curr Biol 18, 1649-1658.

Fuller, B.G., Lampson, M.A., Foley, E.A., Rosasco-Nitcher, S., Le, K.V., Tobelmann, P., Brautigan, D.L., Stukenberg, P.T., and Kapoor, T.M. (2008). Midzone activation of aurora B in anaphase produces an intracellular phosphorylation gradient. Nature 453, 1132-1136.

Funabiki, H., Yamano, H., Kumada, K., Nagao, K., Hunt, T., and Yanagida, M. (1996). Cut2 proteolysis required for sister-chromatid seperation in fission yeast. Nature 381, 438-441.

Fuxreiter, M., Tompa, P., and Simon, I. (2007). Local structural disorder imparts plasticity on linear motifs. Bioinformatics 23, 950-956.

Giet, R., Petretti, C., and Prigent, C. (2005). Aurora kinases, aneuploidy and cancer, a coincidence or a real link? Trends Cell Biol 15, 241-250.

Giubettini, M., Asteriti, I.A., Scrofani, J., De Luca, M., Lindon, C., Lavia, P., and Guarguaglini, G. (2011). Control of Aurora-A stability through interaction with TPX2. J Cell Sci 124, 113-122.

Goldknopf, I.L., and Busch, H. (1977). Isopeptide linkage between nonhistone and histone 2A polypeptides of chromosomal conjugate-protein A24. Proc Natl Acad Sci U S A 74, 864-868.

Gong, D., and Ferrell, J.E., Jr. (2010). The roles of cyclin A2, B1, and B2 in early and late mitotic events. Mol Biol Cell 21, 3149-3161.

Gorjanacz, M., Jaedicke, A., and Mattaj, I.W. (2007). What can Caenorhabditis elegans tell us about the nuclear envelope? FEBS Lett 581, 2794-2801.

Grant, R., Abdelbaki, A., Bertoldi, A., Gavilan, M.P., Mansfeld, J., Glover, D.M., and Lindon, C. (2018). Constitutive regulation of mitochondrial morphology by Aurora A kinase depends on a predicted cryptic targeting sequence at the N-terminus. Open Biol 8.

Gritsko, T.M., Coppola, D., Paciga, J.E., Yang, L., Sun, M., Shelley, S.A., Fiorica, J.V., Nicosia, S.V., and Cheng, J.Q. (2003). Activation and overexpression of centrosome kinase BTAK/Aurora-A in human ovarian cancer. Clin Cancer Res 9, 1420-1426.

Groen, E.J.N., and Gillingwater, T.H. (2015). UBA1: At the Crossroads of Ubiquitin Homeostasis and Neurodegeneration. Trends Mol Med 21, 622-632.

Groisman, I., Huang, Y.S., Mendez, R., Cao, Q., Theurkauf, W., and Richter, J.D. (2000). CPEB, maskin, and cyclin B1 mRNA at the mitotic apparatus: implications for local translational control of cell division. Cell 103, 435-447.

Groisman, I., Jung, M.Y., Sarkissian, M., Cao, Q., and Richter, J.D. (2002). Translational control of the embryonic cell cycle. Cell 109, 473-483.

Hannak, E., Kirkham, M., Hyman, A.A., and Oegema, K. (2001). Aurora-A kinase is required for centrosome maturation in Caenorhabditis elegans. J Cell Biol 155, 1109-1116.

He, J., Chao, W.C., Zhang, Z., Yang, J., Cronin, N., and Barford, D. (2013). Insights into degron recognition by APC/C coactivators from the structure of an Acm1-Cdh1 complex. Mol Cell 50, 649-660.

Hegarat, N., Smith, E., Nayak, G., Takeda, S., Eyers, P.A., and Hochegger, H. (2011). Aurora A and Aurora B jointly coordinate chromosome segregation and anaphase microtubule dynamics. J Cell Biol 195, 1103-1113.

Heride, C., Urbe, S., and Clague, M.J. (2014). Ubiquitin code assembly and disassembly. Current biology : CB 24, R215-220.

Hirota, T., Kunitoku, N., Sasayama, T., Marumoto, T., Zhang, D., Nitta, M., Hatakeyama, K., and Saya, H. (2003). Aurora-A and an interacting activator, the LIM protein Ajuba, are required for mitotic commitment in human cells. Cell 114, 585-598.

Holloway, S.L., Glotzer, M., King, R.W., and Murray, A.W. (1993). Anaphase is initiated by proteolysis rather than by the inactivation of maturation-promoting factor. Cell 73, 1393-1402.

Horn, S.R., Thomenius, M.J., Johnson, E.S., Freel, C.D., Wu, J.Q., Coloff, J.L., Yang, C.S., Tang, W., An, J., Ilkayeva, O.R., et al. (2011). Regulation of mitochondrial morphology by APC/CCdh1-mediated control of Drp1 stability. Mol Biol Cell 22, 1207-1216.

Horn, V., Thelu, J., Garcia, A., Albiges-Rizo, C., Block, M.R., and Viallet, J. (2007). Functional interaction of Aurora-A and PP2A during mitosis. Molecular biology of the cell 18, 1233-1241.

Hu, W., Kavanagh, J.J., Deaver, M., Johnston, D.A., Freedman, R.S., Verschraegen, C.F., and Sen, S. (2005). Frequent overexpression of STK15/Aurora-A/BTAK and chromosomal instability in tumorigenic cell cultures derived from human ovarian cancer. Oncol Res 15, 49-57.

Ikeda, F., and Dikic, I. (2008). Atypical ubiquitin chains: new molecular signals. 'Protein Modifications: Beyond the Usual Suspects' review series. EMBO Rep 9, 536-542.

Jackman, M., Lindon, C., Nigg, E.A., and Pines, J. (2003). Active cyclin B1-Cdk1 first appears on centrosomes in prophase. Nat Cell Biol 5, 143-148.

Jehl, P., Manguy, J., Shields, D.C., Higgins, D.G., and Davey, N.E. (2016). ProViz-a web-based visualization tool to investigate the functional and evolutionary features of protein sequences. Nucleic Acids Res 44, W11-15.

Jeng, Y.M., Peng, S.Y., Lin, C.Y., and Hsu, H.C. (2004). Overexpression and amplification of Aurora-A in hepatocellular carcinoma. Clin Cancer Res 10, 2065-2071.

Joukov, V., De Nicolo, A., Rodriguez, A., Walter, J.C., and Livingston, D.M. (2010). Centrosomal protein of 192 kDa (Cep192) promotes centrosome-driven spindle assembly by engaging in organelle-specific Aurora A activation. Proc Natl Acad Sci U S A 107, 21022-21027.

Kapuy, O., He, E., Uhlmann, F., and Novak, B. (2009). Mitotic exit in mammalian cells. Mol Syst Biol 5, 324.

Kashatus, D.F., Lim, K.H., Brady, D.C., Pershing, N.L., Cox, A.D., and Counter, C.M. (2011). RALA and RALBP1 regulate mitochondrial fission at mitosis. Nat Cell Biol 13, 1108-1115.

Katayama, H., Sasai, K., Kawai, H., Yuan, Z.M., Bondaruk, J., Suzuki, F., Fujii, S., Arlinghaus, R.B., Czerniak, B.A., and Sen, S. (2004). Phosphorylation by aurora kinase A induces Mdm2-mediated destabilization and inhibition of p53. Nat Genet 36, 55-62.

Katayama, H., Zhou, H., Li, Q., Tatsuka, M., and Sen, S. (2001). Interaction and feedback regulation between STK15/BTAK/Aurora-A kinase and protein phosphatase 1 through mitotic cell division cycle. J Biol Chem 276, 46219-46224.

Katsha, A., Belkhiri, A., Goff, L., and El-Rifai, W. (2015). Aurora kinase A in gastrointestinal cancers: time to target. Mol Cancer 14, 106.

Kelly, A.E., Sampath, S.C., Maniar, T.A., Woo, E.M., Chait, B.T., and Funabiki, H. (2007). Chromosomal enrichment and activation of the aurora B pathway are coupled to spatially regulate spindle assembly. Dev Cell 12, 31-43.

Kettenbach, A.N., Schlosser, K.A., Lyons, S.P., Nasa, I., Gui, J., Adamo, M.E., and Gerber, S.A. (2018). Global assessment of its network dynamics reveals that the kinase Plk1 inhibits the phosphatase PP6 to promote Aurora A activity. Sci Signal 11.

Kim, H.T., Kim, K.P., Lledias, F., Kisselev, A.F., Scaglione, K.M., Skowyra, D., Gygi, S.P., and Goldberg, A.L. (2007). Certain pairs of ubiquitin-conjugating enzymes (E2s) and ubiquitin-protein ligases (E3s) synthesize nondegradable forked ubiquitin chains containing all possible isopeptide linkages. J Biol Chem 282, 17375-17386.

Kim, J., Guermah, M., McGinty, R.K., Lee, J.S., Tang, Z., Milne, T.A., Shilatifard, A., Muir, T.W., and Roeder, R.G. (2009). RAD6-Mediated transcription-coupled H2B ubiquitylation directly stimulates H3K4 methylation in human cells. Cell 137, 459-471.

Kimmins, S., Crosio, C., Kotaja, N., Hirayama, J., Monaco, L., Hoog, C., van Duin, M., Gossen, J.A., and Sassone-Corsi, P. (2007). Differential functions of the Aurora-B and Aurora-C kinases in mammalian spermatogenesis. Mol Endocrinol 21, 726-739.

Knoblach, B., and Rachubinski, R.A. (2015). Motors, anchors, and connectors: orchestrators of organelle inheritance. Annu Rev Cell Dev Biol 31, 55-81.

Komander, D., and Rape, M. (2012). The ubiquitin code. Annu Rev Biochem 81, 203-229.

Korobeynikov, V., Deneka, A.Y., and Golemis, E.A. (2017). Mechanisms for nonmitotic activation of Aurora-A at cilia. Biochem Soc Trans 45, 37-49.

Kozyreva, V.K., McLaughlin, S.L., Livengood, R.H., Calkins, R.A., Kelley, L.C., Rajulapati, A., Ice, R.J., Smolkin, M.B., Weed, S.A., and Pugacheva, E.N. (2014). NEDD9 regulates actin dynamics through cortactin deacetylation in an AURKA/HDAC6-dependent manner. Molecular cancer research : MCR 12, 681-693.

Kraft, C., Vodermaier, H.C., Maurer-Stroh, S., Eisenhaber, F., and Peters, J.M. (2005). The WD40 propeller domain of Cdh1 functions as a destruction box receptor for APC/C substrates. Mol Cell 18, 543-553.

Kufer, T.A., Sillje, H.H., Korner, R., Gruss, O.J., Meraldi, P., and Nigg, E.A. (2002). Human TPX2 is required for targeting Aurora-A kinase to the spindle. J Cell Biol 158, 617-623.

Lai, C.H., Tseng, J.T., Lee, Y.C., Chen, Y.J., Lee, J.C., Lin, B.W., Huang, T.C., Liu, Y.W., Leu, T.H., Liu, Y.W., et al. (2010). Translational up-regulation of Aurora-A in EGFR-overexpressed cancer. J Cell Mol Med 14, 1520-1531.

Lake, E.W., Muretta, J.M., Thompson, A.R., Rasmussen, D.M., Majumdar, A., Faber, E.B., Ruff, E.F., Thomas, D.D., and Levinson, N.M. (2018). Quantitative conformational profiling of kinase inhibitors reveals origins of selectivity for Aurora kinase activation states. Proc Natl Acad Sci U S A 115, E11894-E11903.

Lassus, H., Staff, S., Leminen, A., Isola, J., and Butzow, R. (2011). Aurora-A overexpression and aneuploidy predict poor outcome in serous ovarian carcinoma. Gynecol Oncol 120, 11-17.

Lee, Y.C., Liao, P.C., Liou, Y.C., Hsiao, M., Huang, C.Y., and Lu, P.J. (2013). Glycogen synthase kinase 3 beta activity is required for hBora/Aurora A-mediated mitotic entry. Cell cycle 12, 953-960.

Lemas, D., Lekkas, P., Ballif, B.A., and Vigoreaux, J.O. (2016). Intrinsic disorder and multiple phosphorylations constrain the evolution of the flightin N-terminal region. J Proteomics 135, 191-200.

Levinson, N.M. (2018). The multifaceted allosteric regulation of Aurora kinase A. Biochem J 475, 2025-2042.

Lindon, C., Grant, R., and Min, M. (2015). Ubiquitin-Mediated Degradation of Aurora Kinases. Front Oncol 5, 307.

Lindqvist, A., Rodriguez-Bravo, V., and Medema, R.H. (2009). The decision to enter mitosis: feedback and redundancy in the mitotic entry network. J Cell Biol 185, 193-202.

Lioutas, A., and Vernos, I. (2013). Aurora A kinase and its substrate TACC3 are required for central spindle assembly. EMBO Rep 14, 829-836.

Littlepage, L.E., and Ruderman, J.V. (2002). Identification of a new APC/C recognition domain, the A box, which is required for the Cdh1-dependent destruction of the kinase Aurora-A during mitotic exit. Genes Dev 16, 2274-2285.

Littlepage, L.E., Wu, H., Andresson, T., Deanehan, J.K., Amundadottir, L.T., and Ruderman, J.V. (2002). Identification of phosphorylated residues that affect the activity of the mitotic kinase Aurora-A. Proc Natl Acad Sci U S A 99, 15440-15445.

Liu, S.T., and Zhang, H. (2016). The mitotic checkpoint complex (MCC): looking back and forth after 15 years. AIMS Mol Sci 3, 597-634.

Liu, X., Sun, L., Gursel, D.B., Cheng, C., Huang, S., Rademaker, A.W., Khan, S.A., Yin, J., and Kiyokawa, H. (2017). The non-canonical ubiquitin activating enzyme UBA6 suppresses epithelial-mesenchymal transition of mammary epithelial cells. Oncotarget 8, 87480-87493.

Luo, M., Cao, M., Kan, Y., Li, G., Snell, W., and Pan, J. (2011). The phosphorylation state of an aurora-like kinase marks the length of growing flagella in Chlamydomonas. Curr Biol 21, 586-591.

Ma, H.T., and Poon, R.Y. (2011). How protein kinases co-ordinate mitosis in animal cells. Biochem J 435, 17-31.

Macurek, L., Lindqvist, A., Lim, D., Lampson, M.A., Klompmaker, R., Freire, R., Clouin, C., Taylor, S.S., Yaffe, M.B., and Medema, R.H. (2008). Polo-like kinase-1 is activated by aurora A to promote checkpoint recovery. Nature 455, 119-123.

Mahajan, R., Delphin, C., Guan, T., Gerace, L., and Melchior, F. (1997). A small ubiquitin-related polypeptide involved in targeting RanGAP1 to nuclear pore complex protein RanBP2. Cell 88, 97-107.

Mahankali, M., Henkels, K.M., Speranza, F., and Gomez-Cambronero, J. (2015). A non-mitotic role for Aurora kinase A as a direct activator of cell migration upon interaction with PLD, FAK and Src. J Cell Sci 128, 516-526.

Mahen, R., and Venkitaraman, A.R. (2012). Pattern formation in centrosome assembly. Curr Opin Cell Biol 24, 14-23.

Marumoto, T., Hirota, T., Morisaki, T., Kunitoku, N., Zhang, D., Ichikawa, Y., Sasayama, T., Kuninaka, S., Mimori, T., Tamaki, N., et al. (2002). Roles of aurora-A kinase in mitotic entry and G2 checkpoint in mammalian cells. Genes Cells 7, 1173-1182.

Mascanzoni, F., Ayala, I., and Colanzi, A. (2019). Organelle Inheritance Control of Mitotic Entry and Progression: Implications for Tissue Homeostasis and Disease. Front Cell Dev Biol 7, 133.

Meghini, F., Martins, T., Tait, X., Fujimitsu, K., Yamano, H., Glover, D.M., and Kimata, Y. (2016). Targeting of Fzr/Cdh1 for timely activation of the APC/C at the centrosome during mitotic exit. Nat Commun 7, 12607.

Mendez, R., Murthy, K.G., Ryan, K., Manley, J.L., and Richter, J.D. (2000). Phosphorylation of CPEB by Eg2 mediates the recruitment of CPSF into an active cytoplasmic polyadenylation complex. Mol Cell 6, 1253-1259.

Min, M., Mayor, U., Dittmar, G., and Lindon, C. (2014). Using in vivo biotinylated ubiquitin to describe a mitotic exit ubiquitome from human cells. Mol Cell Proteomics 13, 2411-2425.

Min, M., Mayor, U., and Lindon, C. (2013). Ubiquitination site preferences in anaphase promoting complex/cyclosome (APC/C) substrates. Open Biol 3, 130097.

Min, M., Mevissen, T.E., De Luca, M., Komander, D., and Lindon, C. (2015). Efficient APC/C substrate degradation in cells undergoing mitotic exit depends on K11 ubiquitin linkages. Mol Biol Cell 26, 4325-4332.

Mishra, P., Carelli, V., Manfredi, G., and Chan, D.C. (2014). Proteolytic cleavage of Opa1 stimulates mitochondrial inner membrane fusion and couples fusion to oxidative phosphorylation. Cell Metab 19, 630-641.

Mowen, K.A., and David, M. (2014). Unconventional post-translational modifications in immunological signaling. Nat Immunol 15, 512-520.

Nasa, I., and Kettenbach, A.N. (2018). Coordination of Protein Kinase and Phosphoprotein Phosphatase Activities in Mitosis. Front Cell Dev Biol 6, 30.

Nguyen Ba, A.N., Yeh, B.J., van Dyk, D., Davidson, A.R., Andrews, B.J., Weiss, E.L., and Moses, A.M. (2012). Proteome-wide discovery of evolutionary conserved sequences in disordered regions. Sci Signal 5, rs1.

Nikonova, A.S., Astsaturov, I., Serebriiskii, I.G., Dunbrack, R.L., Jr., and Golemis, E.A. (2013). Aurora A kinase (AURKA) in normal and pathological cell division. Cell Mol Life Sci 70, 661-687.

Nishida, K., Yagisawa, F., Kuroiwa, H., Nagata, T., and Kuroiwa, T. (2005). Cell cycle-regulated, microtubule-independent organelle division in Cyanidioschyzon merolae. Mol Biol Cell 16, 2493-2502.

Otto, T., Horn, S., Brockmann, M., Eilers, U., Schuttrumpf, L., Popov, N., Kenney, A.M., Schulte, J.H., Beijersbergen, R., Christiansen, H., et al. (2009). Stabilization of N-Myc is a critical function of Aurora A in human neuroblastoma. Cancer Cell 15, 67-78.

Palazzo, R.E., Vogel, J.M., Schnackenberg, B.J., Hull, D.R., and Wu, X. (2000). Centrosome maturation. Curr Top Dev Biol 49, 449-470.

Pan, J., and Snell, W.J. (2000). Signal transduction during fertilization in the unicellular green alga, Chlamydomonas. Curr Opin Microbiol 3, 596-602.

Paris, J., and Philippe, M. (1990). Poly(A) metabolism and polysomal recruitment of maternal mRNAs during early Xenopus development. Dev Biol 140, 221-224.

Pastore, A. (2010). Further insights into the ubiquitin pathway: understanding the scarlet letter code. Structure 18, 891-892.

Peng, J.Y., Lin, C.C., Chen, Y.J., Kao, L.S., Liu, Y.C., Chou, C.C., Huang, Y.H., Chang, F.R., Wu, Y.C., Tsai, Y.S., et al. (2011). Automatic morphological subtyping reveals new roles of caspases in mitochondrial dynamics. PLoS Comput Biol 7, e1002212.

Peng, Y., and Weisman, L.S. (2008). The cyclin-dependent kinase Cdk1 directly regulates vacuole inheritance. Dev Cell 15, 478-485.

Pesin, J.A., and Orr-Weaver, T.L. (2008). Regulation of APC/C activators in mitosis and meiosis. Annu Rev Cell Dev Biol 24, 475-499.

Peters, J.M. (2006). The anaphase promoting complex/cyclosome: a machine designed to destroy. Nat Rev Mol Cell Biol 7, 644-656.

Petersen, B.O., Wagener, C., Marinoni, F., Kramer, E.R., Melixetian, M., Lazzerini Denchi, E., Gieffers, C., Matteucci, C., Peters, J.M., and Helin, K. (2000). Cell cycle- and cell growth-regulated proteolysis of mammalian CDC6 is dependent on APC-CDH1. Genes Dev 14, 2330-2343.

Pines, J. (2011). Cubism and the cell cycle: the many faces of the APC/C. Nat Rev Mol Cell Biol 12, 427-438.

Pines, J. (2012). A red light in mitosis. Nature reviews Molecular cell biology 13, 482.

Pines, J., and Rieder, C.L. (2001). Re-staging mitosis: a contemporary view of mitotic progression. Nat Cell Biol 3, E3-6.

Plotnikova, O.V., Nikonova, A.S., Loskutov, Y.V., Kozyulina, P.Y., Pugacheva, E.N., and Golemis, E.A. (2012). Calmodulin activation of Aurora-A kinase (AURKA) is required during ciliary disassembly and in mitosis. Mol Biol Cell 23, 2658-2670.

Plotnikova, O.V., Pugacheva, E.N., Dunbrack, R.L., and Golemis, E.A. (2010). Rapid calcium-dependent activation of Aurora-A kinase. Nat Commun 1, 64.

Prosser, S.L., and Pelletier, L. (2017). Mitotic spindle assembly in animal cells: a fine balancing act. Nat Rev Mol Cell Biol 18, 187-201.

Pugacheva, E.N., Jablonski, S.A., Hartman, T.R., Henske, E.P., and Golemis, E.A. (2007). HEF1-dependent Aurora A activation induces disassembly of the primary cilium. Cell 129, 1351-1363.

Qian, J., Beullens, M., Huang, J., De Munter, S., Lesage, B., and Bollen, M. (2015). Cdk1 orders mitotic events through coordination of a chromosome-associated phosphatase switch. Nat Commun 6, 10215.

Qin, L., Guimaraes, D.S., Melesse, M., and Hall, M.C. (2016). Substrate Recognition by the Cdh1 Destruction Box Receptor Is a General Requirement for APC/CCdh1-mediated Proteolysis. J Biol Chem 291, 15564-15574.

Quartuccio, S.M., and Schindler, K. (2015). Functions of Aurora kinase C in meiosis and cancer. Front Cell Dev Biol 3, 50.

Reboutier, D., Benaud, C., and Prigent, C. (2015). Aurora A's Functions During Mitotic Exit: The Guess Who Game. Front Oncol 5, 290.

Reboutier, D., Troadec, M.B., Cremet, J.Y., Chauvin, L., Guen, V., Salaun, P., and Prigent, C. (2013). Aurora A is involved in central spindle assembly through phosphorylation of Ser 19 in P150Glued. J Cell Biol 201, 65-79.

Reboutier, D., Troadec, M.B., Cremet, J.Y., Fukasawa, K., and Prigent, C. (2012). Nucleophosmin/B23 activates Aurora A at the centrosome through phosphorylation of serine 89. J Cell Biol 197, 19-26.

Richards, M.W., Burgess, S.G., Poon, E., Carstensen, A., Eilers, M., Chesler, L., and Bayliss, R. (2016). Structural basis of N-Myc binding by Aurora-A and its destabilization by kinase inhibitors. Proc Natl Acad Sci U S A 113, 13726-13731.

Roghi, C., Giet, R., Uzbekov, R., Morin, N., Chartrain, I., Le Guellec, R., Couturier, A., Doree, M., Philippe, M., and Prigent, C. (1998). The Xenopus protein kinase pEg2 associates with the centrosome in a cell cycle-dependent manner, binds to the spindle microtubules and is involved in bipolar mitotic spindle assembly. J Cell Sci 111 (Pt 5), 557-572.

Rousseau, A., and Bertolotti, A. (2018). Regulation of proteasome assembly and activity in health and disease. Nat Rev Mol Cell Biol 19, 697-712.

Rowan, F.C., Richards, M., Bibby, R.A., Thompson, A., Bayliss, R., and Blagg, J. (2013). Insights into Aurora-A kinase activation using unnatural amino acids incorporated by chemical modification. ACS Chem Biol 8, 2184-2191.

Ruff, E.F., Muretta, J.M., Thompson, A.R., Lake, E.W., Cyphers, S., Albanese, S.K., Hanson, S.M., Behr, J.M., Thomas, D.D., Chodera, J.D., et al. (2018). A dynamic mechanism for allosteric activation of Aurora kinase A by activation loop phosphorylation. Elife 7.

Sasai, K., Treekitkarnmongkol, W., Kai, K., Katayama, H., and Sen, S. (2016). Functional Significance of Aurora Kinases-p53 Protein Family Interactions in Cancer. Front Oncol 6, 247.

Schindler, K., and Schultz, R.M. (2009). CDC14B acts through FZR1 (CDH1) to prevent meiotic maturation of mouse oocytes. Biol Reprod 80, 795-803.

Schumacher, J.M., Ashcroft, N., Donovan, P.J., and Golden, A. (1998). A highly conserved centrosomal kinase, AIR-1, is required for accurate cell cycle progression and segregation of developmental factors in Caenorhabditis elegans embryos. Development 125, 4391-4402.

Schwartz, D.C., and Hochstrasser, M. (2003). A superfamily of protein tags: ubiquitin, SUMO and related modifiers. Trends Biochem Sci 28, 321-328.

Seki, A., Coppinger, J.A., Jang, C.Y., Yates, J.R., and Fang, G. (2008). Bora and the kinase Aurora a cooperatively activate the kinase Plk1 and control mitotic entry. Science 320, 1655-1658.

Serasinghe, M.N., Wieder, S.Y., Renault, T.T., Elkholi, R., Asciolla, J.J., Yao, J.L., Jabado, O., Hoehn, K., Kageyama, Y., Sesaki, H., et al. (2015). Mitochondrial division is requisite to RAS-

induced transformation and targeted by oncogenic MAPK pathway inhibitors. Mol Cell 57, 521-536.

Sessa, F., Mapelli, M., Ciferri, C., Tarricone, C., Areces, L.B., Schneider, T.R., Stukenberg, P.T., and Musacchio, A. (2005). Mechanism of Aurora B activation by INCENP and inhibition by hesperadin. Mol Cell 18, 379-391.

Shagisultanova, E., Dunbrack, R.L., Jr., and Golemis, E.A. (2015). Issues in interpreting the in vivo activity of Aurora-A. Expert Opin Ther Targets 19, 187-200.

Shah, K.N., Bhatt, R., Rotow, J., Rohrberg, J., Olivas, V., Wang, V.E., Hemmati, G., Martins, M.M., Maynard, A., Kuhn, J., et al. (2019). Aurora kinase A drives the evolution of resistance to third-generation EGFR inhibitors in lung cancer. Nat Med 25, 111-118.

Singh, S.A., Winter, D., Kirchner, M., Chauhan, R., Ahmed, S., Ozlu, N., Tzur, A., Steen, J.A., and Steen, H. (2014). Co-regulation proteomics reveals substrates and mechanisms of APC/C-dependent degradation. EMBO J 33, 385-399.

Sivakumar, S., and Gorbsky, G.J. (2015). Spatiotemporal regulation of the anaphase-promoting complex in mitosis. Nat Rev Mol Cell Biol 16, 82-94.

Snell, W.J., Pan, J., and Wang, Q. (2004). Cilia and flagella revealed: from flagellar assembly in Chlamydomonas to human obesity disorders. Cell 117, 693-697.

Strzyz, P. (2018). Chromosome biology: A stairway to mitotic chromosome assembly. Nat Rev Mol Cell Biol 19, 139.

Studer, R.A., Christin, P.A., Williams, M.A., and Orengo, C.A. (2014). Stability-activity tradeoffs constrain the adaptive evolution of RubisCO. Proc Natl Acad Sci U S A 111, 2223-2228.

Sugase, K., Dyson, H.J., and Wright, P.E. (2007). Mechanism of coupled folding and binding of an intrinsically disordered protein. Nature 447, 1021-1025.

Sugimoto, K., Urano, T., Zushi, H., Inoue, K., Tasaka, H., Tachibana, M., and Dotsu, M. (2002). Molecular dynamics of Aurora-A kinase in living mitotic cells simultaneously visualized with histone H3 and nuclear membrane protein importinalpha. Cell structure and function 27, 457-467.

Sullivan, M., and Morgan, D.O. (2007). Finishing mitosis, one step at a time. Nat Rev Mol Cell Biol 8, 894-903.

Taguchi, S., Honda, K., Sugiura, K., Yamaguchi, A., Furukawa, K., and Urano, T. (2002). Degradation of human Aurora-A protein kinase is mediated by hCdh1. FEBS Lett 519, 59-65.

Thornton, B.R., and Toczyski, D.P. (2006). Precise destruction: an emerging picture of the APC. Genes Dev 20, 3069-3078.

Tilokani, L., Nagashima, S., Paupe, V., and Prudent, J. (2018). Mitochondrial dynamics: overview of molecular mechanisms. Essays Biochem 62, 341-360.

Toji, S., Yabuta, N., Hosomi, T., Nishihara, S., Kobayashi, T., Suzuki, S., Tamai, K., and Nojima, H. (2004). The centrosomal protein Lats2 is a phosphorylation target of Aurora-A kinase. Genes Cells 9, 383-397.

Tokuriki, N., Stricher, F., Serrano, L., and Tawfik, D.S. (2008). How protein stability and new functions trade off. PLoS Comput Biol 4, e1000002.

Tsai, M.Y., Wiese, C., Cao, K., Martin, O., Donovan, P., Ruderman, J., Prigent, C., and Zheng, Y. (2003). A Ran signalling pathway mediated by the mitotic kinase Aurora A in spindle assembly. Nat Cell Biol 5, 242-248.

Vader, G., Medema, R.H., and Lens, S.M. (2006). The chromosomal passenger complex: guiding Aurora-B through mitosis. J Cell Biol 173, 833-837.

Valente, C., and Colanzi, A. (2015). Mechanisms and Regulation of the Mitotic Inheritance of the Golgi Complex. Front Cell Dev Biol 3, 79.

Van Roey, K., Uyar, B., Weatheritt, R.J., Dinkel, H., Seiler, M., Budd, A., Gibson, T.J., and Davey, N.E. (2014). Short linear motifs: ubiquitous and functionally diverse protein interaction modules directing cell regulation. Chem Rev 114, 6733-6778.

van Vugt, M.A., Bras, A., and Medema, R.H. (2004). Polo-like kinase-1 controls recovery from a G2 DNA damage-induced arrest in mammalian cells. Mol Cell 15, 799-811.

Violin, J.D., Zhang, J., Tsien, R.Y., and Newton, A.C. (2003). A genetically encoded fluorescent reporter reveals oscillatory phosphorylation by protein kinase C. J Cell Biol 161, 899-909.

Wai, T., and Langer, T. (2016). Mitochondrial Dynamics and Metabolic Regulation. Trends Endocrinol Metab 27, 105-117.

Wasch, R., Robbins, J.A., and Cross, F.R. (2010). The emerging role of APC/CCdh1 in controlling differentiation, genomic stability and tumor suppression. Oncogene 29, 1-10.

Weber, J., Polo, S., and Maspero, E. (2019). HECT E3 Ligases: A Tale With Multiple Facets. Front Physiol 10, 370.

Wieser, S., and Pines, J. (2015). The biochemistry of mitosis. Cold Spring Harb Perspect Biol 7, a015776.

Wike, C.L., Graves, H.K., Hawkins, R., Gibson, M.D., Ferdinand, M.B., Zhang, T., Chen, Z., Hudson, D.F., Ottesen, J.J., Poirier, M.G., et al. (2016). Aurora-A mediated histone H3 phosphorylation of threonine 118 controls condensin I and cohesin occupancy in mitosis. Elife 5, e11402.

Willems, E., Dedobbeleer, M., Digregorio, M., Lombard, A., Lumapat, P.N., and Rogister, B. (2018). The functional diversity of Aurora kinases: a comprehensive review. Cell Div 13, 7.

Wu, J., Yang, L., Shan, Y., Cai, C., Wang, S., and Zhang, H. (2016). AURKA promotes cell migration and invasion of head and neck squamous cell carcinoma through regulation of the AURKA/Akt/FAK signaling pathway. Oncol Lett 11, 1889-1894.

Wysong, D.R., Chakravarty, A., Hoar, K., and Ecsedy, J.A. (2009). The inhibition of Aurora A abrogates the mitotic delay induced by microtubule perturbing agents. Cell Cycle 8, 876-888.

Yamamoto, A., Guacci, V., and Koshland, D. (1996). Pds1p, an inhibitor of anaphase in budding yeast, plays a critical role in the APC and checkpoint pathway(s). J Cell Biol 133, 99-110.

Yamano, K., and Youle, R.J. (2011). Coupling mitochondrial and cell division. Nat Cell Biol 13, 1026-1027.

Yanagida, M. (2014). The role of model organisms in the history of mitosis research. Cold Spring Harbor perspectives in biology 6, a015768.

Yang, N., Wang, C., Wang, Z., Zona, S., Lin, S.X., Wang, X., Yan, M., Zheng, F.M., Li, S.S., Xu, B., et al. (2017). FOXM1 recruits nuclear Aurora kinase A to participate in a positive feedback loop essential for the self-renewal of breast cancer stem cells. Oncogene 36, 3428-3440.

Ye, Y., and Rape, M. (2009). Building ubiquitin chains: E2 enzymes at work. Nat Rev Mol Cell Biol 10, 755-764.

Zeng, K., Bastos, R.N., Barr, F.A., and Gruneberg, U. (2010). Protein phosphatase 6 regulates mitotic spindle formation by controlling the T-loop phosphorylation state of Aurora A bound to its activator TPX2. J Cell Biol 191, 1315-1332.

Zhang, Y., Ni, J., Huang, Q., Ren, W., Yu, L., and Zhao, S. (2007). Identification of the auto-inhibitory domains of Aurora-A kinase. Biochem Biophys Res Commun 357, 347-352.

Zhao, J., Zhang, J., Yu, M., Xie, Y., Huang, Y., Wolff, D.W., Abel, P.W., and Tu, Y. (2013). Mitochondrial dynamics regulates migration and invasion of breast cancer cells. Oncogene 32, 4814-4824.

Zheng, F., Yue, C., Li, G., He, B., Cheng, W., Wang, X., Yan, M., Long, Z., Qiu, W., Yuan, Z., et al. (2016). Nuclear AURKA acquires kinase-independent transactivating function to enhance breast cancer stem cell phenotype. Nat Commun 7, 10180.

Zheng, N., and Shabek, N. (2017). Ubiquitin Ligases: Structure, Function, and Regulation. Annu Rev Biochem 86, 129-157.

Zhou, H., Kuang, J., Zhong, L., Kuo, W.L., Gray, J.W., Sahin, A., Brinkley, B.R., and Sen, S. (1998). Tumour amplified kinase STK15/BTAK induces centrosome amplification, aneuploidy and transformation. Nat Genet 20, 189-193.

Zilfou, J.T., and Lowe, S.W. (2009). Tumor suppressive functions of p53. Cold Spring Harb Perspect Biol 1, a001883.

Zorba, A., Buosi, V., Kutter, S., Kern, N., Pontiggia, F., Cho, Y.J., and Kern, D. (2014). Molecular mechanism of Aurora A kinase autophosphorylation and its allosteric activation by TPX2. Elife 3, e02667.

Zorov, D.B., Vorobjev, I.A., Popkov, V.A., Babenko, V.A., Zorova, L.D., Pevzner, I.B., Silachev, D.N., Zorov, S.D., Andrianova, N.V., and Plotnikov, E.Y. (2019). Lessons from the Discovery of Mitochondrial Fragmentation (Fission): A Review and Update. Cells 8.